Lawrence Berkeley Laboratory
UNIVERSITY OF CALIFORNIA

CHEMICAL BIODYNAMICS DIVISION

THE INTERACTIONS OF 4-NITROQUINOLINE-1-OXIDE WITH NUCLEIC ACIDS

Stephen Alan Winkle
(Ph. D. thesis)

August 1979

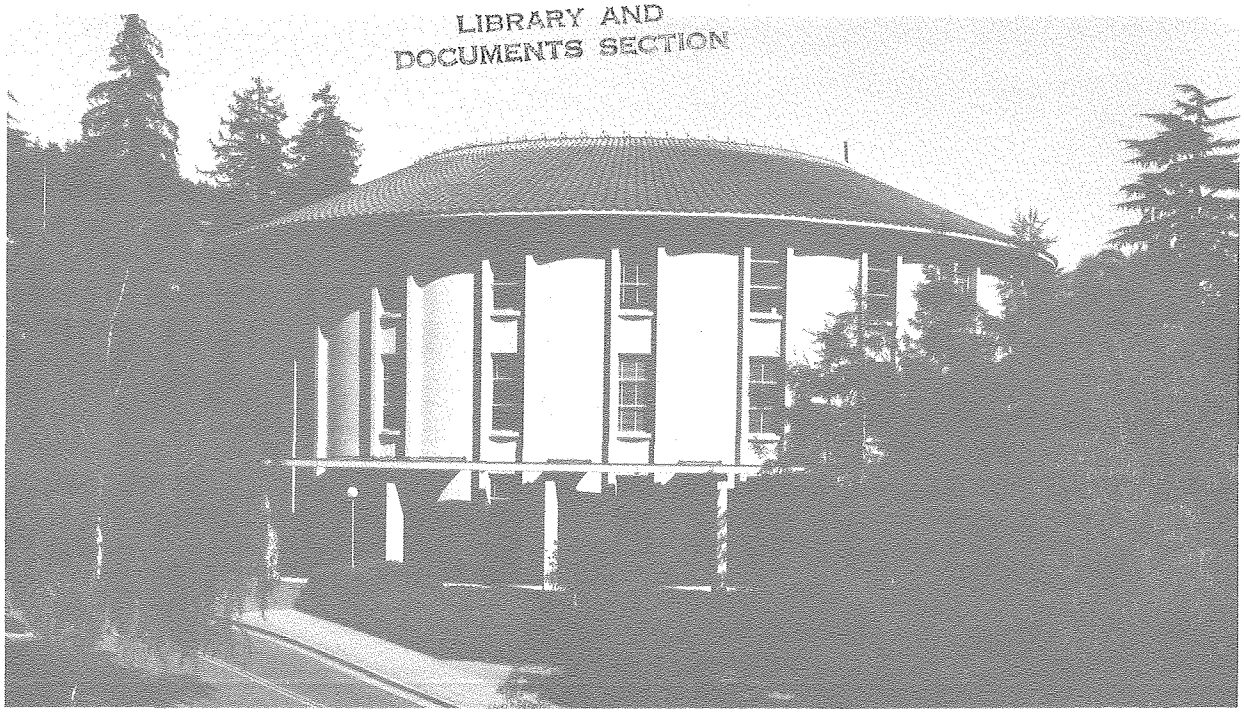

Prepared for the U.S. Department of Energy under Contract W-7405-ENG-48

THE INTERACTIONS OF 4-NITROQUINOLINE-1-OXIDE WITH NUCLEIC ACIDS

by

Stephen Alan Winkle

ABSTRACT

The interactions of the potent mutagen and carcinogen, 4-nitroquinoline-1-oxide (NQO) with deoxyribomononucleotides, deoxyribodinucleotides and DNA's were studied. The non-covalent complexes formed by NQO and either the four 5'= deoxyribonucleotides or the deoxyribodinucleotides were studied using absorption spectra of the charge transfer bands (circa 395-410 nm) and ^{1}H and ^{13}C nuclear magnetic resonance (NMR) spectra of NQO-nucleic acid mixtures. Absorption spectra for the monomer-NQO and dimer-NQO systems were analyzed using Benesi-Hildebrand type equations to yield stoichiometries and equilibrium constants of complex formation. The equilibrium constants for the formation of the 1:1 monomer:NQO complexes at 25°C (K(dpG:NQO) = 16 M^{-1}, K(dpA:NQO) = 12 M^{-1}, K(dpT:NQO) = K(dpC:NQO) = 4 M^{-1}) suggest the preference of NQO for the guanine residue in a DNA. This is in agreement with the data of Okano, T. et al. [(1969) Gann 60, 295]. Non-selfcomplementary dimers form weak 1:1 complexes (dpTpG:NQO, K(25°) = 22 M^{-1}) while self-complementary dimers form strong 2:1 complexes ((dpCpG$_2$:NQO, K(25°C) = 2.2×10^{4} M^{-2}). A mixture of dpTpG and dpCpA with NQO

gives a "2:1" complex (dpTpG:NQO:dpCpA, K(25°C) = 8.6×10^3 M^{-2}). The dinucleotides capable of forming DNA-like minihelices gave similar values of K for NQO complex formation. From ^{13}C and ^{1}H NMR data, it is proposed that in the dpG:NQO complex the (NO_2), (NO) containing NQO is stacked over the guanine imidazole ring while in the dpG:NQO complex the NQO benzenoid ring is over the adenine imidazole ring. Analyses of the changes in ^{13}C and ^{1}H NMR chemical shifts with complex formation for dimer-NQO mixtures gave approximate orientations for the intercalation of NQO with self-complementary dimer minihelices. In the $(dpCpG)_2$:NQO and $(dpGpC)_2$:NQO complexes, the (NO_2) group of NQO probably lies in the major groove and the (NO_2), (NO) containing NQO ring is stacked near the purine imidazole ring. In the $(dpTpA)_2$:NQO and $(dpApT)_2$:NQO complexes, the (NO_2) seems to project into the minor groove and the NQO benzenoid ring is over the purine imidazole ring.

Irradiation of NQO-polynucleotide (poly(rA), poly(rU), poly(rC)) mixtures and NQO-DNA mixtures using either a Hg lamp source (340-420 nm) or a dye laser (400-415) nm produced photoadducts. With the polymers, poly(rC) gave the greatest number of adducts per residue. Poly(rC) and DNA also reacted with NQO in the dark. A dpC-NQO photo-adduct was produced.

DNA-NQO equilibria were studied using analyses of the complex absorption bands (415 nm) and using the phase partition technique. Two NQO molecules bind strongly and cooperatively to a small number of sites on the DNA. The equilibrium constants and binding ratios at 25°C ranged from 4.3×10^{9} M^{-2} and 100 base pairs (bp)/site for calf thymus DNA to 4.0×10^{14} M^{-2} and 3600 bp/site for superhelical SV 40 DNA. The binding ratio for calf thymus DNA was temperature dependent, e.g., 7°C, 500 bp/site; 25°C, 100 bp/site; 35°C, 840 bp/site. The equilibrium constants dropped when supercoiled DNA was converted to the linear form (pBR 322, 2.2×10^{13} to 6.8×10^{11} M^{-2}; SV 40, 4.0×10^{14} to 1.3×10^{13} M^{-2}). NQO inhibits the cutting of superhelical SV 40 DNA and pBR 322 by S_1 endonuclease which cuts "denatured regions" in superhelical DNA's [Beard, et al. (1973), J. Virology 12, 1303]. Restriction enzyme digests of pBR 322 or SV 40 reacted photochemically with ^{3}H-NQO located NQO binding sites (5 on pBR 322; 2 on SV 40, one coinciding with an S_1 cutting site). The DNA unwinding angle of noncovalently bound NQO was 830° per NQO (1700°/site) and for covalently bound NQO (photochemical addition), the DNA unwinding angle was 770°/NQO (1500°/site). Based on these features of the noncovalent binding of NQO to DNA, it is suggested that NQO binds to cruciform-like structures in the DNA.

This dissertation is dedicated to my parents, Vernon and Patsy Jean Winkle, who gave me my start in science, and supported me in every way possible.

ACKNOWLEDGEMENTS

Professor Ignacio Tinoco, Jr. (Chemistry), my research director, provided numerous suggestions and the opportunity for many lively discussions. Nacho served to temper my youthful exuberance by providing a continuous critical appraisal of this work.

Professor John E. Hearst (Chemistry), chairman of my prelim committee and member of my thesis committee, provided useful suggestions and critiques and furnished much in the way of materials and equipment.

Dr. Beatrice Singer Fraenkel-Conrat (Molecular Biology Laboratory), member of the thesis committee also provided useful suggestions relating to the covalent reactions of NQO.

Professor Stan Smith (Chemistry, University of Kentucky), friend and advisor, gave me my start in NMR.

Rudi Nunlist, NMR specialist, was of great value in keeping the NMR's running and obtaining the NMR spectra.

Dr. Gary Wiesehahn, in addition to being the source of enzymes and other materials, gave much valuable advice on aspects of molecular biology: gels, enzyme digests, and such. Doug Youvan was also an extremely valuable source of information on these esoteric techniques. Steve Isaacs, Corliss Chun and Rick Reisbig, also of the Hearst group, also gave useful suggestions.

Barbara Dengler must be acknowledged, as always, for keeping the lab morale high and for keeping the lab in working order. Barbara would merit special praise, if for no other reason, then, for listening to my complaints. David Koh, the coach, could either fix "it" or tell you where to take it. David always had the answer (even if there was not a question). Thanks, coach.

Among the post-docs, Robert Lee and I had many "stimulating" but enjoyable discussions on aspects of NMR. Frank Martin not only provided a wealth of information and suggestions on drug binding but was also someone with whom aspects of "Ole South" and mideast could be discussed. Jim McMahon did write a useful DNA sequence analysis program but that is incidental relative to the value of our discussions of the finer points of science fiction, wargames, dragon slaying and so on. Bruce Johnson was a constant non-stoppable source of advice on just about everything.

Regarding the graduate student members of Nacho's Nucleases, Soo Frier, Mark Watts and Kyong Yoon were available for many informative discussions during my first years in the group. (Kyong also procurred my supply of pBR 322.) Adrienne Drobnies was a comrade in anarchy in the department and group. Carlos Bustamante provided the opportunity for theoretical discussions and a different perspective on the USA, the world and space. Art Pardi gave the opportunity for much jousting while serving as

a source of suggestions and comments. Ken Dahl was a comrade-in-arms, trading friendly insults, pitchers of beer, social commentary (such as on the "merits" of OHSA's carcinogen regulations) and even a little scientific expertise. Jeff Nelson stoically took a lot of grief and returned useful comments.

Fred Grieman and Tony O'Keefe provided a needed dye laser.

The acknowledgements would not be complete without a mention of the Chem Pistols. The Chem Pistols showed our prowess at Basketball, football and softball but really shined at beer drinking and partying. The Chem Pistols provided the escape valve, the measure of insanity necessary.

All of the special people who made my years in Berkeley just fine, y'all, need mention: Steve, Sally, Mike, Shanta, Mark, Susan, the Jim's, the Tony's, Fred, Floyd, Dave and all the rest.

TABLE OF CONTENTS

CHAPTER I

INTRODUCTION

Many carcinogens act as mutagens (McCann, et al., 1975) and may therefore interact with DNA. These interactions can be noncovalent, covalent or a noncovalent interaction followed by a covalent reaction. The possible consequences of such interactions may include either frameshift or point mutations. Numerous studies have been done on the interactions of mutagens/carcinogens with nucleic acids. Among the more popular molecules for study have been the acridines such as 9-aminoacridine (Sakore, et al., 1977), ethidium salts (Krugh & Reinhardt, 1975), benzo(a)pyrene and metabolites (Jeffrey, et al., 1976; Koreeda, et al., 1976; Nakanishi, et al., 1977), N-acetoxyacetyl-2-aminofluorene and related compounds (Fink, et al., 1970; Agarawa & Weinstein, 1970; Krick et al., 1967) and 4-nitroquinoline-1-oxide (NQO) (for example, see Okano, et al., 1969 a-c). From such investigations, information such as the strengths of interactions, binding orientations or adduct structures and sequence preferences have been obtained. In this dissertation, the results of research on the noncovalent binding of the potent mutagen and carcinogen NQO to deoxymononucleotides, deoxydinucleotides and various types of DNA are presented. The dissertation will also include experiments dealing with photochemically induced NQO-nucleic acid adducts.

The existing literature on NQO-nucleic acid interactions can be divided into studies on noncovalent complexes and studies on the formation of adducts. Work on the noncovalent complexes, which will be discussed first, has dealt primarily with monomeric units of nucleic acids (free bases and mononucleosides). Only a few papers have dealt with DNA interactions. On the other hand, a much larger body of work has been done on NQO adduct formation. These studies centered around the metabolism of NQO and the formation of DNA adducts by metabolites such as 4-hydroxyaminoquinoline-1-oxide (HAQO).

Some of the earlier work on noncovalent nucleic acid interactions of NQO was performed by Nagata and coworkers (Nagata et al., 1963; Nagata et al., 1966). Nagata et al. (1966) were the first to present spectroscopic evidence of NQO-DNA complexes, utilizing both flow dichroism spectra and difference absorption spectra. Their studies suggested that NQO lies in plane with the bases of DNA and that a new band appears in the absorption spectrum of NQO-DNA solutions at between 400-420 nm. Subsequent spectral studies also used difference absorption spectra for the observation of this complex band.

Theoretical studies by Nagata et al. (1963) and Karreman (1962) indicated the possible existence of charge transfer in the interactions of NQO with the aromatic base moieties of nucleic acids. Okano and cowerkers (1969a) reported that the addition

of NQO or related quinoline compounds to DNA or deoxyribonucleoside solutions produced hypochromic changes in the UV spectra of the nucleic acids (in the bands near 260 nm). With DNA, deoxyguanosine and deoxyadenosine the percentage hypochromicities of the various quinoline compounds correlated well with the previously reported polarographic half-wave potentials (Tachibana et al., 1967). Subsequently, Okano and coworkers (1969b) reported that there was a linear correlation between the wavelength maxima of the deoxymononucleoside-NQO complex bands (at ca. 400 nm) and the energy levels of the highest-occupied molecular orbitals of the bases. Also, the absorbances at complex wavelength maxima for the four deoxymononucleoside-NQO complexes changed sigmoidally with pH. Okano and coworkers stated that these results showed the presence of charge transfer in the NQO-nucleic acid interactions and showed that the complex bands are due to the charge transfer interaction.

The presence of this charge transfer band provides a means for monitoring the equilibria of NQO and nucleic acids. Kawashima and Tomoeda (1970) obtained complex band spectra for mixtures of NQO with the purine or pyrimidine bases. Using a form of the Benesi-Hildebrand equation (Benesi & Hildebrand, 1949) to analyze the spectral data for the adenine-NQO system, they obtained an equilibrium constant for the formation of the 1:1 adenine:NQO complex

($K = 14\ m^{-1}$). Okano and coworkers (1969b) performed a more extensive spectral study on the NQO-deoxymononucleoside systems. For the four deoxyribonucleosides, they determined equilibrium constants for the formation of 1:1 complexes: $NQO + dN \overset{K}{\rightleftharpoons} NQO{:}dN$. Again, complex band absorption vs. nucleoside concentration data (at fixed NQO concentrations) were analyzed by a form of the Benesi-Hildebrand equation:

$$\frac{[dN]_T[NQO]_T\ell}{A_T} = \frac{1}{\varepsilon}[dN] + \frac{1}{K\varepsilon}$$

where $[dN]_T$ and $[NQO]_T$ are the total concentrations of nucleoside and NQO, ℓ is the cell pathlength, A_T is the total absorbance at the complex λ_{max}, and ε is the molar absorptivity of the complex. The absorption spectra taken were difference spectra: the spectra of the deoxynucleoside-NQO solutions were taken vs. a solution of equal $[NQO]_T$. Okano's work showed that the equilibrium constants for the complexes with the purine deoxynucleosides dG and dA are larger than those for the pyrimidine compounds dT and dC. It may be noted that the equilibrium constant for the dA:NQO complex is very similar to that for the adenine:NQO system. This shows that the presence or absence of the sugar group does not greatly affect the strength of binding.

Okano and coworkers (1969c) also conducted a ^1H NMR study of mixtures of the deoxyribonucleosides and NQO. However this study was done in dimethylsulfoxide-d_6 rather than in

aqueous media and was performed at high concentrations (nucleoside and NQO at ca. 0.30 mol kg^{-1}). The ring protons of the purine bases shifted upfield indicating stacking of the NQO and the bases. Much smaller shifts were seen with the pyrimidines but this could be explained by the smaller equilibrium constants for the pyrimidine systems (less complexed pyrimidines).

Other than the study by Nagata mentioned earlier, only a limited number of studies have been done on the interactions of NQO with DNA. That the presence of NQO increases the T_m's for native DNA as well as for poly(G)·poly(C) and to a lesser extent for poly[d(A-T)·d(A-T)] was reported by Paul and Montgomery (1970). They also investigated the DNA-NQO equilibrium through analysis of the complex absorption bands.

As stated earlier, much more work has been done on the metabolism of NQO and the structural determination of possible DNA adducts. To date, however, no definite adduct structures have been elucidated. Several studies (e.g., Sugimura et al., 1966; Kawazoe et al., 1969a) have indicated that most of the NQO entering an animal is reduced to HAQO, leading to HAQO being considered the ultimate carcinogen. Further metabolism of HAQO has been suggested. One such carcinogenic metabolite could be the 0,0'-diacetyl-4-HAQO (Kawazoe et al., 1969b). Thus, most studies of covalent adducts of "NQO" have actually involved HAQO. Notable investigations of the adducts

have been conducted by Tada and Tada. The covalent adducts isolated from such studies have been between the purine bases and the quinoline moiety. Tada and Tada (1976) subjected DNA containing bound radioactively labeled quinoline moieties (isolated from carcinogen treated cells) to acid hydrolysis. Chromatography of the hydrolysates showed that most (90%) of the quinoline is bound to the guanines. Thus, they concluded that the *in vivo* preference of metabolized HAQO is for guanine.

This dissertation will focus on the noncovalent interactions of NQO with nucleic acids. The orientation which a mutagen assumes in forming a noncovalent complex with DNA determines, at least partially, the structure of the covalent adduct. Studies on DNA sequence or DNA structural feature dependence of the noncovalent binding provide insight into where the covalent adducts will form. Several reasons for using NQO rather than an "activated metabolite" such as the O,O'-diacetyl-HAQO may be offered. The stability of NQO in aqueous media is greater than that of any of the metabolites, including HAQO, on the metabolism pathway leading to reaction with DNA. In general, the reactivities of NQO and HAQO are similar, so NQO could model any proposed active metabolite. As will be discussed further in Chapter IV, there is evidence to suggest that NQO need not be metabolized to react with DNA.

The plan of this research is to sequentially study the interactions of NQO with deoxymononucleotides, then with deoxydinucleotides, and finally with various DNA's. The object is to characterize the nature of NQO-DNA binding. The information obtained may then be related to possible mechanisms by which NQO produces mutations.

From the study using the deoxymonomers, base specificity and complex orientations were obtained. The mononucleotides also provided a relatively simple system in which the methodology could be developed. Difference absorption spectra of the complex bands were analyzed to provide equilibria data. To determine the complex orientations, ^{13}C and ^{1}H NMR spectra of NQO-nucleotide mixtures were used.

These methods were then utilized in monitoring facets of the binding of NQO to deoxydinucleotides. The self-complementary dinucleotides may be induced to form mini-helices or duplexes through the binding of drug molecules. Thus the orientations assumed by NQO in a DNA-like environment could be examined. From the determination of equilibrium constants for different dinucleotides, possible sequence selectivity of NQO could be assayed.

In the studies with DNA's, the methods used changed. Using the charge transfer band to monitor the NQO-DNA equilibria was only partially successful. It was desirable to use lower NQO concentrations than were feasible for optical studies. Thus, tritium labeled NQO and the phase partition method

of monitoring equilibria developed by Waring (1975) were used to determine equilibrium constants and binding ratios. More detailed information about the nature of the binding sites was obtained using the sequenced, well defined DNA's, the plasmid pBR 322 and simian virus 40 (SV40) DNA. Approximate locations of the binding sites were determined using restriction enzymes and the photochemical attachment of NQO to the DNA. The effects of NQO on DNA secondary structure were assayed using HeLa cell unwinding enzyme and S_1 (a single strand cutting enzyme). From the various experiments performed on the NQO-DNA systems, a picture of NQO's interaction and the effects of it could be drawn.

The other topic of discussion is the photochemical reaction of NQO with DNA. The photoreactivity of NQO was discovered accidentally (while looking for NQO fluorescence). Only a limited number of experiments on NQO photoreactions were performed since this did not fall under the main topic of noncovalent interactions of NQO. The thrust of the photochemical experiments was to show that the reaction with DNA did occur. Base specificity and the nature of the adducts were studied. In the main, however, the photoreaction was used as a tool in the characterization of the nature of the binding sites in DNA - in terms of structural or sequence features.

The outline of the dissertation follows the sequence of experiments. In Chapters II and III, the experiments with the

mononucleotides and dinucleotides and their results are discussed, respectively. The photochemistry is presented in Chapter IV. The equilibrium studies with NQO and the DNA's occupy Chapter 5 and Chapter VI is a discussion of the experiments involving the nature of DNA binding sites for NQO. The last chapter, Chapter 7, contains the conclusions, speculations and suggestions for future experiments.

Included as Appendix II is a collection of ^{13}C NMR data for various nucleic acids. Sample spectra, tables of chemical shifts and plots of chemical shift vs. concentrations of the mononucleotides are presented here.

CHAPTER II

DEOXYMONONUCLEOTIDE-NQO COMPLEXES

INTRODUCTION

In Chapter I, the study by Okano et al. (1969b) on the deoxymononucleosides and Kawashima and Tomoeda (1970) on the nucleoc acid bases were discussed. Both groups studied the complex absorption bands arising from the base-NQO interactions. From analysis of these bands using a version of the Benesi-Hildebrand equation, Okano determined equilibrium constants for the formation of 1:1 deoxynucleoside:NQO complexes. The study with the deoxymononucleosides was conducted in 5 mM NaCl, 0.5 mM sodium citrate (pH 7.0) at 25°C. Larger values were found for the purine nucleosides [K(dG) = 12.2 m^{-1}; K(dA) = 11.5 m^{-1}] than for the pyrimidine nucleosides [K(dT) = 5.20 m^{-1}; K(dC) = 2.29 m^{-1}].

For further insight into the base specificity of NQO binding, studies were made of the 1:1 complexes of NQO with the 5'-deoxyribonucleotides:

$$NQO + dpN \overset{K}{\rightleftharpoons} NQO{:}dpN$$

Data from nucleotide concentration vs. complex band absorption spectra were analyzed by a Benesi-Hildebrand equation which was modified to account for nucleotide absorption and changes in the nucleotide and NQO concentrations due to complex

formation. The interactions were also examined using ^{1}H and ^{13}C NMR spectroscopy in aqueous media. From the magnitudes and signs of the changes in chemical shifts of the protons and carbons on the molecules in the complex, it was possible to propose structures for the complexes.

EXPERIMENTAL

Materials

The four 5'-deoxyribonucleotides, dpG, dpA, dpT, dpC were obtained from Calbiochem.

The NQO was synthesized from quinoline-1-oxide (Aldrich Chemical Co.) using the procedure of Ochiai (1953); 5 gm quinoline-1-oxide were dissolved with stirring in 10.8 ml of concentrated H_2SO_4. To this solution at 60 - 70°C, approximately 5.6 ml concentrated HNO_3 were added over a 30 min period. Occasional cooling with an ice bath was necessary to maintain the desired temperature range (70-75°C) while adding the HNO_3. The mixture was stirred at 70-75°C for 2 hr. At the end of 2 hr, the reaction mixture was poured over ice with a yellow precipitate forming. The collected precipitate was washed with distilled cold H_2O, dilute cold Na_2CO_3, more cold H_2O and finally cold 95% EtOH. The precipitate was then recrystallized 3 times from hot acetone. 1.2 gm NQO was collected (22% of the theoretical yield). The low yield was due to impurities in the quinoline-1-oxide (e.g., quinoline absorbed into the quinoline-1-oxide crystals) and excessive washing. The determined melting point after recrystallization,

140 - 145°, was lower than the reported 153 - 154°C. However, the UV spectrum, in cacodylate buffer (figure 1a), and the NMR spectrum, in cacodylate buffer with D_2O (figure 1b), checked with those reported, indicating no impurities. Thin layer chromatography in a variety of solvents, e.g., mixtures of 1 M NH_4OH and 95% EtOH in varying ratios, supported this. The lower melting point relative to that reported is probably due to the presence of H_2O. Solid NQO and NQO solutions were stored in brown glass bottles. The solid NQO is reasonably stable as are aqueous solutions when stored in the dark. In the light, solutions of NQO slowly turn from the normal yellow to brownish, indicating decomposition. Aqueous solutions of NQO for the various studies were made by placing sufficient NQO to achieve a saturated solution in the buffer and stirring overnight at room temperature. Excess NQO was filtered out and the concentration checked by the absorbance at 250 nm (see below). Since NQO is a potent mutagen and carcinogen, a special protocol for handling it was developed and is presented in Appendix I.

Figure 1.

(a) UV absorption spectrum (240-420 nm) of NQO ($[NQO]_T$ = 5.9×10^{-5} M, in cacodylate buffer, pH 7.0). Spectrum obtained at 25°C *vs.* cacodylate buffer on Cary 118 spectrometer.

(b) 360 mHz ^1H NMR spectrum of NQO ($[NQO]_T$ = 1.8×10^{-3} M, in cacodylate buffer (D_2O, pH = 7.0). Spectrum obtained at 20°C on Stanford Magnetic Resonance Laboratory 360 mHz system. Referenced to DSS (0.00 ppm).

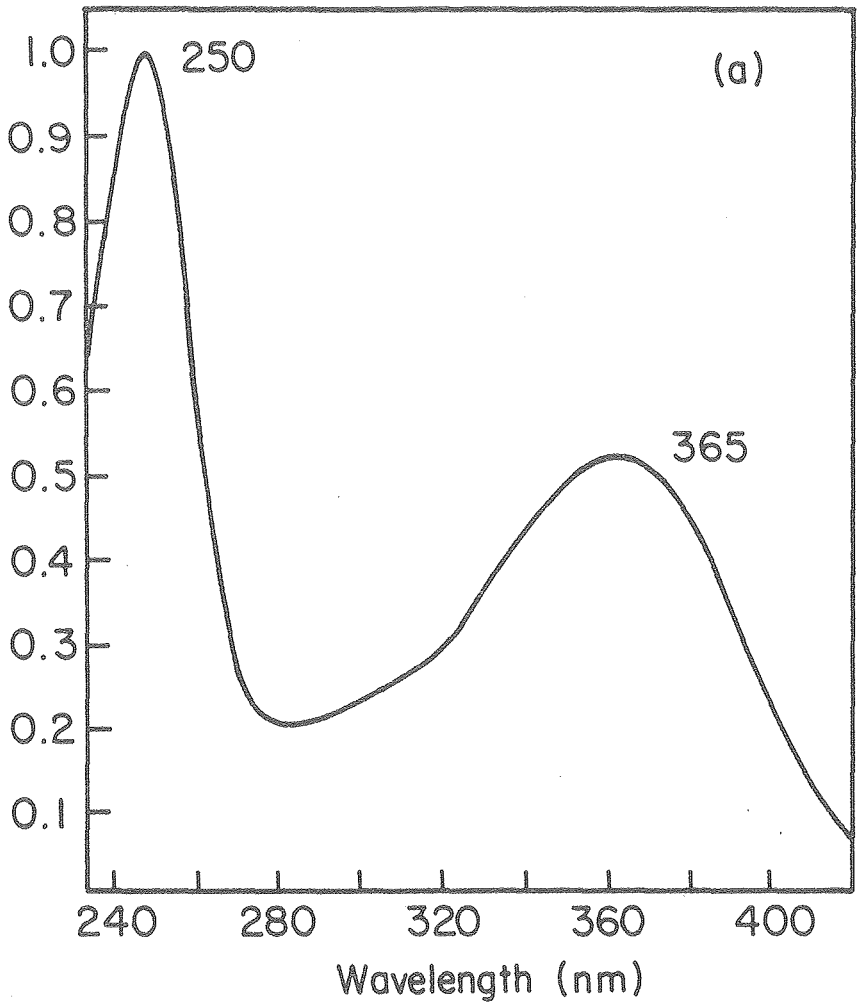

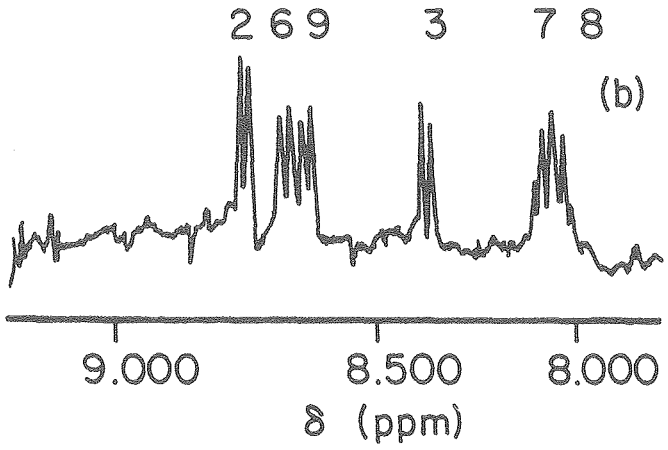

XBL 798-10848

Absorption Spectral Studies

Optical studies were done in a buffer consisting of 0.1 M NaCl and 0.01 M sodium cacodylate, pH 7.0. Concentrations of the nucleotide and NQO solutions were measured using the absorbance at the λ_{max}. (See Table I for the molar absorptivities of NQO at various wavelengths.) Glass tuberculin syringes were used for the measurement of nucleotide and NQO solution volumes. Samples for the optical studies were prepared by placing a fixed volume of stock NQO solution in each sample tube ($[NQO]_T$ for the samples ranged from ca. $6x10^{-4}$ to $2x10^{-4}$ M), adding a given volume of the stock nucleotide solution ($[dpN]_T$ ranged from ca. $9x10^{-2}$ to $2x10^{-2}$ M), and then addition of sufficient cacodylate buffer to produce constant volume. Absorption spectra in the region of the complex band (460-380 nm) were recorded for each dpN-NQO mixture vs. a solution of equal $[NQO]_T$ to produce difference spectra. Absorption spectra were recorded at 25°C on either a Cary 15, Cary 14, or a Beckman Acta MIV spectrometer. For mixtures of dpG and NQO ($[dpG]_T$ from 0.026 to 0.17 M and $[NQO]_T$ from $4.4x10^{-4}$ to $5.5x10^{-4}$ M), absorption spectra (460-380 nm) were recorded at 10°C on a Cary 14 spectrometer. Samples were run in either 0.5- or 1.0-cm pathlength cells vs. a solution of NQO alone of equal concentration. In this manner the spectra obtained were the difference between the sample and reference cells. The $\varepsilon_{(dpN)}$ values at the complex λ_{max} were obtained

TABLE I

Values of the Molar Absorptivity (ε) at Various Wavelengths for NQO (at pH 7.0, Aqueous Media).

Molecule	Wavelength (nm)	Molar Absorptivity x10^3 (M^{-1} cm^{-1})
NQO	250(λ_{max})	16.5[a]
	365(λ_{max})	8.40[a]
	398	3.79[b]
	402.5	3.23[b]
	405	2.69[b]
	406	2.59[b]

[a] T. Okano et al. (1973).

[b] Experimentally determined at the wavelength maxima of the complexes (see Table II).

by measuring the absorption at these λ_{max} of nucleotide solutions of concentrations similar to those for the dpN-NQO mixtures. Values of ε(dpN) from the CRC Handbook of Biochemistry and Molecular Biology (Fasman, 1976) were used at the wavelength maximum for the nucleotides to obtain the nucleotide concentrations. The $\varepsilon_{(NQO)}$ at the various complex band λ_{max} were similarly obtained.

A similar absorption study was attempted using HAQO with dpG and dpA. (The procedure for synthesizing HAQO is in Chapter IV.) Samples of HAQO and either dpG or dpA were prepared in cacodylate buffer in concentrations similar to those employed in the NQO-mononucleotide optical study above. Difference spectra of the charge transfer bands were recorded at 25°C on a Beckman Acta MIV spectrometer. While single peaked complex band spectra were observed with the dpG-HAQO samples, double peaked complex band spectra were observed with the dpA-HAQO samples. This suggested that the HAQO was "decomposing" in the aqueous medium in the presence of light and/or air. Subsequently, the instability of HAQO in aqueous media, especially when exposed to light, was verified by observation of changes in the absorption spectra of what was initially HAQO. In an effort to limit decomposition each sample of nucleotide and HAQO was made up immediately prior to taking the spectrum. This did not help. Due to the apparent instability of HAQO under the experimental conditions, the results with dpG were discounted and further optical experiments on HAQO-nucleic acid systems were not attempted.

Circular Dichroism Spectral Study

The CD spectra of mixtures of dpG and NQO were examined for the presence of an induced CD band arising from the formation of the dpG:NQO complex. Spectra were recorded at 25°C on a Cary 60 spectrometer. Concentrations of dpG and NQO were similar to those of the absorption study - $[dpG]_T \approx 3.0 - 4.0 \times 10^{-2}$ M and $[NQO]_T \approx 4.0 - 6.0 \times 10^{-4}$ M^{-1}. Samples were made up in the cacodylate buffer described above. Standard 1 cm pathlength CD cells were used. Spectra were recorded from above the region of the complex band to the region of nucleotide absorption (460-310 nm). Spectra of the dpG-NQO mixtures were compared to spectra of NQO of equal concentration alone. Even at the large nucleotide concentrations employed, no evidence of induced CD bands was found. However, the equilibrium constant for dpG:NQO formation, which will be discussed later in this chapter, is rather small, K(25°C) = 16. Thus it is possible that any induced bands were not seen due to insufficient complex being formed. Since the equilibrium constant does not change greatly with temperature changes (also discussed later in this chapter), lowering the temperature will not produce much more complex. Thus attempting to obtain CD spectra at lower temperatures probably would be unsuccessful.

^{13}C NMR Study

Solutions for the ^{13}C NMR studies were prepared in a manner similar to that used for the optical samples. NQO was dissolved in the cacodylate buffer in H_2O and the nucleotides were dissolved in D_2O. Samples were prepared by combining 0.250 ml of the NQO solution ($[NQO]_T$ = ca. 1 mM) with a given amount of nucleotide solution ($[dpN]_T$ ranged from ca. $3x10^{-2}$ to $1.4x10^{-1}$ M) and the total volume was brought up to 0.500 ml with additional D_2O. This gave a buffer concentration of 0.05 M NaCl and 0.005 M sodium cacodylate, pH 7.0. The ^{13}C NMR spectra were obtained at 37°C (ambient temperature on this instrument) on a Nicolet TT-23 system at 25.1 MHz, using quadrature phase detection with 8-mm sample tubes. The ^{13}C NMR spectra were referenced to dioxane (1672.0 Hz). Spectra had spectral width of 5000 Hz with 8K data points, giving a resolution of 1.25 Hz.

^{1}H NMR Study

The ^{1}H NMR samples were prepared by mixing 0.250 ml of the NQO solution (in cacodylate) with nucleotide (in D_2O) and D_2O to a total volume of 0.500 ml. The NQO concentration was ca. $1x10^{-3}$ M and $[dpN]_T$ ranged from $1x10^{-2}$ to $5x10^{-2}$ M. This mixture was lyophilized and 0.500 ml of D_2O used to redissolve it. The ^{1}H NMR spectra were referenced to 3-(trimethyl silyl)-propane sulfonic acid (DSS) (0.00 Hz) and were run at 20°C on the Stanford Magnetic Resonance Laboratory 360 MHz system. Spectral width was 3600 Hz with 16K data points, resolution 0.45 Hz.

RESULTS

Optical Studies

The absorption spectra for the dpN-NQO mixtures were difference spectra obtained by subtracting the NQO absorbances. This allowed for clearer observation of the complex bands which would have otherwise appeared as shoulders on the 365 nm band of the NQO. The complex band maxima and molar absorptivities are tabulated in Table II.

In a mixture of a nucleotide and NQO, the absorbance at the complex band maximum recorded against a solution of NQO of the same initial concentration may be expressed as:

$$A_T = \ell(\varepsilon_c - \varepsilon_{(dpN)} - \varepsilon_{(NQO)})[c] + \ell\varepsilon_{(dpN)}[dpN]_T$$

where A_T, $[NQO]_T$, and ℓ are as defined earlier; ε_c, $\varepsilon_{(NQO)}$, and $\varepsilon_{(dpN)}$ are the molar absorptivities of the complex, NQO, and the nucleotide; $[dpN]_T$ is the total nucleotide concentration; and [c] is the complex concentration. From this absorption expression and the equilibrium equation, a modified version of the Benesi-Hildebrand equation was derived where A_{dpN} is the absorption of the nucleotide at the complex λ_{max}:

$$\frac{\ell[NQO]_T}{A_T - A_{dpN}} = \frac{1}{K(\varepsilon_c - \varepsilon_{(dpN)} - \varepsilon_{(NQO)})} \frac{1}{[dpN]_T} + \frac{1}{\varepsilon_c - \varepsilon_{(dpN)} - \varepsilon_{(NQO)}}$$

This equation was derived with the assumption that $[dpN]_T >> [c]$ so that $[dpN] = ([dpN]_T - [c]) \cong [dpN]_T$, where [dpN]

TABLE II

Equilibrium Constants (K(25°C))

for the Formation of dpN:NQO Complexes

Complex	λ_{max} (nm)	$\varepsilon x10^{-3}$ $(M^{-1}cm^{-1})$	K(25°C)(M^{-1})
dpG:NQO	406	3.3	16 ± 2
dpA:NQO	405	3.8	12 ± 2
dpT:NQO	402.5	4.0	4 ± 3
dpC:NQO	398	4.5	4 ± 3

is the equilibrium concentration. To help maintain this assumption, $[dpN]_T$ was always much larger than $[NQO]_T$. The quantity, A_{dpN}, was calculated using $[dpN]_T$ and $\varepsilon_{(dpN)}$ based on the assumption that the amount of complex was much less than $[dpN]_T$. Since nucleotides do not absorb at $\lambda \simeq 400$ nm, the absorbances (which are linear with [dpN]) observed for the nucleotides at such wavelengths are probably due to the small amounts of impurities which become observable at the high nucleotide concentrations employed. By plotting the term, $\ell[NQO]_T/(A_T-A_{dpN}$ against $1/[dpN]_T$, the equilibrium constants for complex formation were obtained. Figures 2a-d give the plots and least-square fits of the data from the studies at room temperature of the complex absorption bands for the four dpN-NQO complexes. The equilibrium constants of complex formation obtained from these plots are summarized in Table II.

To assay the temperature dependence of the dpG-NQO equilibrium, an optical study of dpG-NQO mixtures was made at 10°C as well as 25°C. The Benesi-Hildebrand type plot is shown in Figure 2e. The equilibrium constant at 10°C was determined to be 23 M^{-1}. From the van't Hoff equation, values of $\Delta H° = -4.2$ kcal mol^{-1} and $\Delta S° = -8.5$ cal $mol^{-1}deg^{-1}$ were calculated. Using these quantities, the equilibrium constants at other temperatures for the dpG-NQO system could be calculated, e.g., $K(20°C) = 18\ M^{-1}$.

Figure 2. (a-e) Benesi Hildebrand type plots of NQO-dpN complex spectral data. Temperatures: (a-d) 25°C; (e) 10°C. Buffer: sodium cacodylate (0.01 M)-NaCl (0.1 M), pH 7.0. Concentrations: $[dpN]_T$, 1.7×10^{-1} to 2×10^{-2} M; $[NQO]_T$, 6×10^{-4} to 2×10^{-4} M.

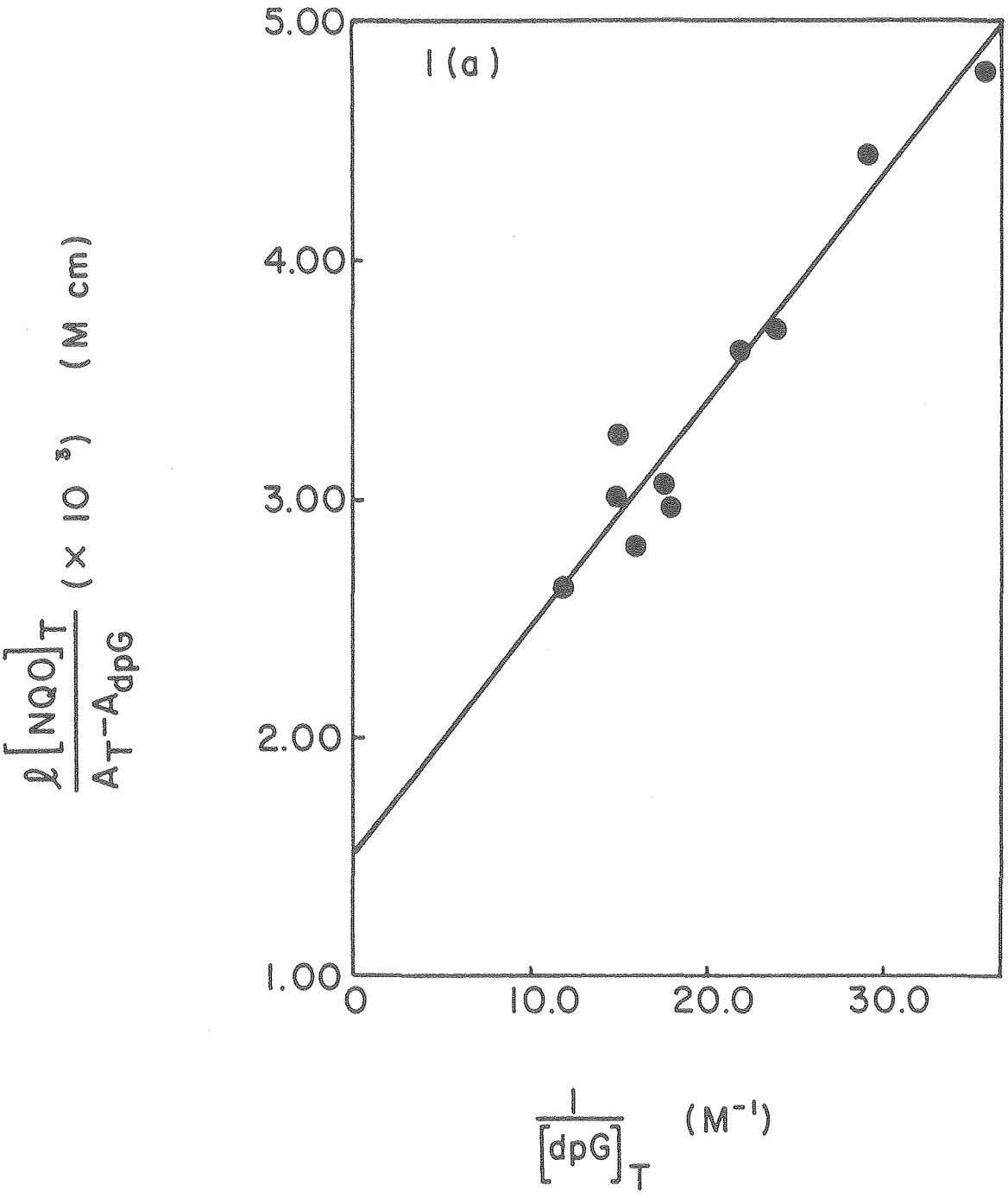
1(a)
5.00
4.00
3.00
2.00
1.00
0
10.0
20.0
30.0
$\frac{\ell[NQO]_T}{A_T - A_{dpG}}$ (x 10^3) (M cm)
$\frac{1}{[dpG]_T}$ (M^{-1})

XBL 778-2987

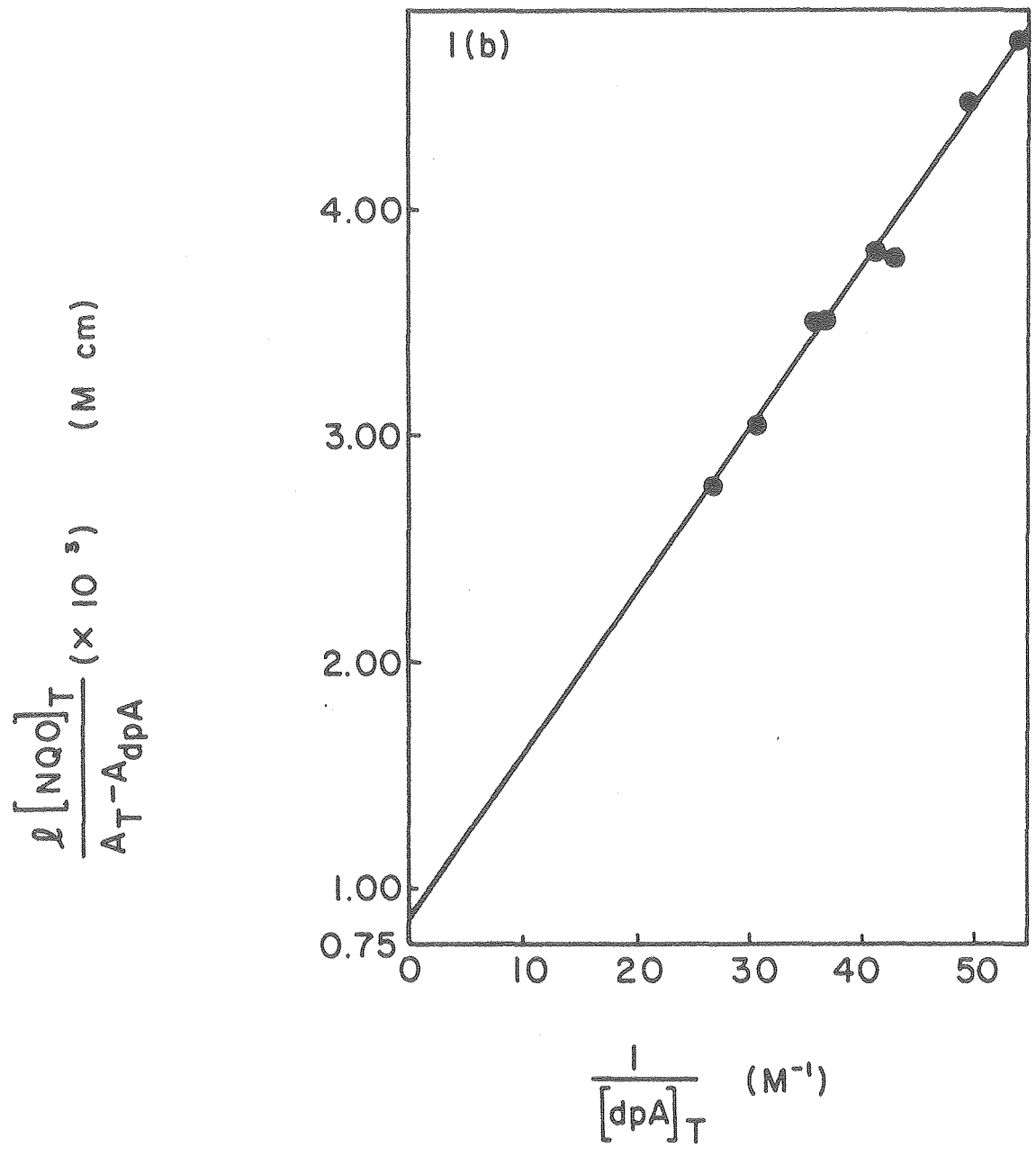
I(b)
4.00
3.00
2.00
1.00
0.75
0
10
20
30
40
50
$\frac{l[NQO]_T}{A_T - A_{dpA}}$ (x 10^3) (M cm)
$\frac{1}{[dpA]_T}$ (M^{-1})

XBL 778-2986

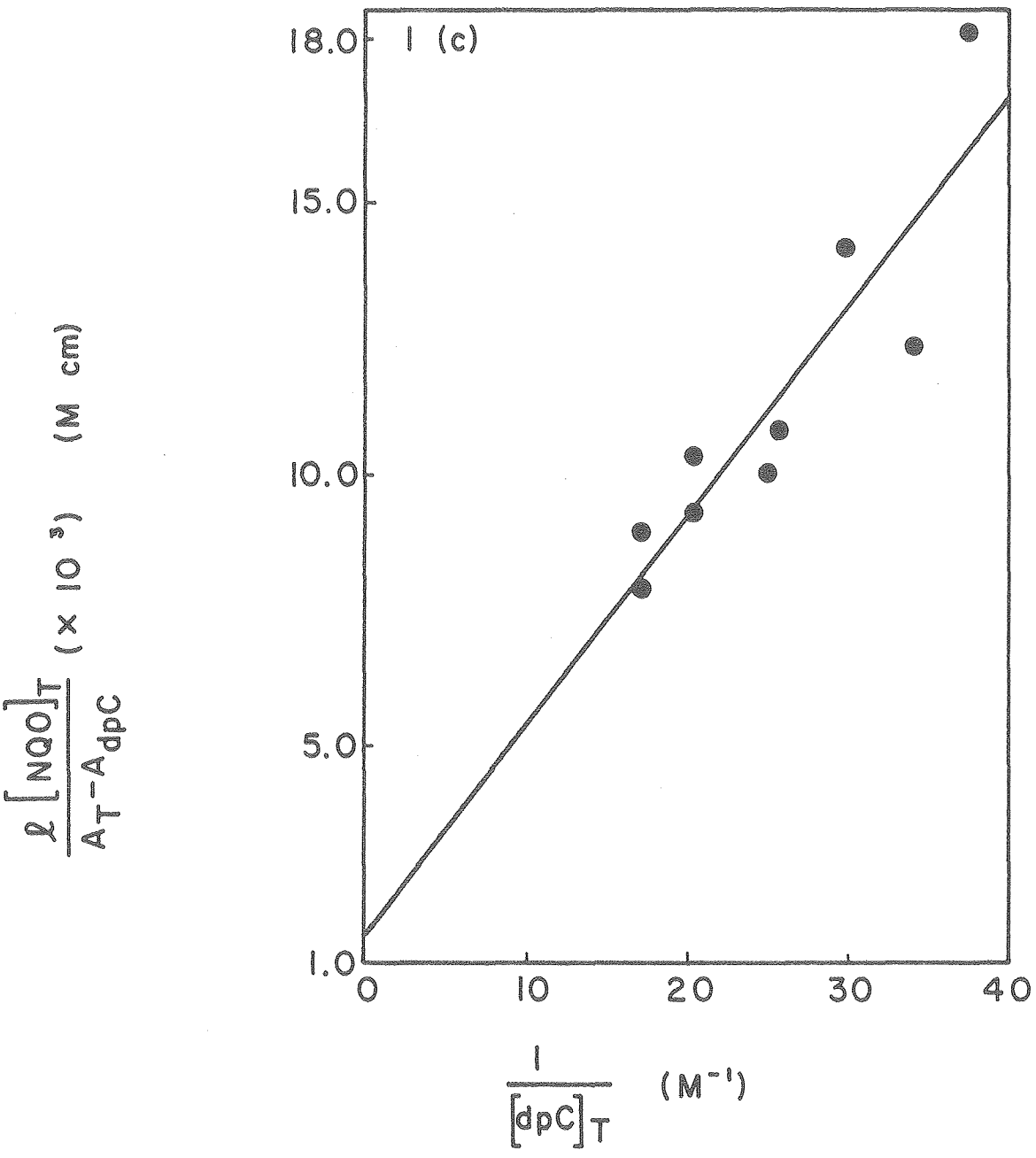
18.0
15.0
10.0
5.0
1.0
0
10
20
30
40
1 (c)
$\frac{\ell [NQO]_T}{A_T - A_{dpC}}$ (x 10^3) (M cm)
$\frac{1}{[dpC]_T}$ (M^{-1})

XBL 778-2983

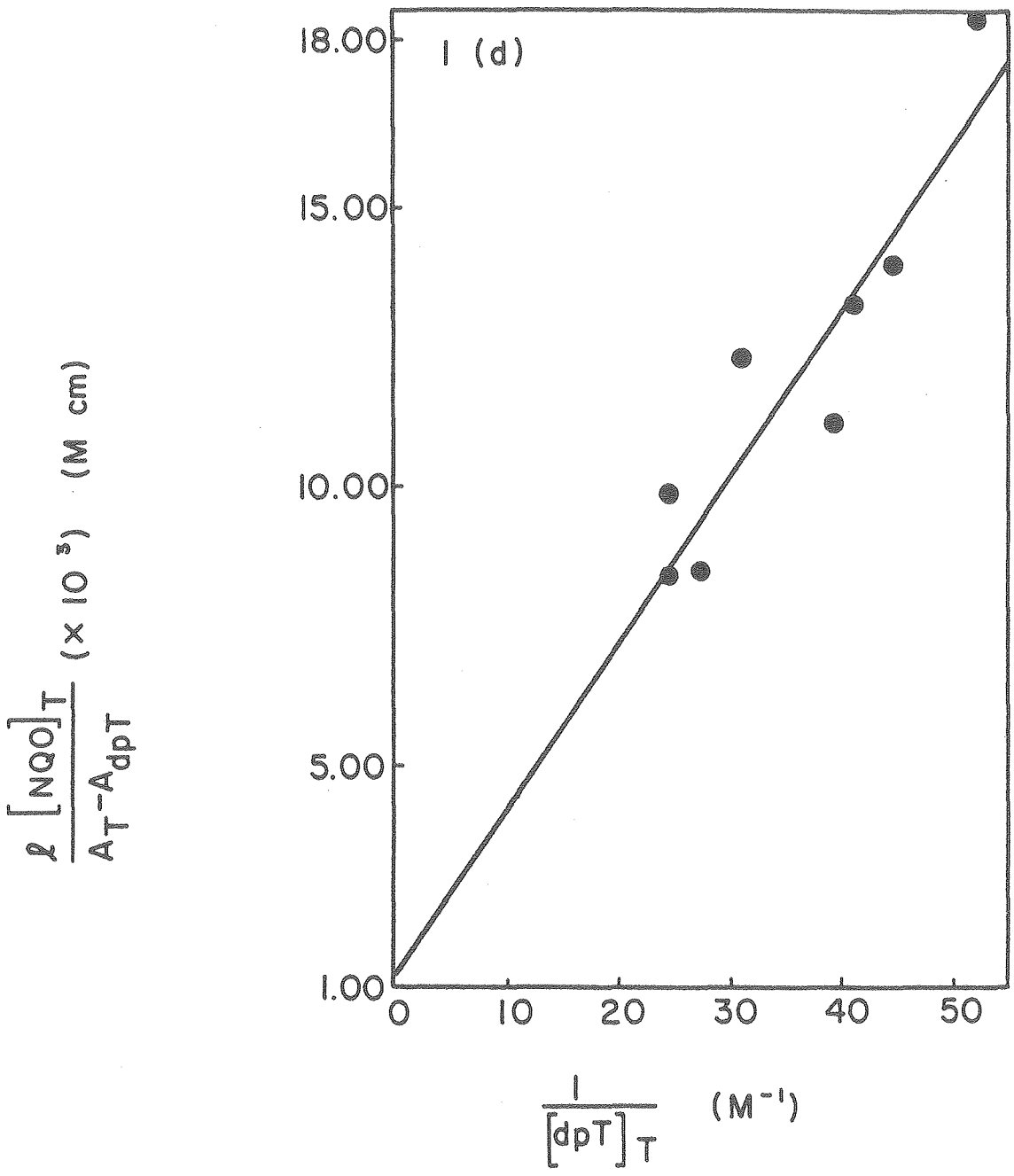
18.00
15.00
10.00
5.00
1.00
l (d)
0
10
20
30
40
50
$\frac{l}{[dpT]_T}$ (M^{-1})
$\frac{l\,[NQO]_T}{A_T - A_{dpT}}$ (x 10^{3}) (M cm)

XBL 778-2985

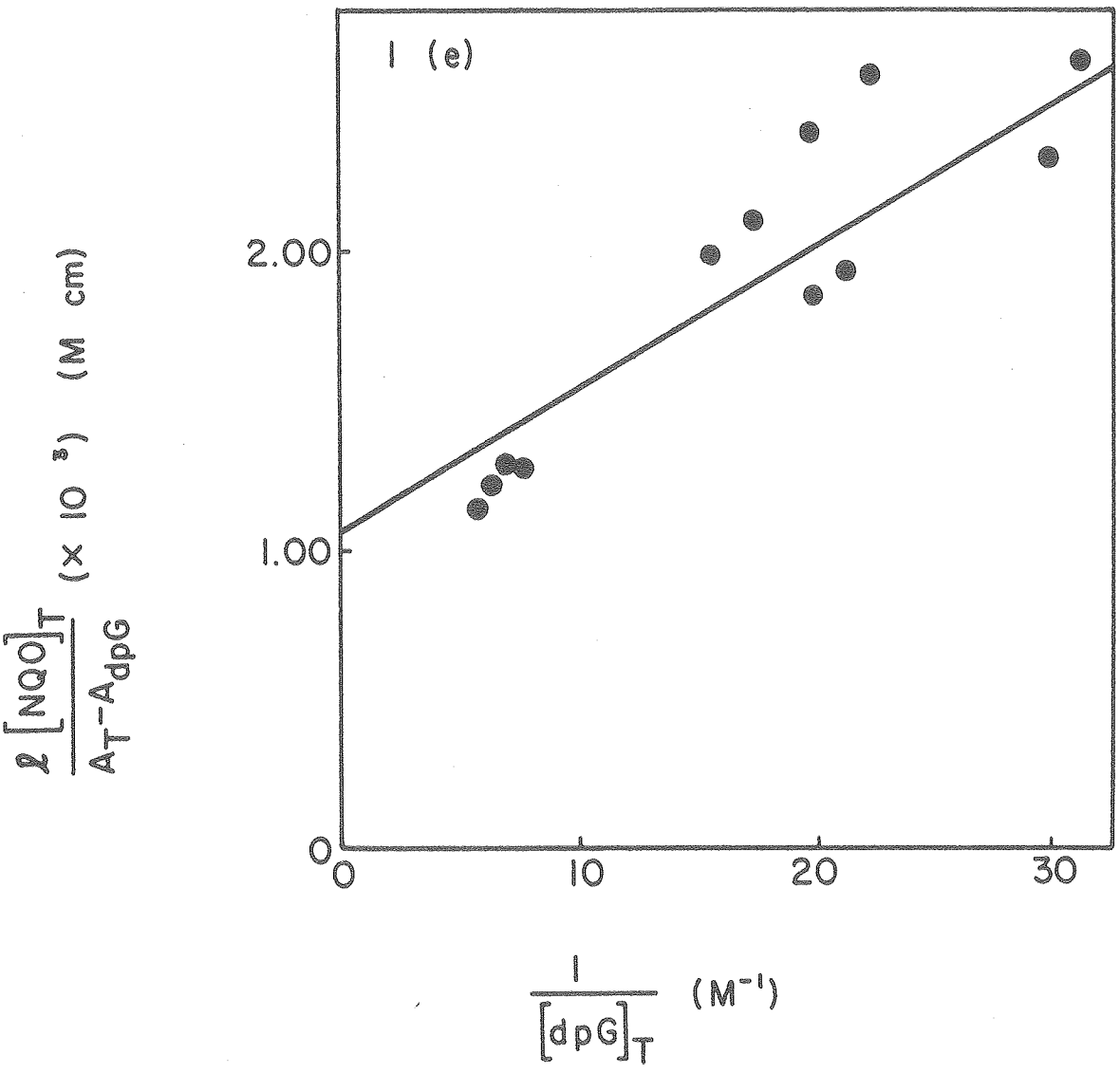

XBL 778-2982

NMR Studies

Because of the low solubility of NQO in aqueous media (ca. 2-3 mM), the ^{13}C NMR spectrum of NQO could not be obtained in a reasonable period of time with the present equipment. Thus, the ^{13}C NMR spectra of dpN-NQO mixtures gave only the spectra of the nucleotide. The observed chemical shifts were the weight averages of the free and bound chemical shifts of the nucleotide carbons.

In Figure 3, the differences between δ_{obsd} for dpG base carbons in the dpG-NQO mixtures and δ_{free} for those carbons (at the same dpG concentrations as in each mixture) are plotted vs. the dpG/NQO ratio. Carbon 8 of the base shows a large downfield shift (to lower field strength) with a decreasing of dpG/NQO ratio (and hence, increasing fraction of bound dpG). The maximum amount of dpG in the complex in these mixtures was approximately 1%. For a sample with 1% of the dpG complexed, a shift change for C-8 of ca. 0.4 ppm is observed. Carbon 6, the carbonyl carbon, shows a lesser, but still fairly large downfield shift. The other observable base carbons (all except C-4) show much smaller downfield shift changes. The only sugar carbon of dpG to show any shift change was C-2' which shifted upfield.

Carbons C-2, C-8, C-4, and C-6 are the only readily observable base carbons of dpA. The relaxation time (T_1) of C-5 and the broadening of this carbon's signal due to complexation inhibit its observation. The chemical shift changes

for the dpA carbons observed in a concentration range similar to that of the dpG-NQO systems are all small downfield shifts. None of the carbons give large shift changes as were observed with C-8 and to a lesser extent C-6 of dpG.

The ^{13}C NMR spectra of dpT-NQO mixtures were measured. No apparent changes due to complexation in any of the dpT carbon chemical shifts were observed.

The chemical shifts of the protons of NQO when complexed with dpG or dpA were calculated from the following relation, where δ_B, δ_{obsd}, δ_{free} are the chemical shifts of a proton in the bound state, in the NQO-dpN mixture and free NQO solution, respectively:

$$\delta_B = \{\delta_{obsd} - \delta_{free}\left(\frac{[NQO]_T - [c]}{[NQO]_T}\right)\} \frac{[NQO]_T}{[c]}$$

The δ_B and the difference between δ_B and δ_{free} for the NQO protons were calculated using the δ_{obsd} from the ^1H NMR spectra of dpN-NQO mixtures. For the dpG-NQO mixtures the equilibrium constant at 20°C (the temperature of the ^1H spectra) was calculated to be 18 M^{-1} from the optical measurements at 10 and 25°C. Having this equilibrium constant enabled us to calculate the complex concentrations for the dpG-NQO mixtures and thus δ_B. For the dpA-NQO mixtues, the [c] at 20°C were estimated using the equilibrium constant at 25°C. The values of δ_B were then calculated using these [c]'s.

Figure 3. ^{13}C NMR chemical shift data for dpG/NQO mixtures. All shifts are downfield. Temperature:37°C. Solvent: sodium cacodylate (0.005 M)-NaCl (0.05 M)-D_2O:H_2O (1:1), pH 7.0. Concentrations: $[dpN]_T$, $3x10^{-2}$ to $1.4x10^{-1}$ M; $[NQO]_T$, ca. 1 mM. With 5000 Hz spectral width, 8K data points. [C-8(●-●); C-6(o-o); C-5(△-△); C-2(□-□)].

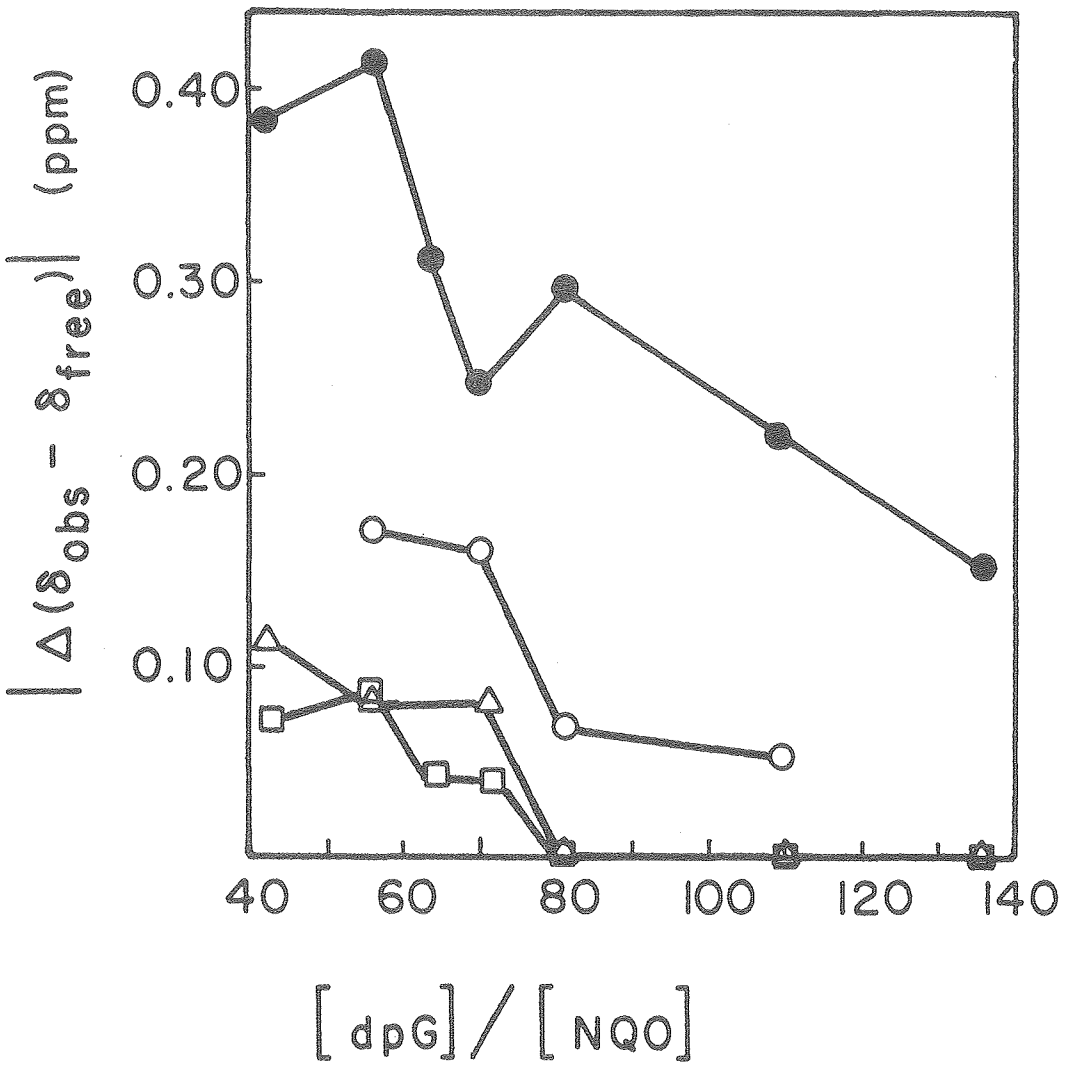

XBL 778-2988

In Table III, the calculated δ_B and $|(\delta_B - \delta_{free})|$ for the NQO protons are presented for dpG-NQO and dpA-NQO mixtures. For NQO complexed with both dpG and dpA, H-6 and H-9 show the largest changes in chemical shift. For NQO in the dpG-NQO mixtures, H-2 and H-3 are the next largest. However, for NQO in dpA-NQO solutions, H-7 and H-8 show the next largest changes after H-6 and H-9. All shifts are upfield, to higher field strength.

TABLE III

Effects of Nucleotide Complex Formation

at 20°C upon NQO Protons

NQO proton	δ_{free} (ppm)	dpG:NQO δ_B (ppm)	dpG:NQO $\lvert\delta_B-\delta_{free}\rvert$ (ppm)	dpA:NQO δ_B (ppm)	dpA:NQO $\lvert\delta_B-\delta_{free}\rvert$ (ppm)
2	8.837	8.728	0.11	8.534	0.30
6	8.730	8.546	0.18	8.146	0.58
9	8.678	8.504	0.17	8.106	0.57
3	8.373	8.310	0.06	8.101	0.27
7	8.084	~ 8.084	~0.00	7.704	0.38
8	8.029	~ 8.029	~0.00	7.611	0.42

DISCUSSION

Optical Studies of the Charge Transfer Bands

The complexes of the four deoxynucleotides with NQO have similar molar absorptivities and the λ_{max} for the four are likewise at about the same wavelength (of about equal energy). The molar absorptivities were obtained from the Benesi-Hildebrand plots. The form of the Benesi-Hildebrand equation used differed from that of Okano through the inclusion of terms for changes in nucleotide and NQO concentration due to complex formation. The ε_c given in Table II differ from those obtained by Okano, although the reciprocals of our intercepts $1/(\varepsilon_c-\varepsilon_{(dpN)}-\varepsilon_{(NQO)})$ are similar to Okano's values of ε_c.

That the data for all four mononucleotides gave linear Benesi-Hildebrand type plots indicates that the four mononucleotides form 1:1 complexes with NQO. The preference of NQO for the purine nucleotides is indicated by the larger magnitude of the equilibrium constants for the purines vs. the pyrimidine systems as found earlier by Okano for the nucleosides. The equilibrium constants for the nucleotide systems are also similar to those obtained by Okano for the nucleosides. For example, the equilibrium constant for the dpG-NQO system is 16 M^{-1} vs. 12.2 M^{-1} for the dG-NQO system. This suggests that the addition (in the 5' position) of a phosphate group to the deoxyribose does not alter to any large extent the binding of NQO to the base portion of the nucleotide.

NMR Studies of the dpG-NQO Mixtures and dpG:NQO Complex Structure

As is shown in figure 3, all dpG base carbon chemical shifts move downfield in the presence of NQO. The proton chemical shift changes for the NQO protons are upfield. This results from the ring current effect of the dpG base on the NQO protons when NQO is stacked with the dpG base. The downfield directions of the dpG ^{13}C shift differences could be explained in terms of the charge transfer interaction. According to current ^{13}C chemical shift theories (Karplus and Pople, 1963; Cheney and Grant, 1967) the paramagnetic shielding term which generally dominates ^{13}C shielding parameters is the most sensitive to changes in the ^{13}C electronic environment. Accordingly, the downfield shifts for the dpG carbons could be explained as being due to the combined effects of a decreased electron density (variable with position in the molecule) and the additional electronic transition (constant for the molecule) (Hanna & Ashbaugh, 1964). The large ^{13}C shift difference of C-8 relative to the other base carbons is consistent with a model in which the imidazole ring of the base is stacked with the electron-withdrawing portion of the NQO, i.e., the nitro and N-oxide containing ring. The shift change for C-6 (though somewhat smaller) implies that the carbonyl group could be involved sith the NO_2, NO ring, as well.

As stated, the shift changes for tne NQO protons are all upfield as would be expected if the ring current of the complexed dpG base dominates the complex effects. However, the shifts are much smaller than those observed for interactions in which aromatic molecules stack without charge transfer, e.g., nucleic acid base stacking (Schweizer et al., 1968) and ethidium bromide-nucleic acid interactions (Che-Hung Lee, personal communication). Hanna & Ashbaugh (1964) observed such a negation of the ring current effect for various charge transfer systems. It was attributed to the addition of a charge transfer excitation energy term to the paramagnetic shift term. The amount of electron transfer is too small to alter to any major degree the magnitude or shape of the ring current. If the assumption is made that the center of the ring current is essentially where Giessner-Prettre & Pullman (1970, 1976) place it, i.e., in the imidazole ring beside the center of the C-4-C-5 bond, the shifts in Table III may be used to help orient the molecules in the complex.

Protons H-6 and H-9 of the NQO show the largest shift and are placed near the C-4-C-5 bond of the base. The ^{13}C NMR data suggest that the nitro and oxide containing ring is stacked with the imidazole base ring so H-2 and H-3 must be placed over that ring and H-7 and H-8 over the other. Additionally, the proton shift changes rule out the placement of the benzene-like ring of NQO with the imidazole ring. After the manipulation of models to arrive at the best fit of proton chemical shift changes, the orientation in Figure 4

Figure 4. Proposed structure of dpG/NQO complex. NQO(●-●) is in a plane parallel to guanine (o-o) and about 3.4 Å above it.

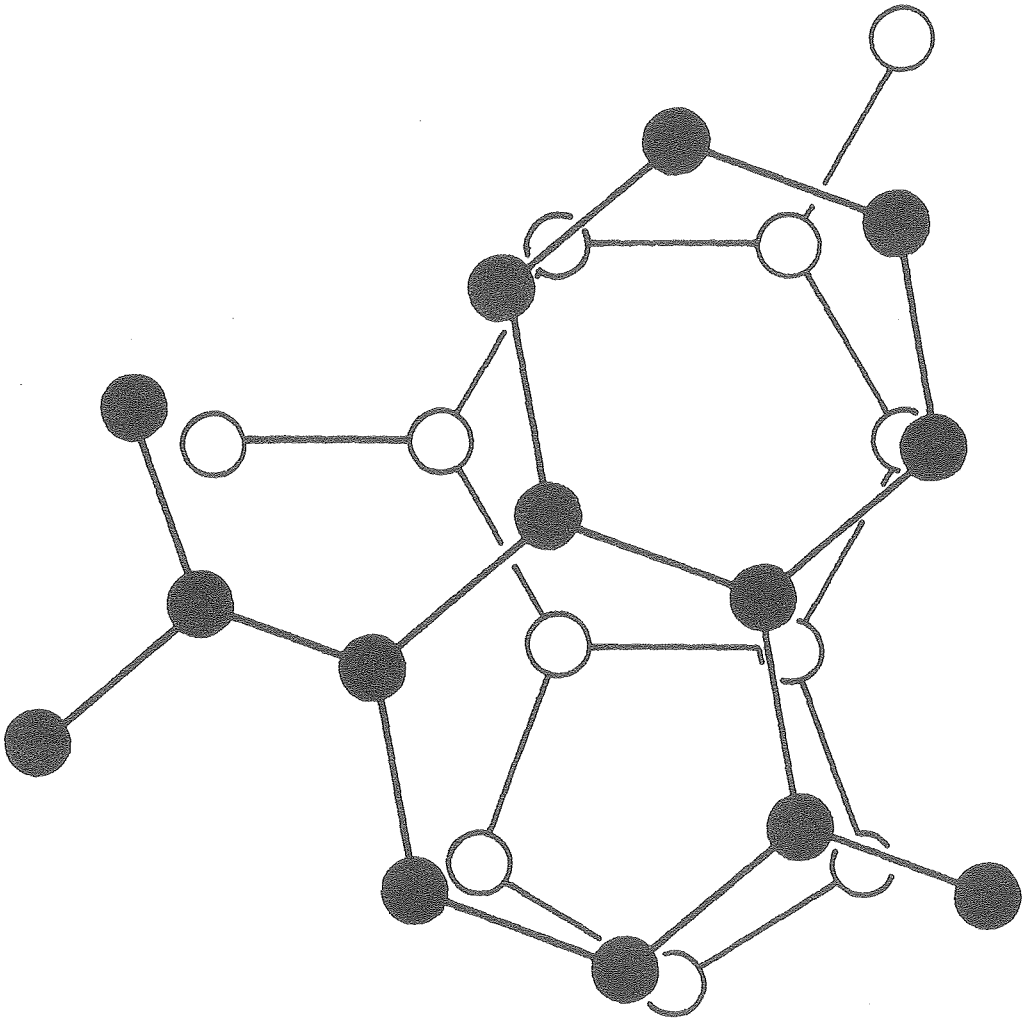

XBL 778-2984

was determined for the dpG:NQO complex. The structure places the positive center of the oxide region of NQO near the electron-rich N-9 of dpG and the electron-attracting region of the NQO nitro group near the carbonyl of dpG. Both areas on dpG contain carbons (C-8 and C-6) showing the largest ^{13}C NMR shift changes.

NMR Studies of the dpA-NQO Mixtures

In the ^{13}C NMR spectra of the dpA in dpA-NQO mixtures, no carbons on the dpA base show the large downfield shift of C-8 of dpG. Indeed, no dpA carbons show different enough chemical shift changes which might distinguish the position in the complex of one region of the dpA base relative to another. This lack of distinguishability and the small size of all the shifts could imply that no single isolated retion of the dpA, such as the imidazole ring and C-8, is near the center of electron withdrawal. The equilibrium constant for dpA:NQO formation is not sufficiently smaller than that of dpG:NQO formation to account for the smaller values of $|(\delta_{obsd}-\delta_{free})|$ in the dpA-NQO mixtures.

The proton chemical shift differences for NQO protons in dpA-NQO mixtures, presented in Table III, are larger than those for dpG-NQO mixtures. This is expected since the ring current of dpA is larger than that of dpG. Whereas for dpG:NQO, the chemical shifts of NQO H-7 and H-8 are apparently unchanged by complexation, for dpA-NQO these protons show the

next largest $|(\delta_{obsd}-\delta_{free})|$ after H-6 and H-9. As in dpG:NQO, the shift changes of H-6 and H-9 for dpA:NQO are the greatest, suggesting that these protons are the closest to the ring current center of dpA. Protons H-2 and H-3 have the smallest shifts and therefore are the farthest from the ring current center.

The lack of a large shift difference for the imidazole ring C-8 implies that the electron-withdrawing ring of NQO is not placed solely over this ring. If this is the case, then the possible orientation of dpA:NQO which gives the best fit to the Giessner-Prettre &Pullman (1976) ring current model of dpA is roughly the reverse of that of dpG:NQO. The benzene-like ring of NQO is over the imidazole ring and the nitro and oxide ring is over the pyrimidine ring. Without the detailed ^{13}C NMR information obtainable for dpG-NQO mixtures, arriving at a more precise picture is difficult.

NMR Studies with dpT

As was stated earlier, no ^{13}C chemical shift changes were observed for mixtures of dpT and NQO. This is probably due to the small equilibrium constant for complex formation. For this reason ^{1}H NMR studies with dpT and ^{1}H and ^{13}C NMR studies with dpC were not attempted.

CONCLUSIONS

Using Benesi-Hildebrand type plots, the equilibrium constants for the formation of 1:1 complexes of dpG, dpA, dpT, and dpC and NQO were obtained. These equilibrium constants, which are similar in value to those obtained for the deoxynucleosides, indicate the preference of NQO for the guanine residues of DNA, a conclusion which the deoxynucleoside studies also suggested. From ^{13}C and ^{1}H NMR studies, an orientation for the dpG:NQO complex was obtained and insight into the dpA:NQO complex orientation was gained.

These studies indicate that the use of NMR and optical methods for studying complexing of NQO with dinucleotides is feasible. Such a study is presented in Chapter III.

CHAPTER III

DEOXYDINUCLEOTIDE-NQO INTERACTIONS

INTRODUCTION

In the previous chapter, the 1:1 complexes of 5'-deoxynucleotides and NQO were discussed. In this chapter, the complexes formed by NQO and deoxydinucleotides will be discussed. While studies with mononucleotides may provide information such as base specificity, it is desirous to examine systems which are more DNA-like. Dinucleotides have the potential of providing DNA-like characteristics. DNA-like minihelices can be formed by self-complementary dimers or appropriate pairs of dimers. At the same time, dinucleotides offer a system which is simple enough that relatively detailed information about complex structures may be obtained.

The methods used in the dinucleotide study are similar to those discussed for mononucleotide complexes in Chapter II. The complex band spectra were analyzed with various Benesi-Hildebrand type equations to obtain equilibrium constants and complex stoichiometries for both self-complementary and non-selfcomplementary dinucleotides. Through ^{1}H and ^{13}C NMR studies, possible geometries for the 2:1 complexes of the self-complementary deoxydinucleotides and NQO were obtained.

EXPERIMENTAL

Materials

The deoxydinucleotides, dpCpG, dpGpC, dpTpA, dpApT, dpTpG, dpCpA, were obtained from Collaborative Research. The NQO was synthesized as described in Chapter II.

Absorption Spectroscopy Studies

Optical studies were done in a buffer consisting of 0.1 M NaCl, 0.01 M sodium cacodylate, 0.2 mM EDTA, pH 7.0. Concentrations of the deoxydinucleotide and NQO solutions were measured using the absorbance at λ_{max}. A molar absorptivity for NQO of $\varepsilon_{250} = 1.65 \times 10^{4}$ $M^{-1}cm^{-1}$ was used (Okano, 1973). For the deoxydinucleotides, the values of ε_{max} for the dinucleoside phosphates were used (P.L. Biochemicals Reference and Price Guide 104). Glass tuberculin syringes were used for the measurement of nucleotide and NQO solution volumes. Samples for the optical studies were prepared by placing a fixed volume of stock NQO solution in each sample tube ([NQO] ranged from 3.3×10^{-4} to 6.7×10^{-4} M), adding a given volume of the stock nucleotide solution ([dpN_1pN_2] ranged from 2.3×10^{-3} to 1.8×10^{-2} M), and then adding sufficient cacodylate buffer to produce a constant volume. The mixed deoxydinucleotide solutions had approximately equal concentrations of the two dinucleotides. Absorption spectra in the region of the complex band (460-380 nm) were recorded for each deoxydinucleotide-NQO

mixture vs. a solution of equal NQO concentration to produce difference spectra. Absorption spectra were recorded at 25°C on a Cary 118 spectrometer. Either 1.0 cm or 0.20 cm pathlength cells were used. The $\varepsilon_{(dpN_1pN_2)}$ values at the wavelength of the complex were obtained by measuring the absorption at this wavelength of nucleotide solutions in concentrations similar to those for the dpN_1pN_2-NQO mixtures. These ε are presented in Table IV.

An attempt was made to obtain the stoichiometries of the dpGpC-NQO and dpCpG complexes using Job plots. Samples of dpGpC plus NQO or dpCpG plus NQO were made up in the cacodylate buffer with concentrations in the optical range. That is, the concentrations of the dimers and NQO ranged from zero to ca. 5×10^{-5} M. Samples were prepared such that the total number of moles remained constant while the mole fractions of dimer to NQO varied. Absorption spectra were recorded at 25°C in 1 cm pathlength cells on the Cary 118 UV spectrometer from 350 - 230 nm for dpGpC/NQO and 450 - 230 nm for dpCpG/NQO. The spectral range for dpGpC/NQO covered from below the shorter wavelength UV bands of NQO and dpGpC to the long wavelength band of NQO. The dpGpC/NQO range covered through the region of the complex band. An isosbestic point was observed at 293 nm for both systems. Plots of the absorbance at a given wavelength vs. mole fraction of either dimer or NQO were made for data at several

TABLE IV

The Molar Absorptivities ($\varepsilon_{dpN_1pN_2}$) at 400 nm of the Deoxydinucleotides in Cacodylate Buffer, pH 7.0, at 25°C.

Dimer	ε ($\times 10^{-1}$) ($\ell\ m^{-1}cm^{-1}$)
dpTpG	0.575
dpCpA	0.606
dpGpC	1.97
dpTpA	0.909
dpApT	1.22
dpCpG	3.21

wavelengths. Such plots should show a deflection at a mole fraction which reflects the complex stoichiometry. For example, a 1:1 complex would have a minimum (or maximum) in the plots at mole fraction equal to 0.5. Small deflections were noted on the plots for dpCpG/NQO and dpGpC/NQO, and these did correspond to 2:1 dimer:NQO complexes. However, the changes in slope were so small that the data was deemed inconclusive. Even the plot using the absorbances in the region of the complex band (ca. 400 nm) for the dpCpG/NQO system gave only a small change in slope in the plot.

Circular Dichroism Study

An attempt was made to observe an induced CD band resulting from the formation of the dpGpC-NQO complex. Spectra were recorded on a Cary 60 in the region (460-310 nm) of the charge transfer absorption band. Sample concentrations were similar to those used in the UV absorption study of the complex band - $[dpGpC]_T$ = 1.9 - 3.8 x 10^{-3} M and $[NQO]_T$ = 2.4 x 10^{-4} M. Samples, prepared in the cacodylate buffer were run at 25°C in low volume 0.5 cm pathlength cells. The dpGpC-NQO spectra were compared to a spectrum of NQO alone (of equal concentration). No induced CD bands were observed. It may be that the induced bands are weak and there was insufficient complex present for observation. Using the equilibrium constant determined for the dpGpC-NQO complex formation (9 x 10^3, to be discussed later), roughly 3 to 12% of the NQO in the sample was in the complex.

Changes in the CD bands (310-220 nm) of dpCpG resulting from the addition of NQO were looked for. Spectra were recorded at 25°C on the Cary 60. The samples were made up in cacodylate buffer with $[dpCpG]_T \approx 4 \times 10^{-5}$ M and $[NQO]_T \approx 1 \times 10^{-6}$ M. No significant changes in the dpCpG CD bands were observed.

Attempted Fluorescence Spectroscopy Study

An attempt was made to obtain the fluorescence spectrum of NQO. The effect (quenching or enhancement) on the NQO fluorescence band intensity when various amounts of dinucleotide were added could be observed and the data analyzed by an equation similar to the Benesi-Hildebrand absorption equations. Unfortunately, NQO undergoes various photochemically catalyzed reactions when excited at 360 nm in the fluoremeter. The NQO samples ($[NQO]_T \approx 3 \times 10^{-6}$ M) were prepared in the cacodylate buffer. Standard 1 cm pathlength fluorescence cells were used. Fluorescence spectra were taken at 25°C on a Perkin Elmer-Hitachi MPF 2A spectrofluoremeter. The excitation wavelength was 360 nm as suggested by Tada, et al. (1967). Spectra were recorded from 380 to 510 nm. The supposed NQO fluorescence band at ca. 475 nm increased in intensity proportionally with the time left in the fluoremeter beam and did not diminish after removal from the fluoremeter. The photoreactions probably occurring will be discussed in Chapter IV. The reported NQO fluorescence band (Tada, et al., 1967) is probably due to one (or more) photoproducts.

^{13}C NMR Studies

For the ^{13}C NMR studies, the initial sample used consisted of about 25 ml of a dinucleotide solution (concentration approximately 4×10^{-3} M) in the pH 7 cacodylate buffer made up in 25-30% D_2O. After obtaining ^{13}C NMR spectra of the pure dinucleotide samples, approximately 25 ml of an NQO solution in D_2O were added to each sample. The resulting solution was concentrated using a rotary evaporator to the volume of the original dinucleotide solutions making [NQO] about 2×10^{-3} M. Successive samples were made by adding a small volume, usually 0.250 ml, of a concentrated dinucleotide stock solution in the cacodylate buffer to the dinucleotide-NQO solution. Thus, $[dpN_1pN_2]$ ranged from about 4×10^{-3} to 6×10^{-3} M. The ^{13}C NMR spectra were obtained in a 25 nm probe at 45.3 MHz using a Bruker 180 MHz magnet and Nicolet 1180 computer system. Samples were measured at 35°C using a 60° pulse with a 10s delay, with broad band proton decoupling, and with quadrature phase detection. About 8,000-10,000 transients were collected for each sample. Samples were referenced to DSS (0.000 ppm). The spectral width was 9000 Hz with 16 K data points to obtain 1 Hz resolution.

^{1}H NMR Study

The ^{1}H NMR samples were prepared in a manner similar to that used for the optical studies. The appropriate amounts of dinucleotide solution in cacodylate buffer, NQO solution

in cacodylate buffer, and cacodylate buffer were combined. The resulting mixture was lyopholized and reconstituted with D_2O. Total sample volume was 0.500 ml, [dpN_1pN_2] ranged from 1.2×10^{-2} to 2×10^{-3} M and [NQO] was about 2×10^{-3} M. The ^1H NMR spectra were measured at 180.09 MHz using the Bruker 180 MHz magnet and Nicolet 1180 computer system. Measurements were made at 25°C and referenced to DSS (0.000 ppm). The spectral width was 1800 Hz with 16 K data points to obtain 0.2 Hz resolution.

RESULTS

The absorption spectra for the dinucleotide-NQO mixtures were difference spectra obtained by subtracting the NQO absorbances. All dinucleotide-NQO complex spectra displayed broad bands with maxima in the region 395-405 nm. The broad nature of the complex bands made it difficult to discern the exact complex λ_{max}. Hence, the absorbance at 400 nm of the dinucleotide-NQO samples was used for the optical studies.

In the case of a dinucleotide and NQO forming a 1:1 complex, the complex band absorption data should fit the equation developed for the mononucleotide-NQO mixtures:

$$\frac{\ell[NQO]_T}{A_T - A_{dpN_1pN_2}} = \frac{1}{K(\varepsilon_c - \varepsilon_{(dpN_1pN_2)} - \varepsilon_{(NQO)})} \frac{1}{[dpN_1pN_2]_T} + \frac{1}{\varepsilon_c - \varepsilon_{(dpN_1pN_2)} - \varepsilon_{(NQO)}}$$

where $[NQO]_T$ and $[dpN_1pN_2]_T$ are the total NQO and dinucleotide concentrations; A_T and $A_{dpN_1pN_2}$ are the total absorbance of the sample at a given λ; ε_c, $\varepsilon_{(dpN_1pN_2)}$, $\varepsilon_{(NQO)}$ are the molar absorptivities of the complex, dinucleotide and NQO at the λ used; ℓ is the cell pathlength and K is the equilibrium constant. For the case of a 2:1 dinucleotide-NQO complex, a similar equation may be derived:

$$\frac{\ell[NQO]_T}{A_T - A_{dpN_1pN_2}} = \frac{1}{K(\varepsilon_c - 2\varepsilon_{(dpN_1pN_2)} - \varepsilon_{(NQO)})} \frac{1}{[dpN_1pN_2]_T^2}$$

$$+ \frac{1}{\varepsilon_c - 2\varepsilon_{(dpN_1pN_2)} - \varepsilon_{(NQO)}}$$

Such a 2:1 complex might be observed for a selfcomplementary dinucleotide-NQO mixture. With a mixture of two different dinucleotides and NQO, a 1:1:1 complex is possible with the data fitting the equation:

$$\frac{\ell[NQO]_T}{A_T - A_{dpN_1pN_2} - A_{dpN_3pN_4}} = \frac{1}{K(\varepsilon_c - \varepsilon_{dpN_1pN_2} - \varepsilon_{dpN_3pN_4} - \varepsilon_{NQO})}$$

$$\times \frac{1}{[dpN_1pN_2]_T[dpN_3pN_4]_T}$$

$$+ \frac{1}{\varepsilon_c - \varepsilon_{dpN_1pN_2} - \varepsilon_{dpN_3pN_4} - \varepsilon_{NQO}}$$

To maintain the assumption, implied in the above derivations, that $[dpN_1pN_2]_T >> [c]$ where [c] is the complex concentration, $[dpN_1pN_t]_T$ was always much larger than $[NQO]_T$. The quantity, $A_{dpN_1pN_2}$ was calculated using $[dpN_1pN_2]_T$ and the experimentally determined $\varepsilon_{dpN_1pN_2}$ (at 400 nm). The values of $\varepsilon_{dpN_1pN_2}$ at 400 nm ranged from 32.1 $M^{-1}cm^{-1}$ for dpCpG to 5.8 $M^{-1}cm^{-1}$ for dpTpG. These small absorbances (which are linear with $[dpN_1pN_2]$) are probably due to small amounts of impurities which become observable at the high nucleotide concentrations employed.

The plots of the absorption data for the different dinucleotide-NQO mixtures fitted to the equation giving best agreement are shown in Figures (5 a-d). Data for two nonselfcomplementary dinucleotides, dpTpG and dpCpA, with NQO fit the 1:1 equation (Figure 5a). With the selfcomplementary dimers, dpCpG, dpGpC, dpTpA, dpApT, the best fits were to the 2:1 equation (Figure 5d). The equilibrium constants for the seven complexes obtained from these plots are presented in Table V. The molar absorptivities at 400 nm for the seven complexes, obtained from the same plots, are very similar. Those for the four 2:1 and the one 1:1:1 complex equal 4100 ± 100 $M^{-1}cm^{-1}$, while the ε_c for the two 1:1 complexes equals 4700 ± 100 $M^{-1}cm^{-1}$.

Figure 5: Benesi-Hildebrand-type plots of NQO-dinucleotide complex spectral data.

(a) dpCpA (o-o), dpTpG (●-●);

(b) dpCpG (o-o), dpGpC (●-●);

(c) dpTpA (o-o), dpApT (●-●);

(d) dpCpA + dpTpG.

Temperature: 25°C. Buffer: sodium cacodylate (0.01 M)-NaCl (0.1 M)-EDTA (0.2 mM), pH 7.0. Concentrations: $[NQO]_T$ 3.3×10^{-4} to 6.7×10^{-4} M, $[dpN_1pN_2]_T$ 2.3×10^{-3} to 1.8×10^{-2} M.

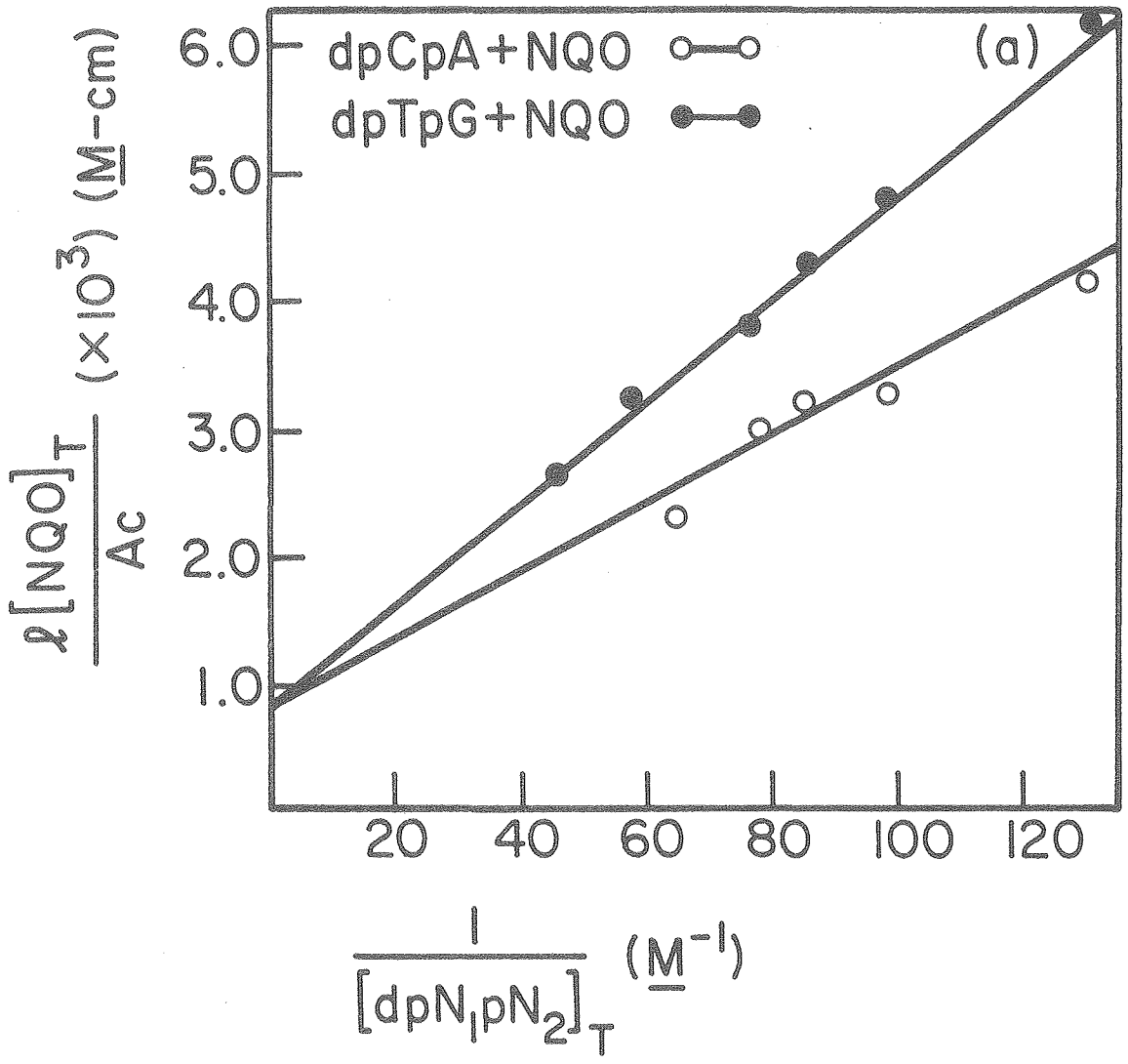
dpCpA+NQO
dpTpG+NQO
(a)
6.0
5.0
4.0
3.0
2.0
1.0
20
40
60
80
100
120
$\frac{\ell[NQO]_T}{Ac}$ (x10^3) (M-cm)
$\frac{1}{[dpN_1pN_2]_T}$ (M^{-1})

XBL 792-8562

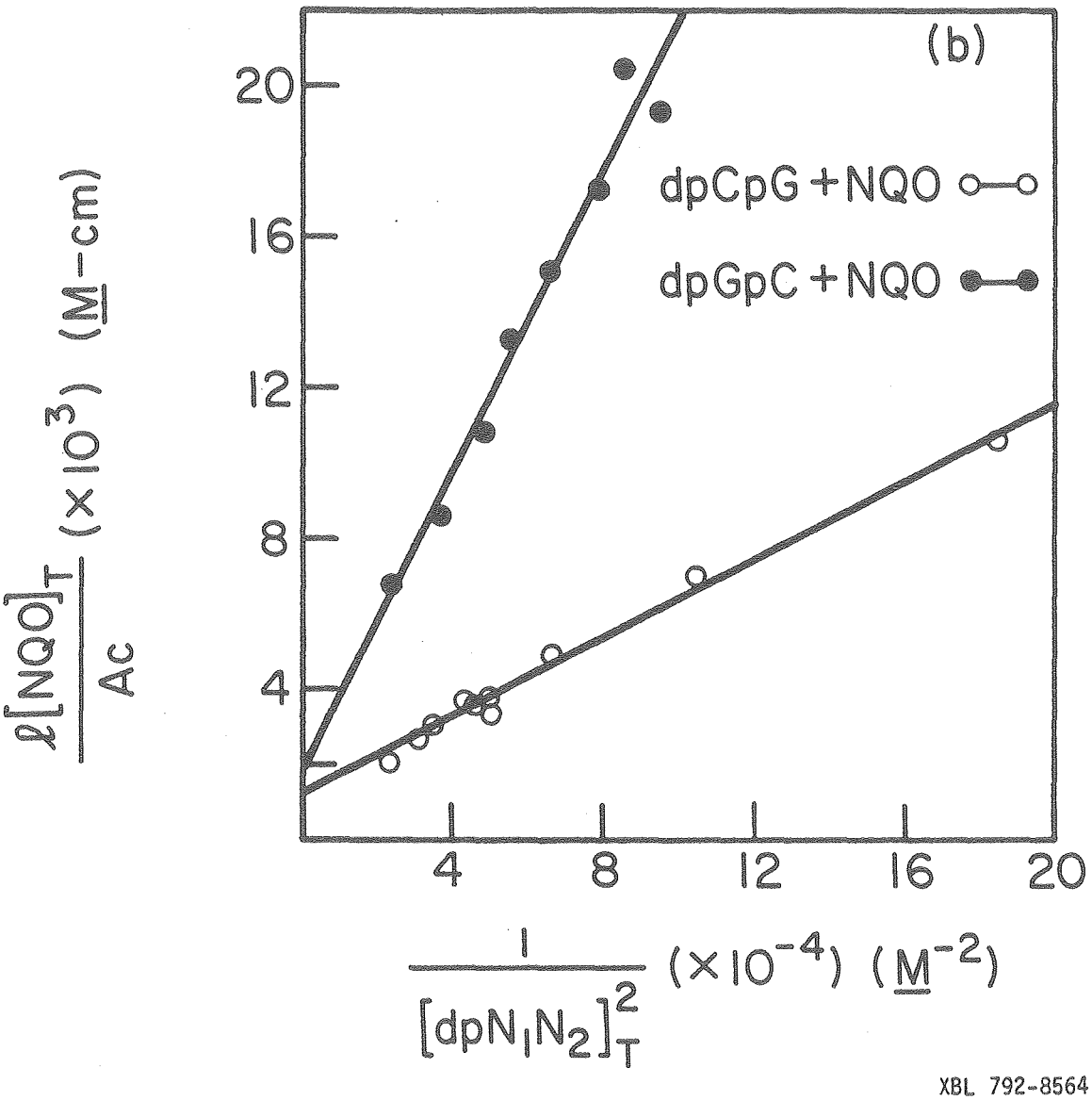
(b)
dpCpG + NQO
dpGpC + NQO
20
16
12
8
4
4
8
12
16
20
$\frac{\ell[NQO]_T}{Ac}$ (×10³) (M-cm)
$\frac{1}{[dpN_1N_2]_T^2}$ (×10⁻⁴) (M⁻²)

XBL 792-8564

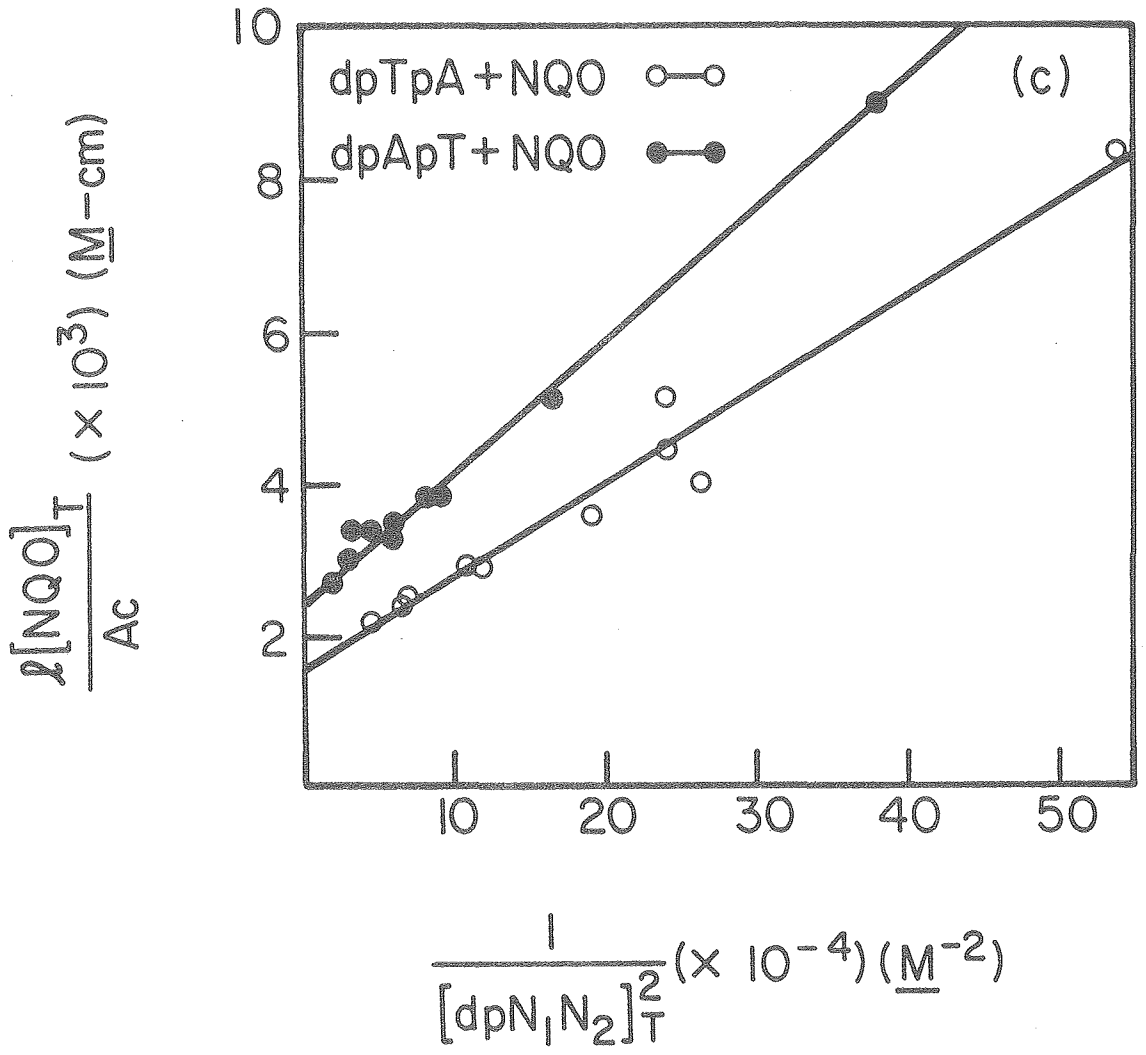
dpTpA+NQO
dpApT+NQO
(c)
10
8
6
4
2
10
20
30
40
50
$\frac{\ell[NQO]_T}{Ac}$ (× 10^3) (M−cm)
$\frac{1}{[dpN_1N_2]_T^2}$ (× 10^{-4}) ($\underline{M}^{-2}$)

XBL 792-8563

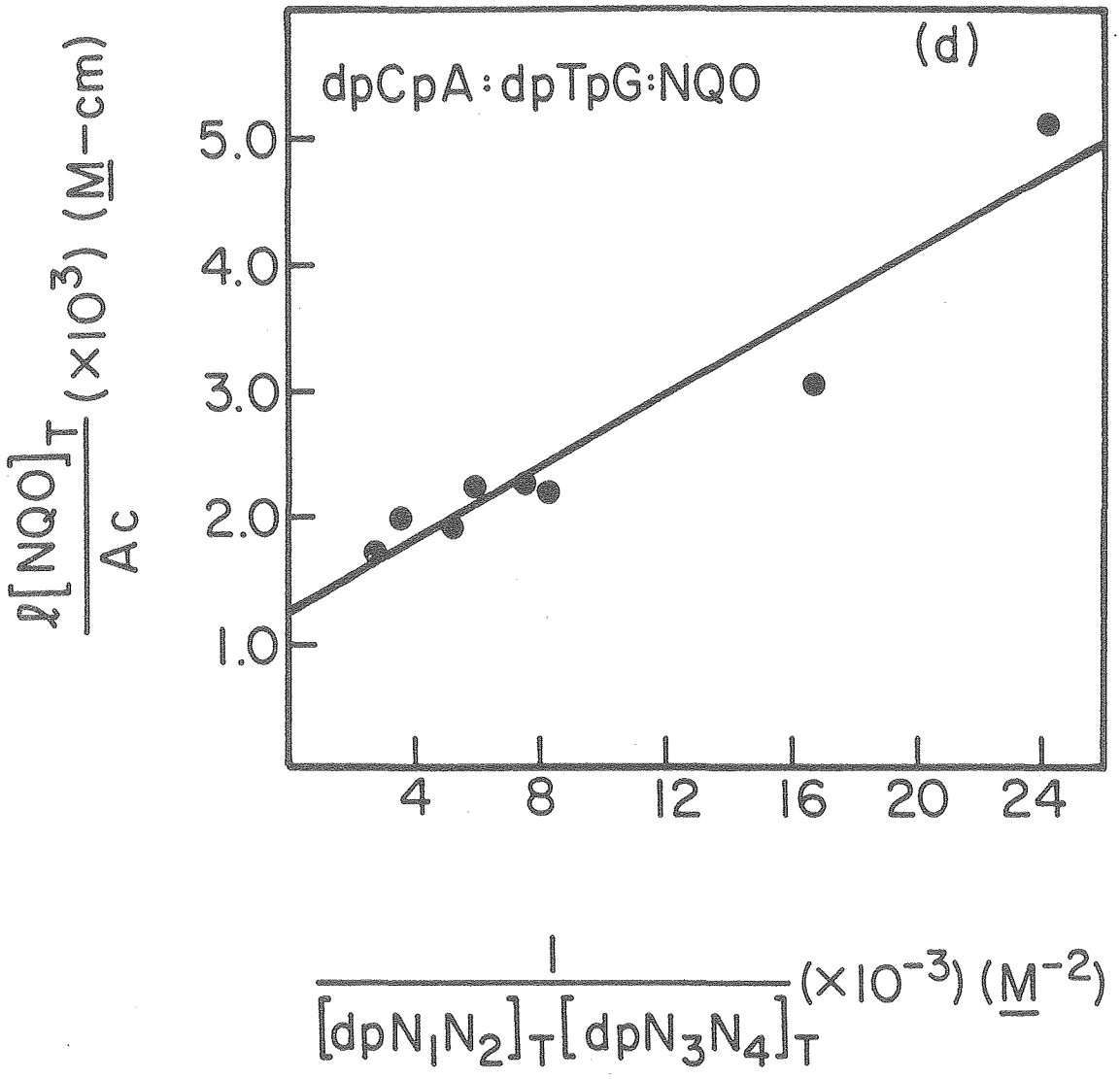
(d)
dpCpA:dpTpG:NQO
5.0
4.0
3.0
2.0
1.0
4
8
12
16
20
24
$\frac{\ell[NQO]_T}{Ac}$ (×10³) (M−cm)
$\frac{1}{[dpN_1N_2]_T[dpN_3N_4]_T}$ (×10⁻³) (M⁻²)

XBL 792 8561

TABLE V

Equilibrium Constants at 25°C for Deoxydinucleotide-Nitroquinoline Oxide Complex Formation

Noncomplementary Dinucleotides

Complex	K^a(25°C), M^{-1}
(dpTpG):NQO	22
(dpCpA):NQO	32

Complementary Dinucleotides

Complex	K^b(25°C), M^{-2}
(dTpG):(dpCpA):NQO	0.9×10^4
$(dpGpC)_2$:NQO	0.9×10^4
$(dpTpA)_2$:NQO	1.3×10^4
$(dpApT)_2$:NQO	1.4×10^4
$(dpCpG)_2$:NQO	2.2×10^4

[a]Maximum estimated error = ± 5 M^{-1}

[b]Maximum estimated error = ± 0.4×10^4 M^{-2}

The use of the large bore 25 mm probe in the ^{13}C NMR study permitted the observation of signals from dilute dinucleotide:NQO samples. The ^{13}C chemical shifts observed for the base carbons in dinucleotide-NQO mixtures are the weighted sums for the chemical shifts of the bound and various free states. We assume (as the ^{1}H NMR data suggest) that there is only one bound species. However, because of the lack of symmetry in the NQO molecule, in any 2:1 intercalation complex formed with self-complementary dinucleotides, the two purine rings are affected differently by the NQO as are the two pyrimidines. Thus the chemical shifts for each of the two purines (or pyrimidines) in the complex will be different. The chemical shift for a nucleus of a base in the bound species is the average of the shifts for the identical bases [$\delta_B = (\delta_{B1} + \delta_{B2})/2$]. The value of δ_B for the base carbons in the 2:1 complex can be obtained from:

$$\delta_B = (\delta_{OBS} - (\frac{[dpN_1pN_2]_T - 2[c]}{[dpN_1pN_2]_T})\delta_F) \frac{[dpN_1pN_2]_T}{2[c]}$$

The complex concentrations, [c], were approximated using the K's determined at 25°C (Table V). The assignments of the free dinucleotide carbon signals, δ_F, are given in Appendix II.

The δ_B's thus obtained for the carbons of the self-complementary dimers were used to calculate the differences (given in Table VI) between δ_B and the chemical shifts, δ_M

TABLE VI. Differences in Average Carbon Chemical Shifts Between Dimers Complexed with NQO and (Comparable) Free Mononucleotides.

Dimer	C2	C4	C5	C6	G2	G4	G5	G6	G8
dpCpG	-0.75	-3.84	+0.12	-0.58	+1.54	-1.32	-1.40	-1.85	-1.40
dpGpC	+1.85	+3.38	+0.48	_0.75	+1.05	+1.54	+1.97	+1.11	+1.51
	T2	T4	T5	T6	A2	A4	A5	A6	A8
dpTpA	-0.51	-0.37	+0.24	-0.53	+0.18	-0.32	-0.91	-0.45	-0.97
dpApT	+1.68	--[a]	+0.04	+0.07	-1.58	+0.39	-0.55	--[a]	+0.12

(NOTE: Positive shift changes are downfield changes.)

[a]Not observable

of the appropriate mononucleotides. The δ_B for the first base in the dimer, i.e., (dpN_1-) in the dimer dpN_1pN_2 are compared with δ_M for the 5'-mononucleotide at pH = 7. The δ_B for (-pN_2) are compared with the δ_M for the 5'-mononucleotide at pH = 5. In Tabel VI, note that (δ_B-δ_M) < 0 represent chemical shift changes to <u>increasing</u> field strength (upfield).

The dinucleotide-NQO complexes of dPu-Py dinucleotides (dpGpC and dpApT) show ^{13}C shift changes which are mainly downfield with the (δ_B-δ_M) for $(dpGpC)_2$:NQO being larger, in general, than those for $(dpApT)_2$:NQO. Conversely the dPy-Pu dinucleotide complexes (involving dpCpG and dpTpA) have values for (δ_B-δ_M) which are either somewhat positive (slightly downfield) or negative (upfield changes). The specifics of the shift changes for each complex will be considered in the Discussion Section.

In the dpCpG-NQO and dpGpC-NQO mixtures, the (dpN_1-) C2' (of the deoxyribose) resonance shifts notably downfield as is shown in Figure 6. No such shifts were observed with dpTpA-NQO or dpApT-NQO mixtures. The (-pN_2) C2' resonances for dpCpG, dpTpA and dpApT did not shift. However, a shift was observed for (-pN_2) C2' of dpGpC. With the possible exception of the C1; resonances, no shifts were observed for the other sugar carbons. The C1' resonances for the (pN_1-) and (-pN_2) sugars generally overlapped making assignment and observation of shift changes unfeasible.

Figure 6: The ^{13}C NMR spectra of the C2' for

(a) dpCpG (4.1 mM), (a') dpCpG (5.8 mM), NQO (2.1 mM)

(b) dpGpC (3.7 mM), (b') dpGpC (5.8 mM), NQO (1.9 mM)

(c) dpTpA (4.0 mM), (c') dpTpA (5.8 mM), NQO (2.1 mM)

Temperature: 35°C, Buffer: sodium cacodylate (0.01 M)-NaCl (0.1 M)-EDTA (0.2 mm), in 25-30% D_2O, pH 7.0.

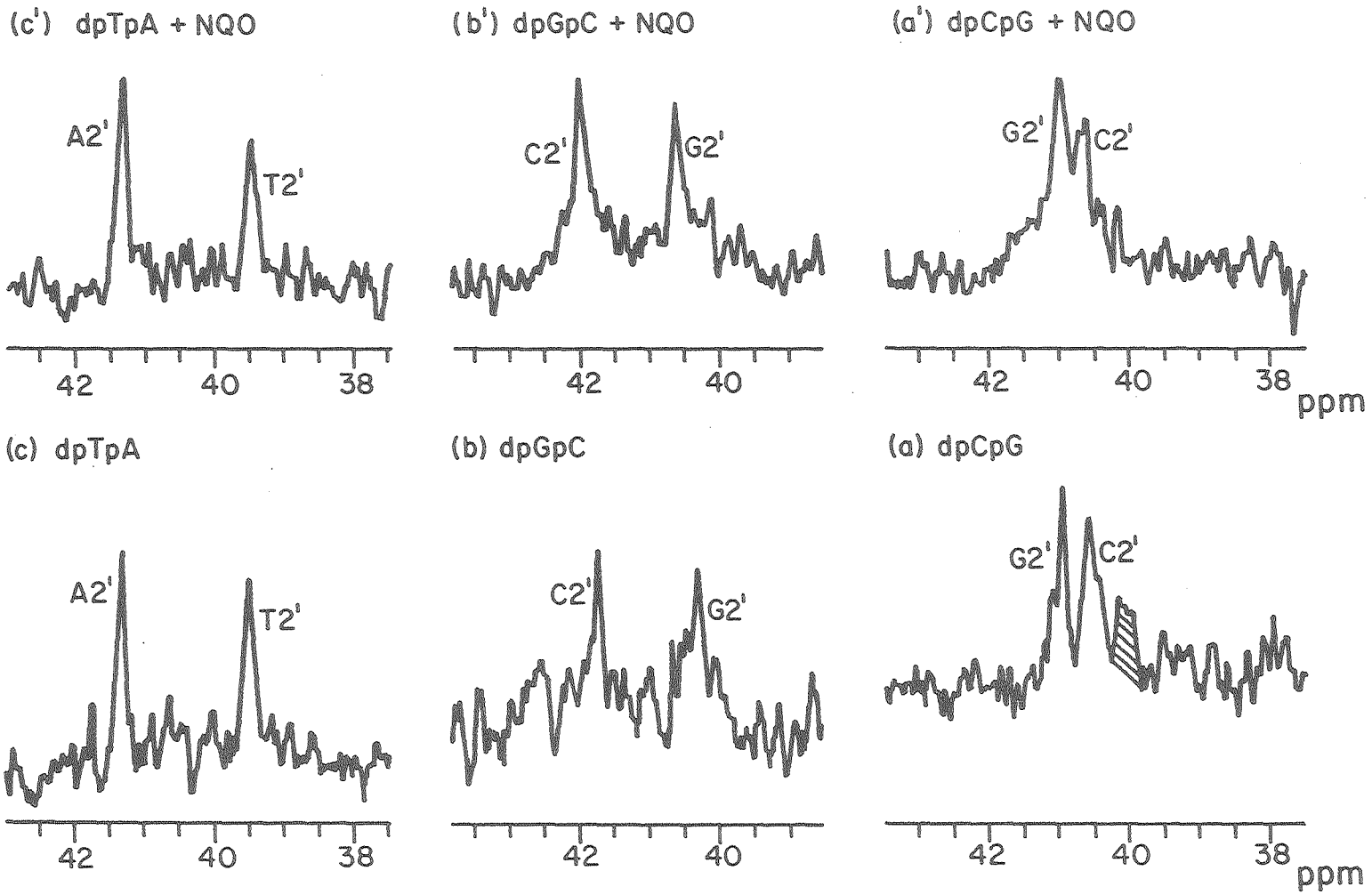
(c') dpTpA + NQO
A2'
T2'
42
40
38
(b') dpGpC + NQO
C2'
G2'
42
40
(a') dpCpG + NQO
G2'
C2'
42
40
38
ppm
(c) dpTpA
A2'
T2'
42
40
38
(b) dpGpC
C2'
G2'
42
40
(a) dpCpG
G2'
C2'
42
40
38
ppm

XBL 792-8556

The observed chemical shifts of the NQO protons are weight averages of the chemical shifts of free and bound species. Thus the chemical shifts of the NQO protons in the complexes with the dinucleotides were calculated in a manner similar to that used for the ^{13}C δ_B of the base carbons.

$$\delta_B = (\delta_{OBS} - \frac{[NQO]_T-[c]}{[NQO]_T} \delta_F) \frac{[NQO]_T}{[c]}$$

The δ_F used for the NQO protons were those given previously in Chapter II. The values of [c] were calculated using the K's at 25°C (Table V). In Table VII, the differences between the δ_B and δ_F for the different dinucleotide:NQO complexes are presented. As expected, different patterns of shift changes are observed for the four complexes. The shift changes were compared to composite ring current diagrams corresponding to a plane (3.4 Å from each base plane) in the interior of a dinucleotide minihelix. (The diagrams were based on the calculated ring currents of Giessner-Prettre & Pullman, 1970, and were constructed by Mr. T. Early, UCSD.) As ring current effects are probably the dominant factor contributing to the NQO proton shifts in an intercalated complex, the comparison can indicate a conformation for each complex.

TABLE VII

Differences in Proton Chemical Shifts between NQO Complexed with Selfcomplementary Dinucleotides and Free NQO

NQO Proton	$\lvert(\delta_B-\delta_F)\rvert$ (ppm) dpCpG	dpGpC	dpTpA	dpApT
2	-0.11	-0.15	-0.17	-0.19
3	-0.09	-0.11	-0.16	-0.17
6	-0.11	-0.17	-0.25	-0.24
7	-0.05	-0.27	-0.17	-0.17
8	-0.12	-0.07	-0.07	-0.21
9	-0.16	-0.16	-0.20	-0.22

DISCUSSION

Opticsl Studies and Equilibrium Constants

The seven dinucleotide-NQO mixtures give charge transfer bands of similar intensities and with similar λ_{max}. The molar absorptivities and λ_{max} for the dinucleotide-NQO complex bands are also very close to those we observe for the 5'-mononucleotides.

The complexes of NQO with two nonselfcomplementary dinucleotides form 1:1 complexes with equilibrium constants (K(25°C)) of the same order of magnitude as the mononucleotides. When the ability to form a minihelix is present as with the selfcomplementary dinucleotides and with a mixture of dpTpG and dpCpA, the complex stoichiometry is two dinucleotides to one NQO. This suggests that, in the complex, the dinucleotides form a minihelix with the NQO bound between the two dinucleotides. The experimentally determined equilibrium constants, K, are representative of the overall equilibrium:

$$2\ dpN_1pN_2 + NQO \overset{K}{\rightleftharpoons} (dpN_1pN_2)_2{:}NQO$$

The equilibrium for the complex may be thought of as the sequence of two reactions:

1) $$2\ dpN_1pN_2 \overset{K_1}{\rightleftharpoons} (dpN_1pN_2)_2$$

2) $$(dpN_1pN_2)_2 + NQO \overset{K_2}{\rightleftharpoons} (dpN_1pN_2)_2{:}NQO$$

The determined K is then equal to the product K_1K_2. Note that the mechanism for complex formation need not necessarily be these two steps. However, by considering the complex formation in this form, the contribution of minihelix formation (reaction (1)), i.e., base stacking and base pairing, to the energy of the complex may be assessed. Young and Krugh (1975) determined equilibrium constants (at 2°C) for minihelix formation by dpGpC (K_1 = 7.8) and dpCpG (K_1 = 3.0). Equilibrium constants were not determined for dpTpA and dpApT but for the mixed system, dpApC + dpGpT, much less duplex formation occurs. No dimerization of the ribodinucleoside monophosphate rApU was observed under similar conditions (4°C) by Krugh and coworkers (1976) although duplex formation of rCpG and rGpC were roughly comparable to their deoxy counterparts.

Since the K's for formation of 2:1 dimer:NQO complexes are all on the order of 10^4 M^{-2} and the contributions of minihelix formation to the complex free energy are small (K_k's are 10 M^{-1} or less), a sizable component of the complex energy is due to NQO-dinucleotide interactions (including the charge transfer interactions). AFter removal of the component of the equilibrium constant due to minihelix formation, the equilibrium constants (K_2) for 2:1 complex formation from the minihelix are still two to perhaps four orders of magnitude greater than those for 1:1 dinucleotide:NQO complexing. The NQO binding affinity is thus much higher for dinucleotides capable of minihelix formation.

With certain intercalating molecules, marked sequence specificities among dinucleotides have been noted. For example, ethidium bromide shows a preference for Py-Pu sequence over Pu-Py sequences (Krugh, et al., 1975; Krugh and Reinhardt, 1977). The situation with NQO is somewhat less clear. The sequence C-G seems to be preferred over G-C, especially if one considers the approximate K_2 (C-G) and K_2 (G-C) obtained by dividing the experimental K's by Krugh's K_1's (which were obtained under different conditions). However it may not be true that C-G in a helix is preferred over A-T, T-A, or C-A:T-G or that Py-Pu sequences are in general preferred to Pu-Py. The similar values of K for the different dimers could indicate that NQO exhibits no distinct sequence preference for dinucleotide helices.

NMR Studies of the Selfcomplementary Dinucleotide:NQO

The information obtained from the ^{1}H and ^{13}C NMR studies (Table VI, Table VII) and Figure 6 was analyzed to provide structural information on the noncovalent complexes. The ring currents of the dinucleotide bases shift the NQO protons upfield. The magnitude of each upfield shift change is related to the distance of each proton from the centers of the composit ring current of the four bases. The magnitudes of all the chemical shift changes observed are somewhat diminished relative to the calculated ring current shifts; however, only the relative shifts are important for our purposes.

Such diminutions were also observed with the mononucleotide NQO complexes. The (δ_B-δ_F) values (Table VII) were compared with ring current diagrams for the four dinucleotide minihelices. Comparisons were attempted to three different ring current diagrams corresponding to threee distinct duplex orientations. In all cases the base pairs were 6.8 Å apart. The first orientation was with the dinucleotide minihelix corresponding to a B DNA structure, that is, with one base pair rotated by 36° with respect to the other. The second orientation had a 10° rotation rather than 36°; this corresponds to a 26° unwinding (Wang, 1974). The third was a 10° rotation of one base pair and a 1 Å displacement of the bottom base pair. In this orientation, one base pair is lined up more or less directly over the other whereas in the first two cases the base pairs are staggered. This last orientation is what has been suggested for ethidium intercalation by Sobell and coworkers (1976). For all four dinucleotides, the best fits were with the base pairs at 36°.

Complexes in which the NQO is intercalated with its long axis roughly perpendicular to the long axis of the base pairs may be ruled out. In such complexes, the NQO protons H-2,3 and/or H7,8 would be far removed from the ring current center. The ring current shift changes (δ_B-δ_F) would be near zero for these protons in such conformations. As is shown in Table VII, for all four systems all protons have (δ_B-δ_F) values of the same order of magnitude.

The approximate complex orientations obtained are given in Figures 7 a-d; it is clear that they represent an average of a dynamic situation. In the $(dpCpG)_2$:NQO and $(dpGpC)_2$:NQO complexes, the electron withdrawing ring of the NQO (the (NO_2), (NO) ring) is closer to the imidazole ring of the guanine. The (NO_2) group of NQO is near the G6 carbonyl and C4 amino groups in what could be termed the major groove. The (NO) group of NQO is near the G2,C2 area.

With the $(dpTpA)_2$:NQO and $(dpApT)_2$:NQO complexes, it is the benzenoid ring of the NQO which is to the side of the intercalation pocket near the imidazole ring. The (NO_2), (NQO)-ring is in the center of the pocket, over the 6-membered rings of the purine bases. The (NO_2) group projects near the A2 hydrogen and T2 carbonyl into what may be called the minor groove.

In making the comparisons, the assumption was made that NQO forms a distinct type of complex with each dinucleotide rather than a range of very different complex structures. If NQO intercalated to form a variety of complexes with each dimer, the differences in $(\delta_B-\delta_F)$ in Table VII for the different NQO protons would tend to disappear. For example, if NQO formed either a complex with its nitro group in the major groove or a complex with its nitro group in the minor groove (in other words, came in from either side) and took up the same position relative to one of the purines, the $(\delta_B-\delta_F)$ for H-2 and H-3 would be very similar to those for the pairs H-7 and H-8 and H-6 and H-9. As the data show, this is not the case.

Figure 7: Proposed structures os selfcomplementary dimer:NQO 2:1 complexes.

(a) $(dpCpG)_2$:NQO;

(b) $(dpGpC)_2$:NQO;

(c) $(dpTpA)_2$NQO;

(d) $(dpApT)_2$:NQO.

Only base atoms (excluding hydrogens) are shown for the dimers. Bottom base pair (o--o); top base pair (o—o); NQO (•—•). These are approximate representations of the complex structures.

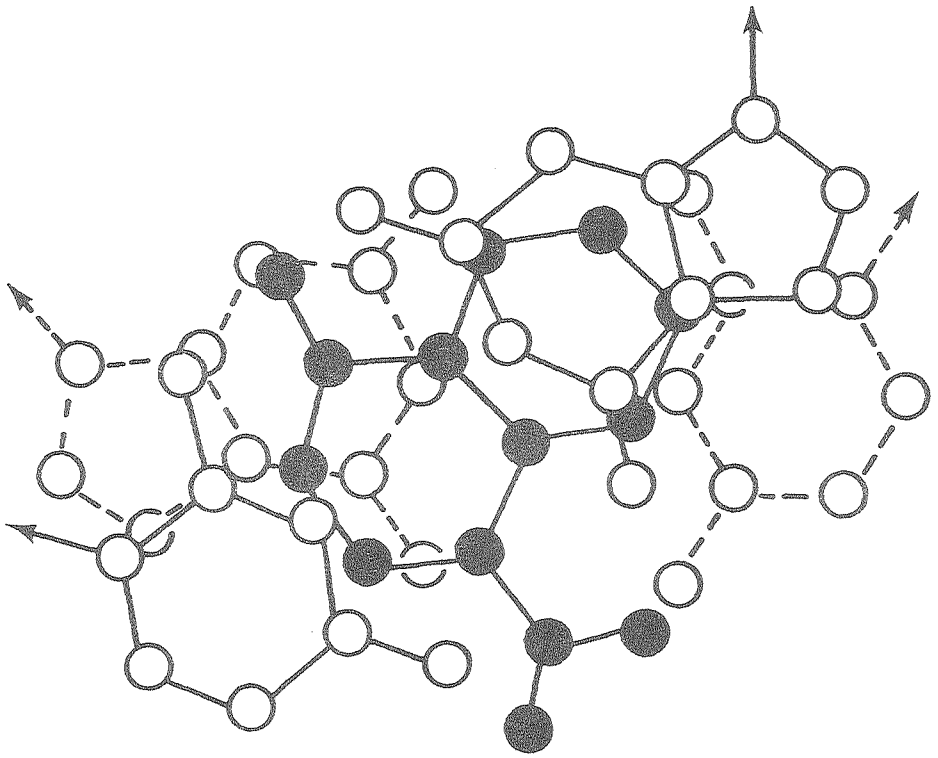

(a)

$(dpCpG)_2$:NQO

XBL 792-8558

(b)

$(dpGpC)_2$:NQO

XBL 792-8557

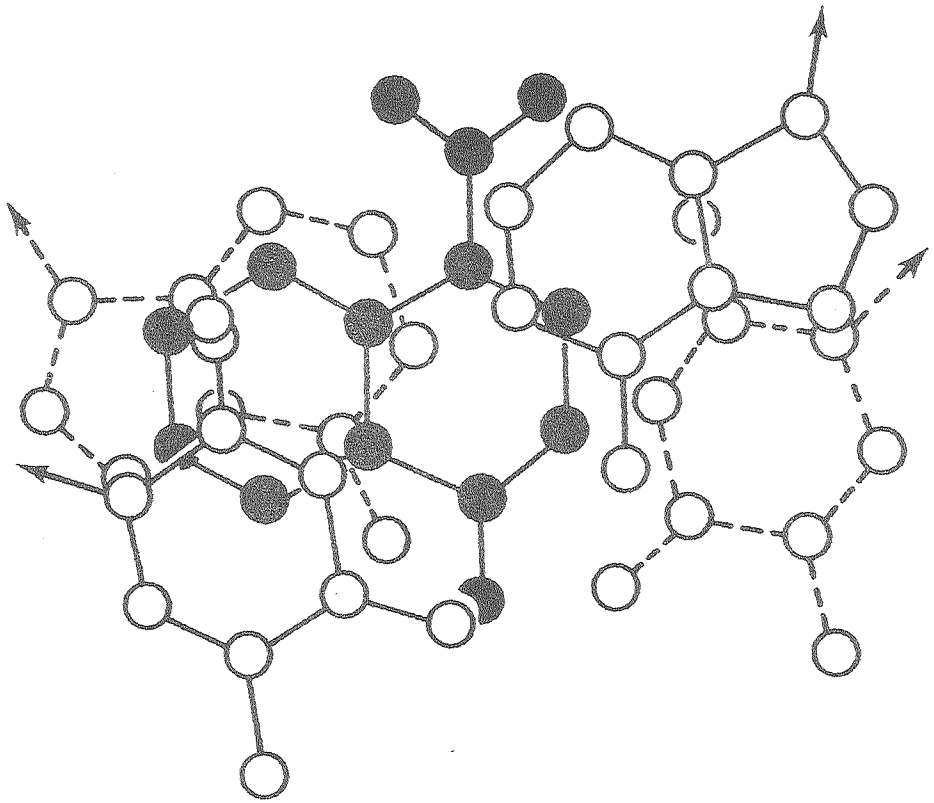

(c)

$(dpTpA)_2$:NQO

XBL 792-8560

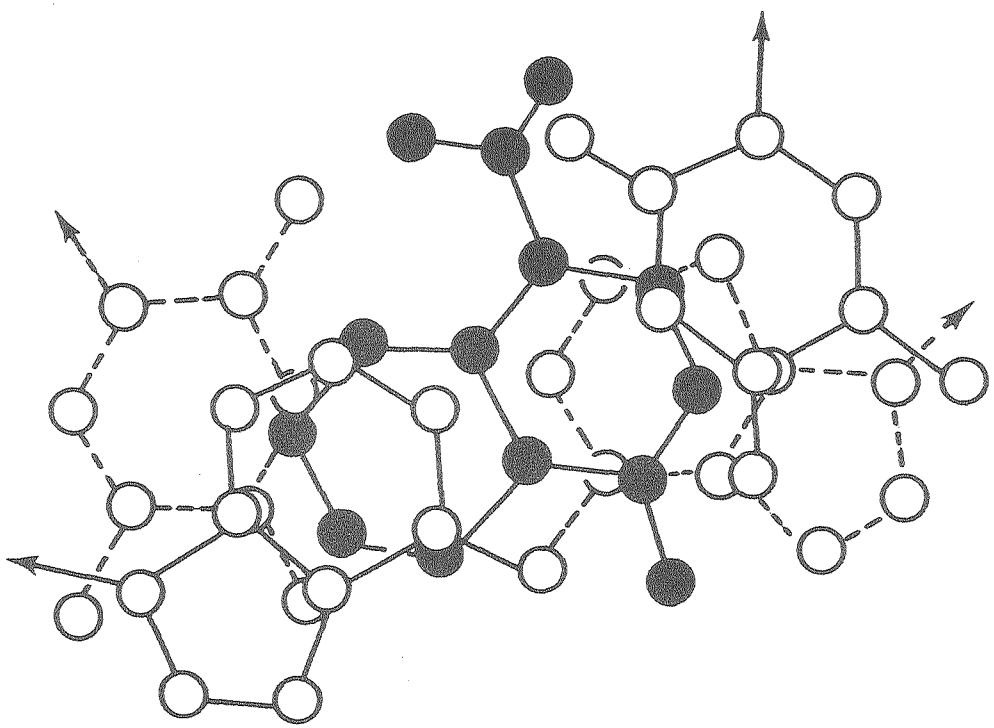

(d)

$(dpApT)_2$:NQO

XBL 792-8559

Furthermore, formation of unique complexes with dinucleotides has been observed with other molecules such as ethidium bromide (Jain et al., 1977), 9-aminoacridine (Sakore et al., 1977) and proflavine (Neidle et al., 1977). The fits of the data for dpTpA and to a lesser degree, dpApT, were not as good as those for dpCpG and dpGpC. This could indicate that there is slippage of the NQO in the intercalation pockets of dpTpA and dpApT duplexes. The proposed structures would allow for this since the NQO is in the center of the intercalation site - with the dpGpC and dpCpG complexes it is to one side. (Note that the self-complementary dimers possess a two-fold axis of symmetry. Thus the complex with the NQO stacked with one purine is identical to that with the NQO stacked in a similar manner with the other purine).

The ^{13}C NMR study of the dinucleotide base carbons provided data which can be interpreted in terms of the complex structures. The changes arising in δ_{B1} and δ_{B2} for each type of base carbon are due primarily to the ring current of the intercalated NQO and to a lesser extent the ring current of the other bases. In addition there are effects from changes in the local atomic anisotropy (local paramagnetic term) due to charge transfer, hydrogen bonding, etc. The ring current effect will produce upfield shift changes (Giessner- Prettre & Pullman, 1979), whereas the charge transfer from the bases apparently produces downfield changes. The more an individual carbon is involved in the electron transfer,

the larger the shielding changes are. This can be rationalized in terms of current theories of ^{13}C shielding parameters (Karplus & Pople, 1963; Cheney & Grant, 1967). In the previous chapter, the ^{13}C NMR spectra of dpG-NQO and dpA-NQO mixtures were discussed. In the dpG-NQO case, a large downfield shift was observed for G8 relative to the other guanine base carbons. This suggested that the electron withdrawing center (the (NO_2), (NO)-ring) of NQO was over the imidazole ring of the guanine. With dpA-NQO no such large shifts were observed for any adenine carbon suggesting that the NQO electron withdrawing ring was more located over both rings of adenine.

With all the dinucleotides, the ^{13}C shift changes were smaller than was observed with the mononucleotides. In the dinucleotide-NQO complexes, the charge transfer can involve four bases and the NQO. Thus the effect of the charge transfer is diminished. This is especially true when the withdrawing "center" is not over one end of the molecule such as the imidazole ring of the purines. Furthermore, as δ_B is the average of δ_{B1} and δ_{B2}, a shift of δ_{B1} and δ_{B2} in opposite directions will also diminish its magnitude.

With the dimer dpGpC the carbons of the imidazole ring of the guanine G5, G8, G4 show ralatively large downfield shift changes; C6 and C5 of cytosine show smaller downfield shifts. This is consistent with having the electron withdrawing ring of NQO, the (NO_2), (NO)-ring over the imidazole ring of

one of the guanines with a lesser interaction with C5, C6. With the dimer dpCpG, only C5 of the non-base pairing carbons shows a downfield shift. However C6 shows a smaller upfield change than other carbons in dpCpG. This suggests that the withdrawing NQO ring is over these regions. The differences in shift changes between the two sequences dPu-Py and dPy-Pu are explained by the conformations of the stacked dimers. With dPu-Py dimers the imidazole ring is exposed, while in dPy-Pu dimers it is covered partially by the dpN_1-sugar. Similarly, in the dPu-Py dimers the pyrimidine residue is partially blocked by the dpN_1-sugar. More overlap by the intercalator with the imidazole ring is therefore possible in the dPu-Py sequence.

With dpApT, much smaller shift changes are seen than with dpGpC and the pattern is different. With dpGpC, the changes on the guanine were in the order G5 > G4 ≃ G8. With dpApT, the order was A4 > A8 > A5 and A5 exhibited an upfield change. The changes on the pyrimidine carbons 5 and 6 were much less downfield with dpApT than with dpGpC. The preferred position of the (NO_2), (NO)-ring may be over the center of the dpApT duplex. Similarly with dpTpA, A4 is shifting less upfield than are A5 and A8. This is also consistent with placing the (NO_2), (NO)-ring over the center of the duplex as the ^1H NMR data suggest.

The dpN_1-sugar 2' carbons of both the dimers dpCpG and dpGpC showed downfield shifts. Such downfield shifts could be caused by the proximity of the NQO molecule. In such a position, the 2' carbons are in the downfield shielding region of the NQO ring current. This is consistent with the orientations proposed in Figures 7 a,b in which the NQO is to the side of the intercalation pocket. With dpApT and dpTpA no shifts of the dpN_1-2' carbons were observed. In the duplexes formed by these two dimers, the NQO is in the center of the pocket.

The orientations which the NQO assumes relative to the guanine residues in the dpGpC and dpCpG complexes are close to the orientation which NQO has with the mononucleotide. Also, the NQO orientation in the dpApT and dpTpA complexes resembles the orientation in the NQO:dpA complex.

CONCLUSIONS

Analyses of charge transfer spectral data for different dinucleotide-NQO mixtures has provided equilibrium constants and stoichiometries for their complexes. The preference of NQO is for dimers which form miniature double strands. No marked sequence specificity was noted among the dimers examined. Results of investigations of DNA-NQO interactions to be discussed in Chapters V and VI indicate the possibility of specificity for some larger structural feature or sequence.

From the NMR studies, structures for NQO:selfcomplementary dimer complexes are proposed. With each dimer, NQO assumes a specific orientation. The structures of the dpCpG complex and the dpGpC complex are similar, as are those for the dpTpA complex and the dpApT complex.

CHAPTER IV

PHOTOCHEMISTRY OF NQO

INTRODUCTION

In the last chapter, it was stated that when an aqueous solution of NQO was excited at 360 nm, the result was not the expected fluorescence spectrum of NQO but rather apparent photochemistry of the NQO. Tada, et al. (1967) had reported that irradiation of NQO at 360 nm resulted in a fluorescence band at 480 nm. Their study implied that the fluorescence was due to the NQO. The results of the attempt to measure NQO fluorescence led to a brief exploration of the photoreactivity of NQO.

Kataoka, et al. (1966) reported that when NQO was irradiated with a mercury lamp (which would cover the UV region including the 365 nm transition of NQO) strong electron spin resonance signals were observed. Using NQO with ^{15}N substituted for either or both NQO nitrogens, they probed the nature of the photo-induced radicals in dioxane, benzene and hexane. For example, in dioxane, the free radical delocalization was reported to be limited to the benzenoid ring and N-oxiate group. An ESR study by Okano and Uekama (1968) on NQO free radicals showed that the presence of DNA enhanced the formation of NQO free radicals as measured by increased ESR signals. This could suggest that the formation of the NQO-DNA base charge transfer complex promotes the production of NQO free

radicals. As was discussed in Chapter I, the results of many experiments indicate that most NQO is converted *in vivo* to HAQO which is "activated", possibly by conversion to the very reactive 0,0'-diacetyl-4-HAQO (Sugimura, et al., 1966; Kawazoe, et al., 1969; Kawazoe, et al., 1969). The discovery of the photoreactivity of NQO suggested that photochemical or non-enzyme catalyzed reactions of NQO with DNA might occur, as well.

This chapter will focus on the photoreactions of NQO with nucleic acids. The aim of this series of experiments was *not* to completely characterize all such reactions. Rather, the experiments were designed to define approximately the nature of the photoadducts and the conditions for producing them. The photoaddition of NQO to DNA may then be used as a probe for the sites of NQO interaction with DNA. These last experiments are discussed in Chapter VI.

The format of this chapter is varied from the other chapters describing sets of experiments in that the experimental procedures and results are presented together.

EXPERIMENTAL

Materials

The mononucleotides were obtained from Calbiochem. The calf thymus DNA was from Worthington. The poly(rA) was from Sigma, the poly(rU) was from Miles Laboratories and the poly(rC) was a gift from Dr. Frank Martin. The NQO was synthesized and purified as described in Chapter II.

The HAQO was prepared from NQO using phenylyhdrazine as described by Ochiai, et al. (1957). The actual method used was that of Kawazoe & Tachihana (1967) for 5-methyl-4-HAQO. NQO (1.89 gm) was dissolved in 75 ml 95% EtOH and the mixture heated to 75%. Phenylhydrazine (12.0 ml) was added with stirring. Approximately 5 min later the first whitish precipitate appeared accompanied by the release of gaseous N_2. The mixture was heated for 45 min (until generation of N_2 ceased). The whitish precipitate was collected and dissolved in HCl saturated MeOH for recrystallization. The material, HAQO·HCl, was recrystallized two times with approximately 0.5 gm recovered (yield 28%). The melting point was 178-185°C (reported melting point is 192°C) and the material gave only one spot with TLC (in 95% EtOH, $CHCl_3$, and 1:1 EtOH (95%):$CHCl_3$ on cellulose plates). The UV spectrum in cacodylate buffer checked with that reported by Ochiai, et al. (1957). The HAQO is farily stable when stored as the HCl salt in a dark bottle. In solution, the stability is much lower. Freshly prepared aqueous solutions of purified HAQO were bright yellow. When the HAQO decomposed the solutions become orangish.

Aqueous Photoreactions of NQO: Non-Nucleic Acid Reactions

Samples of NQO, ca. 2×10^{-3} M, in the cacodylate buffer were typically irradiated for 1 hr at 20-25°C. The irradiation device consisted of 2 400 W general Electric Hg-arc lamps

mounted on either side of the double walled sample chamber. A $CoCl_2$ solution (40% (w/w)) was circulated through the outer jacket of the sample chanber to cut off light below ∿ 340 nm and significant amounts of light above ∿ 420 nm. (See figure 8 for a representative absorption spectrum of the $CoCl_2$ solution in this region.) The peak intensity 100 mW was at ca. 360 nm which is near the long wavelength UV transition of NQO.

After irradiation, thin layer chromatography using prepared cellulose plates (Eastman Kodak, with fluorescent indicator) was performed on the reaction mixtures. The solvent systems were mixtures of 1 M NH_4OAc(aq) and 95% EtOH, e.g., 1:3 NH_4OAc:EtOH. Four photoproducts were observed. Characteristics of the bands in 1:3 NH_4OAc:EtOH were: the first, rf = 0.68, yellos color; the second, rf = 0.83, light purple under a Mineralight UVS-12 UV lamp; the third, rf = 0.87, yellow, dark under uv; the fourth, rf = 0.93, dark purple under UV. In this solvent mixture, NQO has an rf of 0.88. (The rf's were calculated as the distance traveled by the band on the TLC plate divided by the distance from the start to the solvent front.)

Preparative scale TLC was then done to obtain sufficient quantities for UV analysis. It should be noted that lengthy drying of the plates after running the TLC's was necessary to remove most of the acetic acid. To extract the photo-products from the plates, the bands were scraped off the

Figure 8: UV absorption spectrum (320-440 nm) of a 40% (w/w) $CoCl_2$ solution (used in the Hg lamp irradiation device) obtained at 25°C vs. H_2O on a Cary 118 spectrometer.

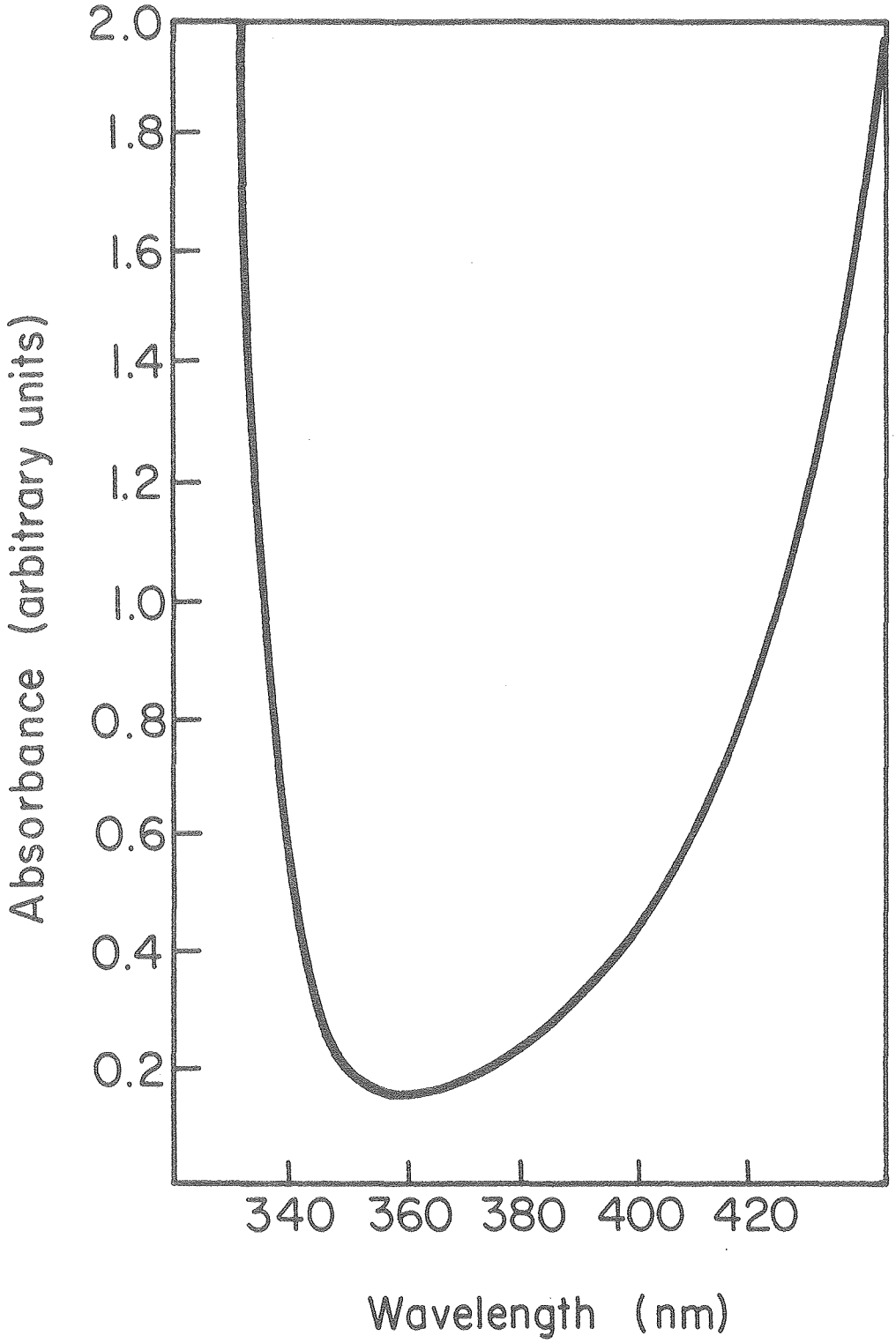

XBL 798-10852

plates and combined with stirring with a small quantity of H_2O or $CHCl_3$. The slurries were then filtered through a glass funnel and a Millipore filter to remove the cellulose. The absorption spectra, vs. H_2O, were run on a Cary 118 spectrometer.

For comparison of the UV spectra, reference may be made to the NQO UV spectrum in Chapter II, figure 1. The UV spectra of the photoproducts are given in figure 9. The first photoproduct band gave a UV spectrum which is identical to that of quinoline-1-oxide. The second photoproduct band gave a UV spectrum which matches well in the region 290-330 nm with the spectrum of 4-hydroxyquinoline-1-oxide with the allowance for a long wavelength shoulder ($\sim$ 340 nm). This shoulder may be due to the N-oxide group. The third component presents a curious case. The spectrum did not match well with the published spectra of various quinoline compounds, e.g., 4-nitrosoquinoline-1-oxide. When this band was extracted with $CHCl_3$, evaporated to dryness and reconstituted in H_2O, the UV spectrum was the same as that of NQO. Thus this photoproduct is unstable and is capable of being easily converted (oxidized (?)) to NQO. The fourth component initially gave a UV spectrum which was distinctive and which did not agree well with published spectra. After an aqueous solutions was allowed to stand, the compound's UV spectrum was similar to that of the second component.

Figure 9: UV spectra (250-390 nm) of the four NQO photoproducts. Component I (—— - - - ——); component II (———); Component III (—— ——); component IV (—— – – ——). Spectra taken at 25°C vs. H_2O on a Cary 118 spectrometer. Relative intensities of the spectra of the four components are arbitrary and do not reflect relative amounts of the products formed. Spectral characteristics below 250 nm obscured by impurity bands, e.g., acetic acid (see text).

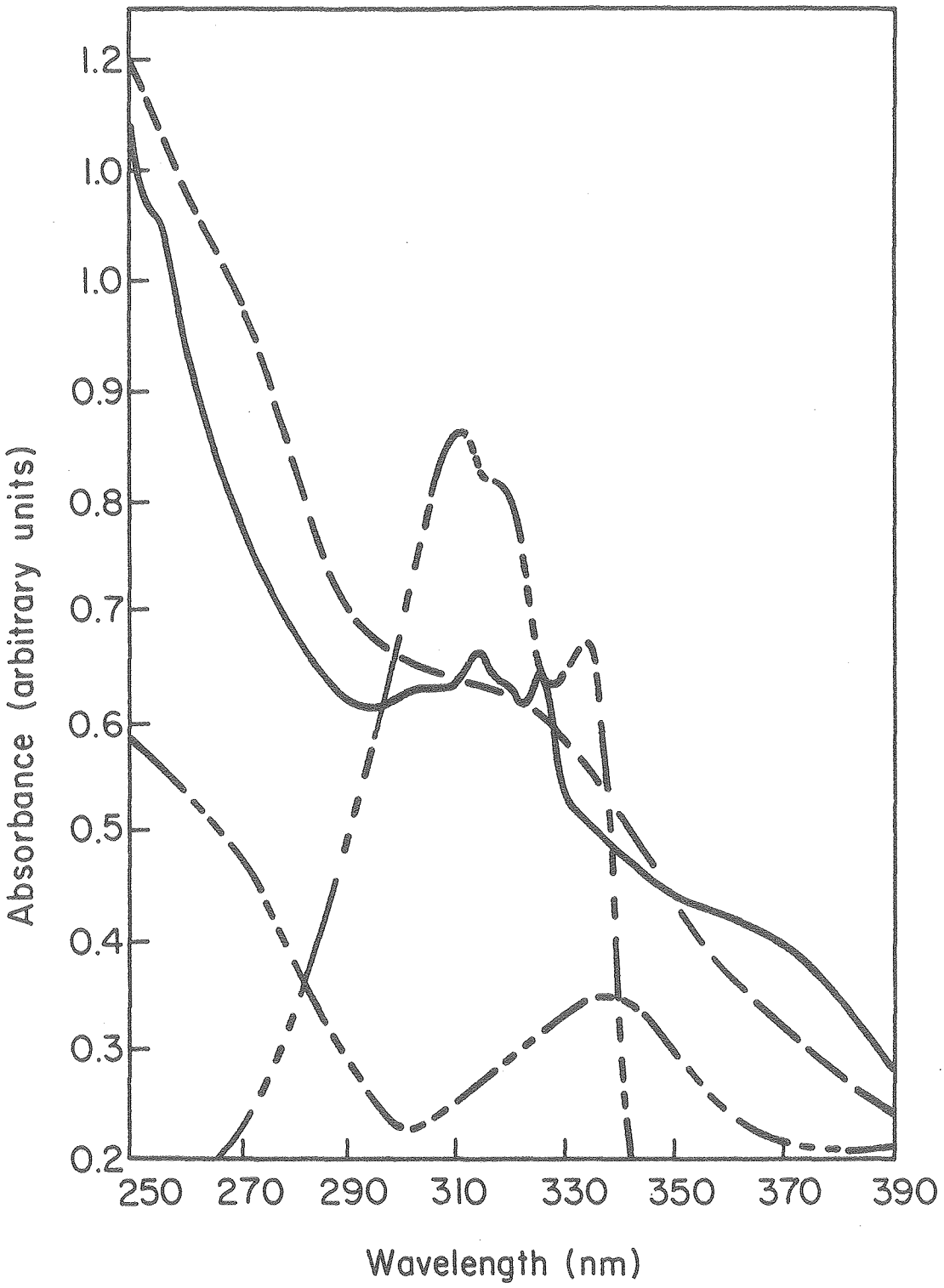

XBL 798-10851

Further, the solution then gave two components with TLC- corresponding to the initial components two and four. This suggested that components two and four are isomers.

A 95% EtOH solution of NQO (ca. 2×10^{-3} M) was irradiated for 1 hr at 20-25°C on the irradiation device described above. A photoproduct with a UV spectrum very similar to component two from the aqueous reactions was isolated using TLC. This compound could be 4-ethoxyquinoline-1-oxide.

To 10 ml of an approximately 2 mM solution of NQO (in cacodylate buffer), two drops of 2 M NaOH were added. The solutions was then stirred in the dark for 24 hr. A component was isolated from the TLC plate (rf = 0.82 in 3:1 NH_4OH (1 M):EtOH (95%)) which gave a UV spectrum matching with that of component two (the 4-hydroxyquinoline-1-oxide of the photoreaction.

Photoreactions of HAQO

Samples of HAQO (ca. 2 mM) in cacodylate buffer were irradiated at 20-25°C for 1 hr on the described Hg lamp irradiation device. Thin layer chromatography was performed on the irradiated samples as described for NQO. The TLC suggested a somewhat different set of photoproducts than occurred with NQO. Characteristics of the components eluted with 1:3 NH_4OAc:EtOH were: component one, rf = 0.037, bright blue under UV; two, rf = 0.068, also bright blue under UV; three, rf = 0.76, dark blue under UV; four, rf = 0.83, bright purple under UV; five, rf = 0.86, yellow, blue under UV;

sic, rf = 0.92, dark purple under UV. In this solvent system, HAQO has an rf of 0.88. Components were extracted from preparatory scale TLC plates and UV spectra in H_2O taken. The fourth and sixth components matched in rf and UV spectra with components two and four of the NQO photoreaction (which were apparently isomers).

Photoreactions of NQO with Mononucleotides

Since NQO showed the greatest affinity for binding to dpG (Chapter II), attempts were made to isolate NQO-dpG photoproducts. Solutions of dpG (concentrations varied from $5x10^{-2}$ to $2x10^{-1}$ M) with NQO (2 mM) in cacodylate buffer were irradiated at 4°C for 1 hr as previously described. In the TLC (under conditions such as those described above) of such reaction mixtures, no obvious adduct components were detected. A Sephadex A-25 ion exchange column with aqueous triethylamine (TEAB) (pH 7.6) gradient (0.1 - 2.0 M) also did not show any such products. It is possible that adduct bands could have been hidden under the dpG bands in both systems. Thus, the fact that no adducts were seen does not rule out their existence.

The pyrimidine nucleotide, dpC, was tried next. A cacodylate buffer solution of dpC (0.2 M) and NQO (2 mM) was irradiated for 1 hr at 4°C with stirring on the irradiation device. The TLC in 3:1 NH_4OAc (1 M): EtOH (95%) did not reveal any adducts. However, from a Sephadex

A-25 ion exchange column with an aqueous TEAB (pH 7.6) gradient (0.1-2.0 M), a bright yellow component was eluted at 1.1-1.2 M TEAB. The component in the gradient buffer was evaporated using a rotary evaporator and reconstituted in H_2O. Subsequently, TLC on cellulose plates in 3:1 NH_4OAc (1 M):EtOH (95%) was used to further purify the compound (rf = 0.52). The compound was lyopholized after extraction from the TLC plate. In the UV spectrum in cacodylate buffer (figure 10 a), absorption bands were observed at 410, 335, 280 (shoulder), 255 (shoulder) and 230 nm. The 230 nm band was somewhat obscured by impurities (probably associated with the TLC, e.g., acetic acid. The 180 MHz ^1H NMR spectrum (figure 10 b) in D_2O at 25°C gave in the aromatic region signals at δ 9.20 (singlet; δ 8.28 (doublet, J ≈ 8 Hz); δ 7.97 (apparent triplet $J_1 \approx J_2 \approx 8$ Hz); δ 7.75 (doublet, J ≈ 8 Hz); δ 6.62 (broad singlet). Chemical shifts are given relative to the DSS reference. The sugar region of the spectrum, approximately 2 - 5.5 ppm, was partially obscured by the HOD signal and/or the ^1H decoupling used to decrease the HOD signal intensity. A sample of the compound was submitted to the Mass Spectroscopy Laboratory, Space Sciences Laboratory, UCB. After treatment with alkaline phosphatase, field desorption mass spectroscopy was attempted by Dr. Kenneth Straub. The mass spectra gave signals which could be assigned to quinoline compound or

Figure 10:

(a) UV absorption spectrum (225-450 nm) in H_2O of dpC-NQO photoproduct. Spectrum taken at 25°C on Cary 118 spectrometer.

(b) 180 MHz ^1H NMR spectrum in D_2O of dpC-NQO photoproduct. Spectrum of aromatic protons referenced to DSS (0.00 ppm). Spectrum taken at 25°C using a 180 MHz Bruker magnet with Nicolet 1180 computer system.

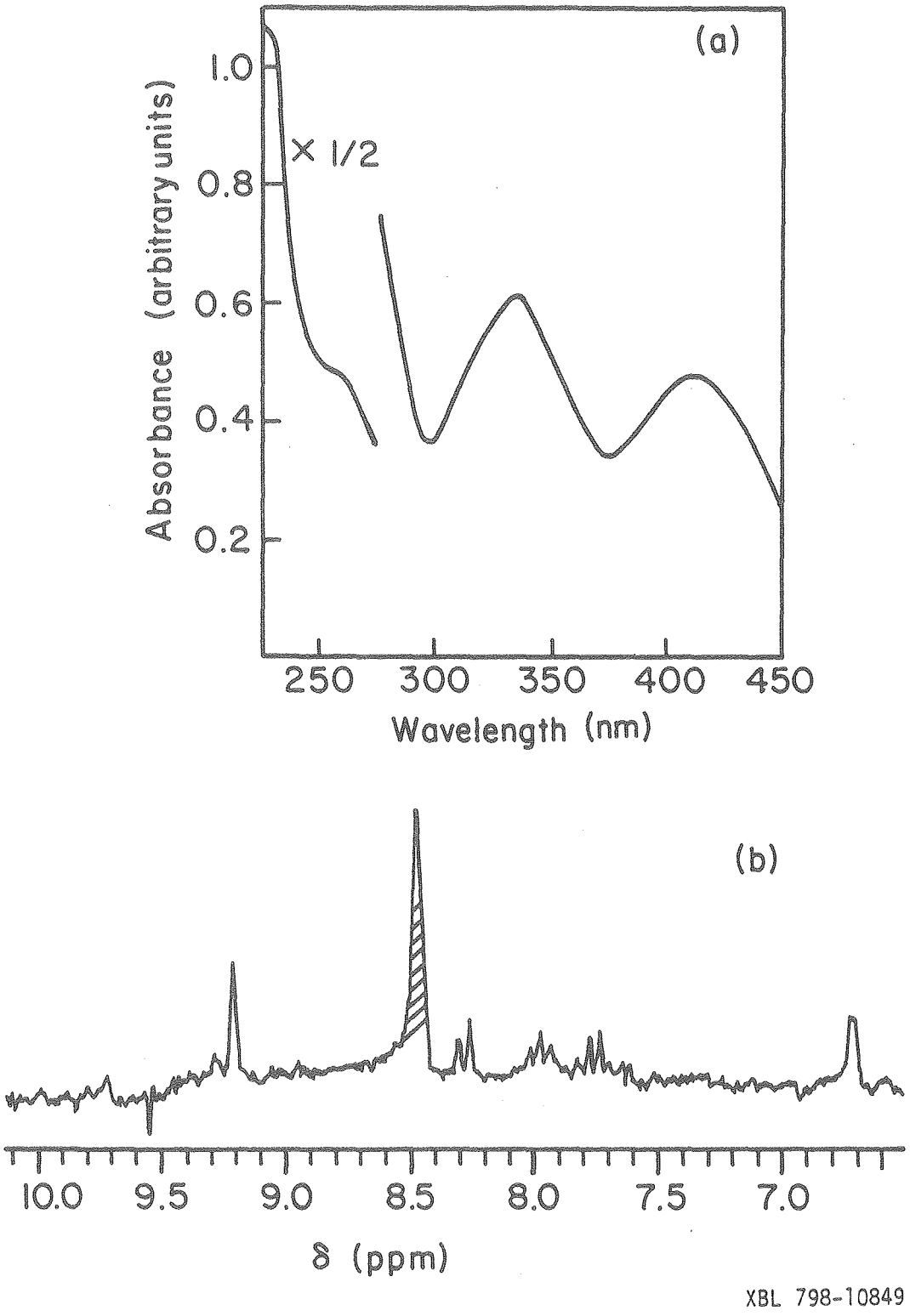

XBL 798-10849

cytidine fragments. However, there were also sizable peaks which could not be assigned to the types of fragments normally observed (see, for example, Dejongh, 1973). Furthermore, there was no apparent molecular ion signal. It is possible that the procedures used on the compound, e.g., the alkaline phosphatase digestion, decomposed (in part) the sample leading to spurious impurity signals.

The reactions of NQO with dpA and dpT were also attempted. Cacodylate solutions of dpA or dpT (0.2 M) with NQO (2 mM) were irradiated as before. Products were sought using TLC as before. No evidence of products was found, but as with dpG, products could have been obscured by the large nucleotide bands.

Photoreactions of NQO with the Ribonucleotide Polymers poly(rC), poly(rA), poly(rU)

A. Light Reactions

Cacodylate solutions (0.1 to 0.3 ml) of poly(rA), poly(rU), or poly(rC) [poly(rA), 5.3×10^{-4} to 2.7×10^{-3} M; poly(rU), 8.8×10^{-4} to 4.4×10^{-3} M; poly(rC), 6.64×10^{-4} to 3.3×10^{-3} M] and ^{3}H-NQO (1 to 5 x 10^{-5} M) were irradiated using the irradiation device for 15-30 min at 30°C. Polymer concentrations were checked using the absorbances at 260 nm at the published ε_{260} (PL Biochemicals Reference and Price Guide 105). Concentrations are expressed as moles of residues per liter. The ^{3}H-NQO was synthesized

as described in Chapter V. Initial ^{3}H-NQO concentrations were determined by counting the radioactivity using a liquid scintillation counter (Beckman LS-230). Details of the scintillation counting are also in Chapter V. After irradiation, the solutions were dialyzed for 48 hrs in cellulose dialysis tubing vs. H_2O (ca. 1 ℓ H_2O changed 2-3 times). In one experiment, the polymers were precipitated from the reaction mixtures using 2 volumes of NaCl saturated 95% EtOH. The precipitated polymers were redissolved in the amount of buffer needed to give the initial volume. The polymer concentrations after precipitation were checked using the absorbances at 260 nm. Insufficient NQO was covalently bound to greatly affect the absorption spectra. The quantities of covalently bound NQO were determined by counting the radioactivity after dialysis or precipitation.

Samples of the polymers [poly(rA), 5.3×10^{-4} M; poly(rU), 8.8×10^{-4} M; poly(rC), 6.64×10^{-4} M] with ^{3}H-NQO ($9.6\text{-}9.9\times10^{-6}$ M) were irradiated for 1 min at room temperature using a Molectron pulsed dye laser, from Professor B. Mahan's research group, UCB, operating at 407 nm (average power was ca. 30 mW at 407 nm). Use of the dye laser was provided by A. O'Keefe and F. Grieman. The polymers were precipitated with 95% EtOH (NaCl saturated), redissolved in buffer and counted as before. Polymer concentrations after precipitation were checked using the solution absorbances at 260 nm.

With Hg lamp irradiation, poly(rC) gave covalently bound NQO in the amount 1600 residues/bound NQO; poly(rA) 3000 residues/bound NQO; poly(rU) 4400 residues/bound NQO. Using the dye laser, poly(rC) had 4800 residues/NQO, poly(rA) had 5500 residues/NQO, and poly(rU) had 25000 residues/NQO.

B. Dark Reaction

Of cacodylate solutions of poly(rA) (2.7×10^{-3} M), poly(rU) (4.4×10^{-3} M), poly(rC)(3.3×10^{-3} M), 0.5 ml was combined with an equal volume of concentrated ^{3}H-NQO solution in 1:1 n-amylacetate:cyclohexane. These biphasic mixtures were shaken in the dark for 66 hr. The aqueous phases of each were separated and extracted with $CHCl_3$ to remove most of the nonreacted NQO from the aqueous solutions. The aqueous polymer solutions were then dialyzed against H_2O for 24 hr. The quantity of covalently bound ^{3}H-NQO for each polymer was determined by counting the radioactivity. Both poly(rA) and poly(rU) gave no evidence of covalently bound ^{3}H-NQO. Poly(rC) had one bound NQO per 85000 residues.

Reaction of NQO with DNA

A. Light Reactions

One ml of a cacodylate solution of calf thymus DNA (1.7×10^{-4} M in moles of residues per liter) and ^{3}H-NQO (1.0×10^{-6} M) was irradiated for 15 min at 15°C on the HG lamp irradiation device. The sample was then dialyzed against 300 ml H_2O for three days with the H_2O changed twice daily. The amount of NQO incorporated was determined by tritium counting - 4.6×10^{-7} M ^{3}H-NQO incorporated or 1 NQO per 370 bases. A later reaction irradiated for 2.3 min at room temperature with $[DNA]_T = 1.5 \times 10^{-3}$ M and $[^{3}H\text{-}NQO]_T = 9.0 \times 10^{-6}$ M yielded 1 NQO/3800 bases.

Another sample with $[DNA]_T = 1.5 \times 10^{-3}$ M and $[^{3}H\text{-}NQO]_T = 9.2 \times 10^{-6}$ M was irradiated for 2.3 min at 402 nm on the molectron pulsed dye laser (20 pulses/sec, average power = 2 mW). This sample was dialyzed and tritium counted as before. The yield was 1 NQO/7900 bases.

B. Dark Reaction

A solution of calf thymus DNA (1.7×10^{-3} M) and ^{3}H-NQO (6.0×10^{-5} M) was wrapped in foil and placed in a water bath at 37°C for five days. The sample was dialyzed for several days vs. H_2O. Tritium counting of the sample showed that 4.7×10^{-7} M of ^{3}H-NQO were incorporated into the DNA. This gives 1 NQO/3600 bases.

DISCUSSION

The formation of 4-hydroxyquinoline-1-oxide by NQO with either base catalysis or irradiation suggests that NQO will undergo substitution reactions at the 4-portion. The photochemically induced production in 95% EtOH of what was tentatively identified as 4-ethoxyquinoline-1-oxide further supports this suggestion. Previous studies have shown NQO to be susceptible to nucleophilic attack and substitution at the 4-position. For example, NQO seems to be particularly reactive towards the SH moiety (e.g., Okabayaski, 1953; Endo, 1958). A review by Kawazoe (1971) covers the reactions of NQO with the SH moiety as well as hydroxyl, amino, and other groups.

Not surprisingly, photoreactions of HAQO are also observed. The instability of HAQO in the light had been previously noted (Chapter II). At least one of the HAQO photoreactions in aqueous media is apparently the same as that of NQO - the production of 4-hydroxyquinoline-1-oxide. Thus, both NQO and HAQO appear susceptible to nucleophilic substitution at the 4-position.

NQO reacts photochemically with DNA which sports a variety of nucleophilic moieties, hydroxyl groups, amino groups, phosphate oxygens, and the 8-positions on the guanine and adenine bases. As is shown in figure 8, the $CoCl_2$ solution surrounding the sample cell allows the maximum amount of

light through at 360 nm - which is near the 365 nm n-π* transition of NQO. (The 365 nm NQO transition shifts with changes in solvent polarity, suggesting that it is an n-π* transition). This solutions also lets through light in the region (390-420 nm) of the bands arising from nucleic acid-NQO complexes. While the NQO photoreaction in the absence of a nucleic acid certainly involve excitation of the 365 nm transition, at least some of the NQO-nucleic acid reactions could involve excitation of the charge transfer transition. When a calf thymus DNA-NQO mixture was irradiated at 402 nm using a dye laser, a significant amount of NQO was covalently bound to the DNA. Thus, at least one of the possible NQO-DNA adducts results from exciting the charge transfer transition rather than the NQO n-π* transition. All three polynucleotides, poly(rC), poly(rU), poly(rA), also gave covalently bound NQO adducts when excited in the region (407 nm) of the charge transfer bands.

Irradiation at the charge transfer band wavelengths would appear to be preferable to irradiation with the Hg lamp source. When the Hg lamp is used, NQO not associated with the nucleic acid will also be excited, leading to production of the various photoproducts of NQO. This can cut down on the yield of photoadducts. The presence of these non-desired NQO products makes purification of the nucleic acid (with bound NQO) more of a problem. If the laser source is utilized, the NQO that has not reacted with the nucleic acid is removable using

$CHCl_3$ extraction. Further, there is circumstantial evidence (see Chapter VI) that irradiation with the Hg-lamp source produces nicking of the DNA. Some of the superhelical SV 40 DNA in samples that were irradiated using the Hg lamp source was converted to relaxed circular form. The most likely explanation for this is that the irradiation somehow nicked the DNA. Such "relaxing" or "nicking" was not observed when the laser source operating at charge transfer band wavelengths was used.

NQO was shown to react with DNA in the dark-without photo-excitation or enzymatic metabolism. The predominant concept of NQO's in vivo carcinogenic activity centers on the metabolic reduction of NQO to HAQO which might then be further activated. The finding that NQO will react without catalysis in vitro in the dark with DNA supports the view that NQO might directly react in vivo with DNA. This pathway of NQO's in vivo activity could occur in addition to the metabolic pathway. Previous authors have considered the possibility of unmetabolised NQO as the carcinogenic agent (Nakahara, 1984). The carcinogenicities of substituted NQO derivatives have been shown to correlate with their reactivities with nucleophilic reagents (Okamota & Itoh, 1963; Kawazoe & Araki, 1970). HAQO reacts photochemically, as well, to give a nucleophilic substitution product which is the same as one of those from NQO. It is then conceivable that HAQO could react with DNA in a manner very similar to that of NQO.

The base specificity of the NQO-nucleic acid reaction(s) was probed using the ribonucleotide polymers poly(rA), poly(rU), poly(rC). The use of the polymers permits easy quantitative isolation, using dialysis or ethanol precipitation, of the covalently reacted NQO from the unreacted NQO and photobreakdown products. After irradiation on the Hg lamp irradiation device, covalently bound NQO was found with all three polymers. Poly(rC) gave the greatest number of adducts. That all three polymers reacted is not extremely surprising since all possess photoreactive and/or nucleophilic groups. After irradiation on the pulsed dye laser at 407 nm, bound NQO was also found with all three polymers. Again poly(rC) had the greatest amounts of products. The charge transfer bands for all the base-NQO complexes have about the same molar absorptivities at 407 nm. Thus one might expect reactions with all the bases. In the dark reactions, only poly(rC) had covalently bound NQO. In the photoreactions poly(rC) gave more adducts per residue than did poly(rA) or poly(rU). Poly(rC) would appear to have an increased reactivity towards NQO addition relative to the other bases. (It might be noted that although poly(rG) was not studied, poly(rG) could be expected also to react with NQO.) The pyrimidine bases have been shown previously to be photo-active. For example, studies have been reported on thymine dimerization and the reactions of psoralens with the pyrimidines (Isaacs, et al., 1978). Photoaddition of alcohols to purines and pyrimidines has been reported by Frimer, et al. (1976).

Attempts were made to isolate the photoproducts of the NQO-mononucleotide reactions. While no products were isolated form dpG, dpA or dpT reaction mixtures, this does not mean that the reactions did not occur. Obviously, as the polymer experiments show NQO reacts photochemically with bases other than cytosine. An apparent photoadduct was isolated from the dpC/NQO reaction. The material eluted from a Sephadex A-25 ion exchange column at 1 M TEAB (pH = 7.6). Mononucleotides with a minus two charge at this pH elute at ca. 0.5 M TEAB; dinucleoside monophosphates at 0.15-0.25 M TEAB. The charge on the supposed adduct would appear to have roughly the equivalent of two phosphate groups. On the cellulose TLC plate, the sample traveled much more slowly than do mononucleotides. The ^{1}H NMR spectrum in the aromatic region may be assigned as follows: the broad singlet at δ 6.62 ppm from two equivalent cytidine protons probably at the 6 position (the proton at the 5 position is usually much further down field); the doublets at δ 8.28 and δ 7.75 ppm from quinoline ring protons 6 and 8; the triplet at δ 7.97 ppm from quinoline H-7; and the singlet at δ 9.20 ppm from quinoline H-2. This substitution pattern on the NQO is consistent with the published studies of the reactivity of various positions of NQO (other than the 4-position) (Kawazoe & Ohnishi, 1967). The presence of the long wavelength transition in the UV spectrum, i.e., 410 nm, would perhaps be an argument for extended conjugation.

The 335 nm transition could be due to the N-oxide group. A speculated structure for the adduct is given in figure 11. The cytosines are attached to the quinoline at positions 3 and 9. The nature of the group at position 4 is still unknown. This structure must be taken as tentative without the existence of other supportive evidence, e.g., mass spectra. The fact that the adduct isolated is a di-adduct, two cytidine residues to one quinoline moiety, does not necessarily imply that, in DNA, such diadducts would occur. The diadduct formation may merely be a consequence of the large excess of dpC in the reaction mixture and the reactivity of multiple sites on the NQO towards addition. In DNA, the reaction might occur at either position.

Figure 11: Proposed structure of the dpC-NQO photoadduct. The two dpC species are attached through their 6-positions to the 3- and 9-positions of the quinoline. The (?) at the quinoline 4-position denotes that the moiety at this position is undetermined.

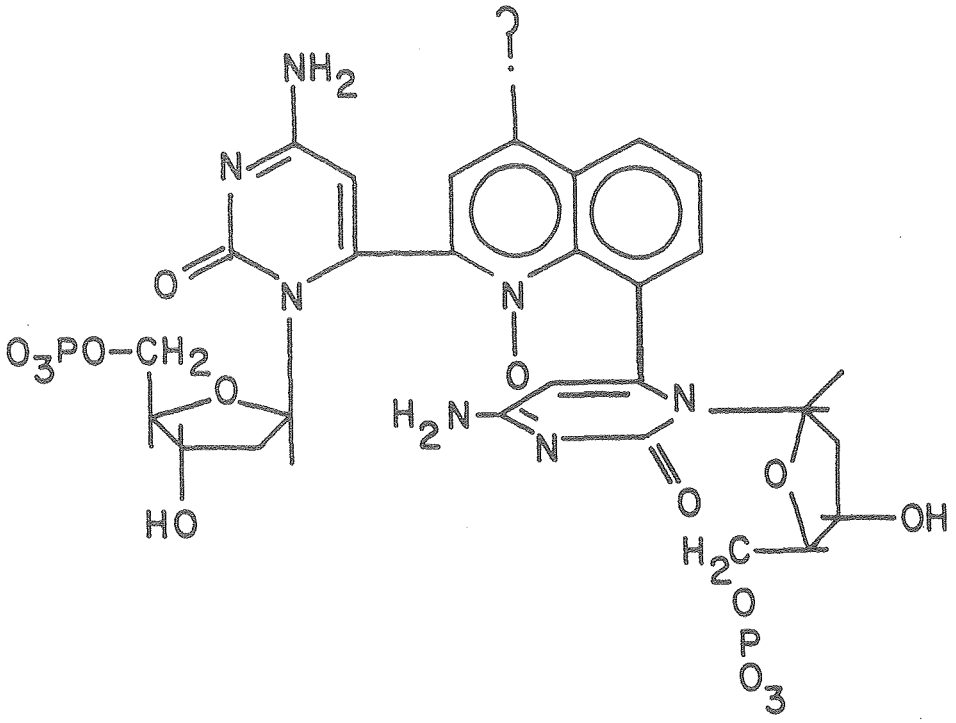
?
NH2
N
O
N
O3PO-CH2
O
HO
N
O
H2N
N
N
O
O
H2C
O
P
O3
OH

CONCLUSIONS

These studies show, as they were designed to do, that NQO reacts, both in the presence and the absence of irradiation, directly with nucleic acids. Some of the reactions with the different bases involve the charge transfer transition. A structure (figure 11) for the dpC-NQO diadduct was proposed. Much more work could be done on delineating other NQO-nucleic acid adduct structures, such as those found in poly(rA) and poly(rU). The information obtained gives sufficient background for employing the photoaddition of NQO as a probe for sequence or structural feature specificity of NQO-DNA interactions. This work will be discussed in Chapter VI.

CHAPTER V

EQUILIBRIA OF NONCOVALENT NQO BINDING TO DNA

INTRODUCTION

In this chapter the focus will again be on noncovalent NQO-nucleic acid interactions - specifically, the equilibrium binding of NQO to different DNA's. Paul & Montgomery (1970) investigated the NQO-calf thymus DNA equilibrium. DNA melting in the presence of NQO was monitored by observing the change with temperature in the absorbance at 260 nm. These experiments showed that NQO increased the T_m's of native calf thymus DNA, poly[dG·dC] and to a lesser extent poly[d(A-T)·d(A-T)]. Based on data obtained by monitoring the charge transfer band from NQO-DNA base interactions, they reported equilibrium constants for what they termed "strongly" and "weakly" reactive sites. Their binding data gave a curved Scatchard plot and it is not obvious that it represents two types of binding. The curvature, rather than representing two (or more) types of binding, could be due to competition for the binding sites. Their solutions of DNA and NQO had a high NQO molecule to DNA phosphate ratio. If there existed in the DNA a small number of "primary" NQO binding sites accompanied by a larger number of "secondary" sites, the use of high NQO molecule to DNA phosphate ratios could fill completely the primary sites. Under such experimental conditions, the binding to the "secondary" rather than primary sites would be observed.

Paul and Montgomery did not apparently correct in their complex band difference spectra for DNA absorption. If the DNA solution absorbs at the complex band wavelengths, then the absorbances recorded in the difference spectra for the DNA-NQO mixtures would be a sum of the DNA absorbance and the complex absorbance. Without the correction for DNA absorption, the amounts of complex determined from the difference spectra will be too high.

In this chapter, the experiments on the equilibrium binding of NQO to calf thymus DNA, E. coli DNA, SV 40 DNA and the plasmid pBR 322 are reported. The initial experiments with calf thymus and E. coli DNA made use of the charge transfer bands to monitor the equilibria. It was desirable to study the equilibria at very high DNA phosphate to NQO ratios. To attain this condition, very low NQO concentrations were needed - below the optical spectroscopy range. Attempts at using equilibrium dialysis or filter assay methods with tritium labeled NQO were unsuccessful since NQO binds to both the cellulose dialysis tubing and the Millipore filters. The method finally chosen was the phase partition method, developed by Waring (1975). Phase partitioning has been used successfully by Waring (1975), Davanloo & Crothers (1976), and recently by Hogan et al. (1979) to study drug-nucleic acid equilibria.

In this method, the drug is dissolved in a solvent that is not miscible with water and that has a high boiling point. The partition coefficient in the absence of DNA between the aqueous and organic phases is determined. The excess amount going from the organic phase into the aqueous phase with DNA present is the quantity bound to the DNA. Data from the phase partition experiments using NQO with the different DNA's was analysed to give the equilibrium constants and binding ratios for NQO-DNA complex formation.

EXPERIMENTAL

Materials

Calf thymus DNA and *E. coli* DNA were obtained from Worthington Biochemicals. The pBR 322 plasmid (a mixture of relaxed and superhelical circular DNA) was a gift from Dr. Kyong Yoon. Partially purified SV 40 DNA from infected green monkey cells was obtained from Dr. James Bartholomew. This DNA was further purified using phenol extraction and centrifugation to obtain supercoiled SV 40 (a mixture of circular relaxed and superhelical DNA). An additional amount of supercoiled SV 40 was obtained from Bethesda Research Laboratories. The synthesis of the "cold" NQO was described in Chapter II.

For the synthesis of ^{3}H-labeled NQO, 300 mg quinoline-1-oxide (Aldrich, recrystallized from diethyl ether) were sent to New England Nuclear for labeling. 100 mg of impure

^{3}H-quinoline-1-oxide were returned. 50 mg of the obtained ^{3}H-quinoline-1-oxide was dissolved in 0.4 ml of concentrated HNO_3, followed by stirring. The reaction mixture was maintained at 65-70°C for 2 hr in a water bath. Ice chips were then added to precipitate the ^{3}H-NQO. The mixture was filtered through a millipore filter to collect the precipitate. The precipitate was removed from the millipore filter with acetone (which also dissolved the filter). The acetone solution was then sent through an acid washed alumina column to purify. The acetone was then evaporated from the sample and the ^{3}H-NQO redissolved in the solvent which was required for a given experiment. Purity was checked using the UV absorption spectrum and TLC. The n-amylacetate: cyclohexane solutions of ^{3}H-NQO used in the phase equilibrium studies below could also be passed through the alumina column. Solutions of ^{3}H-NQO were stored in a refrigerator to limit decomposition.

Tritium Counting

The liquid scintillation counting cocktail consisted of 2000 ml toluene, 1000 ml Triton X-100 (a solubilizer, Sigma) and 12 gm Omnifluor (New England Nuclear). For counting, 10 ml of this cocktail was mixed with approximately 1 ml of cacodylate buffer to which had been added an aliquot of the sample, e.g., 50 µl. Tritium counting was done on a Beckman LS-230 liquid scintillation counter. To determine the cpm-to-molarity conversion factor, counts were made of solutions

of ^{3}H-NQO for which concentrations had been determined optically. The determined conversion factor was 3.79×10^{-11} mmoles/cpm. For the conversion: (cpm of the sample) x (3.79×10^{-11} mmoles/cpm) ÷ (volume of the aliquot in ml) gives the molarity of the sample. Specific activity was calculated assuming a 40% counting efficiency by the Beckman LS-230 counter. The calculated specific activity of the ^{3}H-NQO was 30 mCi/mmole.

Optical Studies of DNA-NQO Equilibrium Binding

Stock solutions of calf thymus DNA, E. coli DNA and "cold" NQO were made up in the cacodylate buffer described in Chapter III. The DNA solutions were dialysed overnight against the buffer. Concentrations were measured using the absorbance at λ_{max} (250 nm) for NQO and the absorbance at 260 nm for the DNA's (ε_{260}(calf thymus) = 6.25×10^{3} ℓ $M^{-1}cm^{-1}$ per residue; ε_{260}(E. coli) = 6.54×10^{3} ℓ $M^{-1}cm^{-1}$ per residue (Allen, et al. (1972))). It should be noted that the DNA concentrations given in this dissertation are, unless otherwise noted, in terms of moles of residues per liter. Glass tuberculin syringes were used for the measurements of DNA and NQO solution volumes.

Two types of optical studies were conducted. In the first, difference spectra of the complex bands were recorded. Samples were prepared by placing a fixed volume of stock NQO solution in each sample tube ($[NQO]_T$ ranged from ca.

1.5×10^{-4} to 2.6×10^{-4} M), adding a given volume of DNA solution ($[DNA]_T$ ranged from 6.7×10^{-3} to 1.3×10^{-3} M) and then adding sufficient buffer to give constant volume. Absorption spectra in the region of the complex band (460-380 nm) were recorded for each DNA-NQO mixture vs. a solution of equal $[NQO]_T$ to produce difference spectra. Absorption spectra of the samples in 0.2 cm pathlength cells were recorded at 25°C on a Cary 118 spectrometer.

In the second study, the total absorption spectra in the region (460-380 nm) of the charge transfer band were recorded. Samples were prepared in the same way as above, except the DNA concentration was fixed and the NQO concentration was varied. Absorption spectra of samples in 0.2 cm cells were recorded on the Cary 118. The $[DNA]_T$ ranged from ca. 2 to 6×10^{-3} M and $[NQO]_T$ ranged from ca. 6×10^{-6} to 3×10^{-4} M. For calf thymus DNA, the experiments were conducted at 7, 15, 25, 30, 35°C and for E. coli DNA, the experiments were carried out at 25°C. The study was also done at 25°C with heat denatured calf thymus DNA prepared by boiling and quickly cooling a solution of double stranded DNA. The sample concentrations for the experiment with single strand DNA were in the same range as for the double strand DNA.

The ε(DNA) values at the complex λ were obtained by measuring the absorption at these λ of DNA solutions of concentrations similar to those of DNA-NQO mixtures. The ε(NQO) at complex λ were similarly obtained.

Phase Partition Studies of DNA-NQO Equilibrium Binding

After trying $CHCl_3$, $CHCl_3$:n-amyl acetate (1:1), and cyclohexane as the non-aqueous solvent for the phase partition experiments a 1:1 n-amyl acetate:cyclohexane solution was chosen. This solvent system was used because the boiling points of these two organic compounds were relatively high (compared to $CHCl_3$, for example) and because the partition coefficient of NQO was low [P(aqueous/organic) ≈ 0.08]. A low "background" amount of free NQO in the aqueous layer is desirable so that small concentrations of bound material can be detected. Having a small aqueous/organic partition coefficient gives this. (Some of the data for calf thymus DNA were collected using $CHCl_3$ as the organic phase.) Stock solutions of ^{3}H-NQO were prepared in the 1:1 n-amylacetate:cyclohexane and were stored in a refrigerator. Stock solutions of calf thymus DNA (native or denatured), E. coli DNA, SV 40 DNA (supercoiled or linear) and pBR 322 (supercoiled or linear) were prepared in the cacodylate buffer as described in the optical study. The percentages of supercoiled DNA in the "superhelical" SV 40 and pBR 322 samples were estimated using gel electrophoresis on 1% agarose (see Chapter VI for details of the electrophoresis procedures). The relative amounts of the two forms of circular DNA were judged by the relative intensities of the relaxed and superhelical bands. For pBR 322, the DNA was approximately 2:1 superhelical:relaxed; for SV 40 DNA, the ratio was 8:2 superhelical:relaxed. DNA concentrations were

determined using the absorbance at 260 nm. For pBR 322, the ε_{260}(*E. coli*) was used and for SV 40, ε_{260} = (6.3×10^3 ℓ $M^{-1}cm^{-1}$ per residue (which is roughly that of calf thymus DNA) was used. Again, glass tuberculin syringes were used to measure volumes. Samples were prepared by combining a a fixed volume of DNA stock solution with a fixed volume of cacodylate buffer to produce the desired DNA concentration ($[DNA]_T$ ranged from ca. 8.0×10^{-6} to 1.1×10^{-3} M). The organic phase was prepared by combining a variable amount of stock NQO solution with a sufficient volume of 1:1 n-amyl acetate:cyclohexane to produce constant volume ($[NQO]_T$ in the aqueous phase after mixing ranged from ca. 2×10^{-8} to 1×10^{-5} M). Equal volumes (typically 0.2 ml of the aqueous and organic solutions were combined in capped 0.5 ml plastic Eppendorf centrifuge tubes and were shaken on a mechanical shaker for a minimum of 2 hr at room temperature. The mixtures were centrifuged at low speed for 30 sec to separate the phases. Aliquots, e.g., 30 µl, from the aqueous and organic phases were tritium counted to give the NQO concentrations. Gel electrophoresis was conducted with SV 40 and pBR 322 DNA samples after the mixing to ensure that the phase partition method does not damage the DNA. If the shaking of the aqueous DNA solutions with the organic NQO solutions produced nicks in the DNA, the relaxed DNA linear DNA gel bands would increase in magnitude and the superhelical gel bands would decrease. This did not happen. The partition

coefficient for NQO between these two phases was determined by shaking cacodylate buffer with the organic solution. The partition coefficient was checked periodically to monitor possible changes in organic solution composition.

The linear SV 40 and pBR 322 DNA's used in these experiments were prepared by cutting the circular DNA's with the restriction enzyme Eco R1 (Miles Laboratories). Eco R1 has one cutting site on both DNA's. A solution of either DNA was dialyzed from the cacodylate buffer into the Eco R1 buffer (100 mM Tris-HCl, 5 mM $MgCl_2$, 2 mM 2-mercaptoethanol, 50 mM NaCl, pH 7.2). An appropriate amount of enzyme (20 units for 35 µg pBR 322 DNA, 500 units (excessive) for 140 µg SV 40 DNA) was combined with each DNA solution and the mixtures were incubated at 37°C for 1 hr. The enzyme was extracted with 90% phenol and the DNA was precipitated by addition of 2 volumes cold 95% EtOH. The DNA was dissolved in cacodylate buffer and dialyzed vs. cacodylate buffer to remove any phenol.

DNA-NQO Phase Equilibrium in the Presence of Ethidium

Samples of superhelical SV 40 DNA (1.02×10^{-4} M) with ethidium (8.22×10^{-7} M) were made up in cacodylate buffer from stock SV 40 and ethidium solutions. The ethidium solution was prepared by dissolving ethidium bromide (Sigma) in cacodylate buffer. The aqueous SV 40-ethidium solutions were combined with ^{3}H-NQO in 1:1 n-amyl acetate:cyclohexane and shaken for 2 hr at room temperature. In the aqueous

phase after shaking, $[NQO]_T$ ranged from ca. $2\text{-}9\times10^{-7}$ M. The phases were separated and worked up as above. The partition coefficient for ^3H NQO in the presence of ethidium between aqueous and organic phases was determined by shaking a cacodylate solution of ethidium (8.22×10^{-7} M) with the organic ^3H-NQO solution.

Phase Equilibria of t-RNA and ^3H-NQO

Samples of yeast phenylanine ε-RNA (Boerhinger Man or Sigma) ($[\varepsilon RNA]_T$ ranged from 5×10^{-6} to 1×10^{-4} M) and ^3H NQO ($[NQO]_T$ (in aqueous phase after mixing) ranged from ca. 1×10^{-7} to 6×10^{-6} M) were prepared as described for the DNA experiments. Mixtures of the aqueous tRNA and NQO dissolved in 1:1 n-zmyl acetate:cyclohexane were shakend for 2 hr at rrom temperature. Phases were separated by centrifugation and aliquots counted. No significant equilibrium binding of NQO to tRNA was observed.

RESULTS

In the difference absorption spectra, the charge transfer bands ($\lambda_{max} \approx 415$ nm) for the NQO-DNA complexes were observed. The difference spectral studies were used to obtain the complex molar absorptivities, ε_c, for the NQO-DNA complexes. Plots of $1/A_c$ (where $A_c = A_T - A_{DNA}$) vs. $1/[DNA]_T$ were made. The A_{DNA} were calculated using the $[DNA]_T$ and the experimentally determined $\varepsilon_{415}(DNA)$. In the difference spectra, $A_c = \ell(\varepsilon_c - \varepsilon_{NQO} - \varepsilon_{DNA})c$ where c is the complex concentration at very large $[DNA]_T$ ($1/[DNA]_T \rightarrow 0$), all of the NQO is bound, i.e., $[NQO]_T = c$. From the

extrapolated value of $1/A_c$ where $1/[DNA]_T = 0$, the term $(\varepsilon_c-\varepsilon_{NQO}-\varepsilon_{DNA})$ was obtained for each DNA used. The values of ε_c thus obtained at 25°C were 2500±100 $\ell\ M^{-1}cm^{-1}$ for calf thymus DNA and 2700±100 $\ell\ M^{-1}cm^{-1}$ for E. coli DNA. The values of ε_c were used to obtain the [c] in the DNA-NQO solutions of the second optical study.

In the second optical study the total absorption spectra in the region of the complex bands was recorded. Thus, $A_T = A_{DNA} + A_{NQO} + \ell(\varepsilon_c-\varepsilon_{NQO}-\varepsilon_{DNA})c$. The values of A_{DNA} and A_{NQO} were calculated using $[DNA]_T$ and $[NQO]_T$ and the experimentally determined $\varepsilon_{415}(DNA)$ and $\varepsilon_{415}(NQO)$. The complex concentrations were then calculated:

$$c = A_c/\ell(\varepsilon_c-\varepsilon_{NQO}-\varepsilon_{DNQ})$$

where $A_c = A_t-A_{DNA}-A_{NQO}$, and $(\varepsilon_c-\varepsilon_{NQO}-\varepsilon_{DNA})$ had the value determined above. The amount of free NQO in solution was $c_F = [NQO]_T - c$. The obtained values of c and c_F were then used to obtain the equilibrium constants and binding ratios as will be described later in this section.

Using tritium counting counting, the total amounts of ^3H NQO in the aqueous and organic phases from the phase partition experiments were determined. The amount of free NQO in the aqueous phase, c_F, was calculated for each sample:

$$c_F = Pc_o$$

where c_o is the concentration in the organic phase and P is the aqueous to organic partition coefficient. The amount of NQO complexed is simply $c = [NQO]_T - c_F$, where $[NQO]_T$ is in this case the total amount of NQO in the aqueous phase. The data for each type of DNA from both methods of determining c were combined in one analysis. For calf thymus DNA, E. coli DNA, and superhelical SV 40 and pBR 322, the obtained values of c and c_F at each $[DNA]_T$ and $[NQO]_T$ were used to make a Scatchard plot:

$$r/c_F = (R-r)K$$

In this equation $r = c/[DNA]_T$, $c_F = [NQO]_T - c$, R is the binding ratio (bound NQO/residue). The Scatchard plots for the different DNA systems at 25°C are given in figures 12 a-d and for calf thymus DNA at other temperatures in fig. 12e. The equation for this type of plot assumes independent binding sites for each NQO, i.e., no cooperativity or competition in the binding. If there were two types of sites, the observed plot would be a combination of the curves for both. This situation would appear similar to binding with competition for the sites. As fitures 12a-d show, the binding curves for the different DNA's go through maxima. This is indicative of cooperativity in the binding of NQO to the DNA's.

Figure 12a-e: Scatchard plots for NQO binding to the various DNA's. Concentrations $[DNA]_T$ from ca. 8×10^{-6} to 6×10^{-3} M, $[NQO]_T$ (in the aqueous phase) from ca. 2×10^{-8} to 3×10^{-4} M in cacodylate buffer (pH 7.0.

(a) - (d), 25°C.

(e) 7°(△--△), 15°(o—o), 30°(▲--▲), 35°C(●—●).

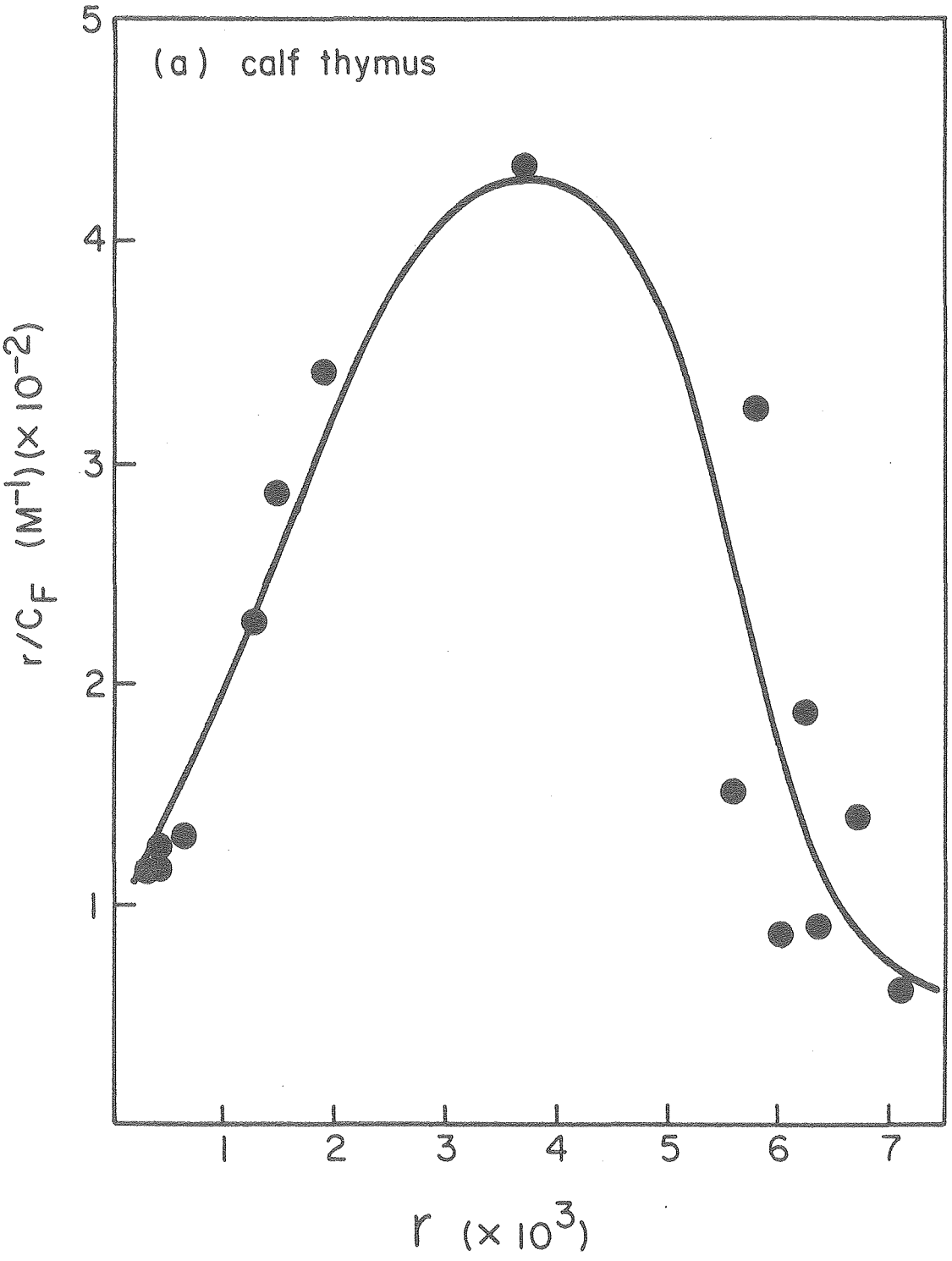

XBL 797-10715

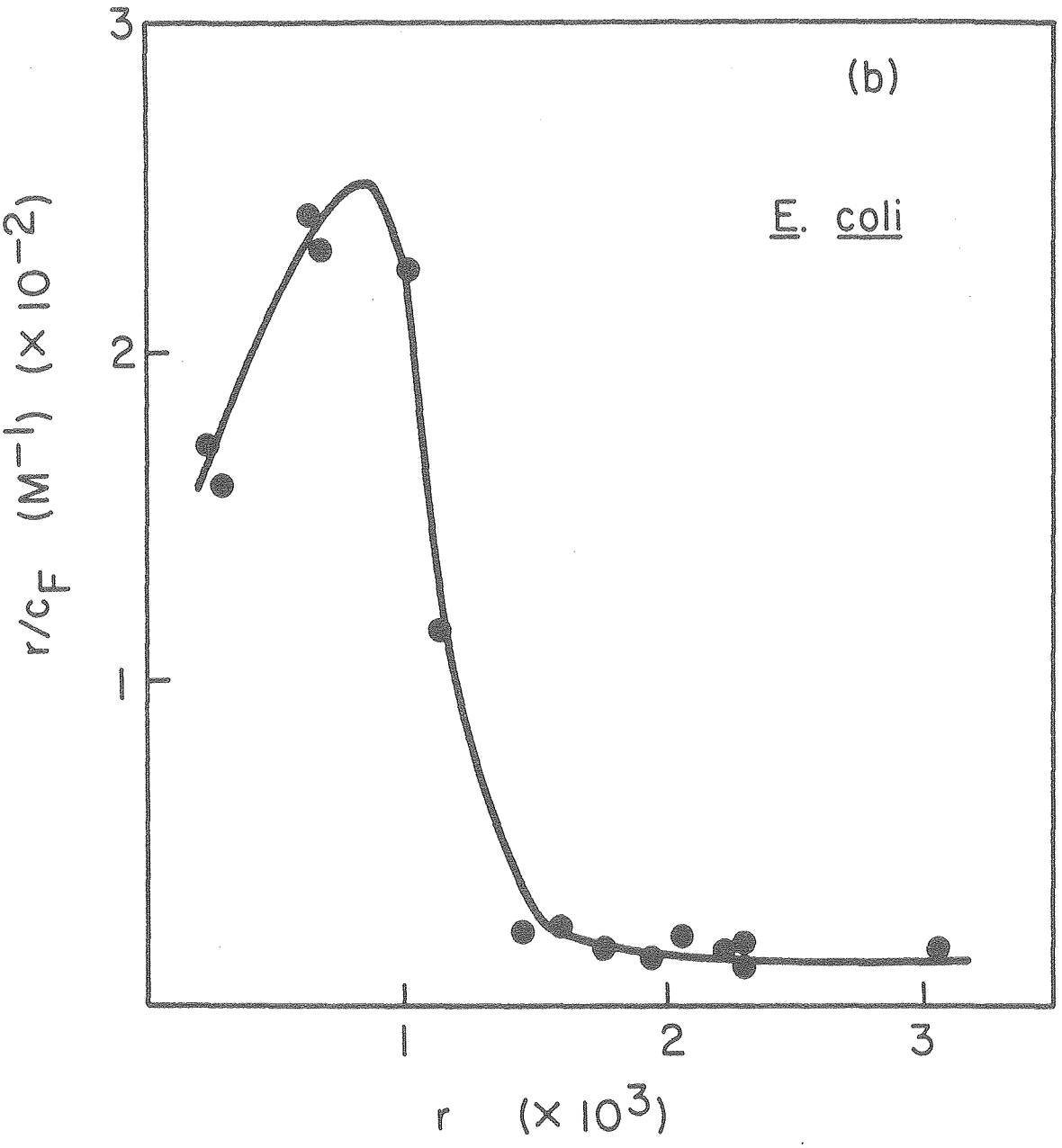

XBL 798-10855

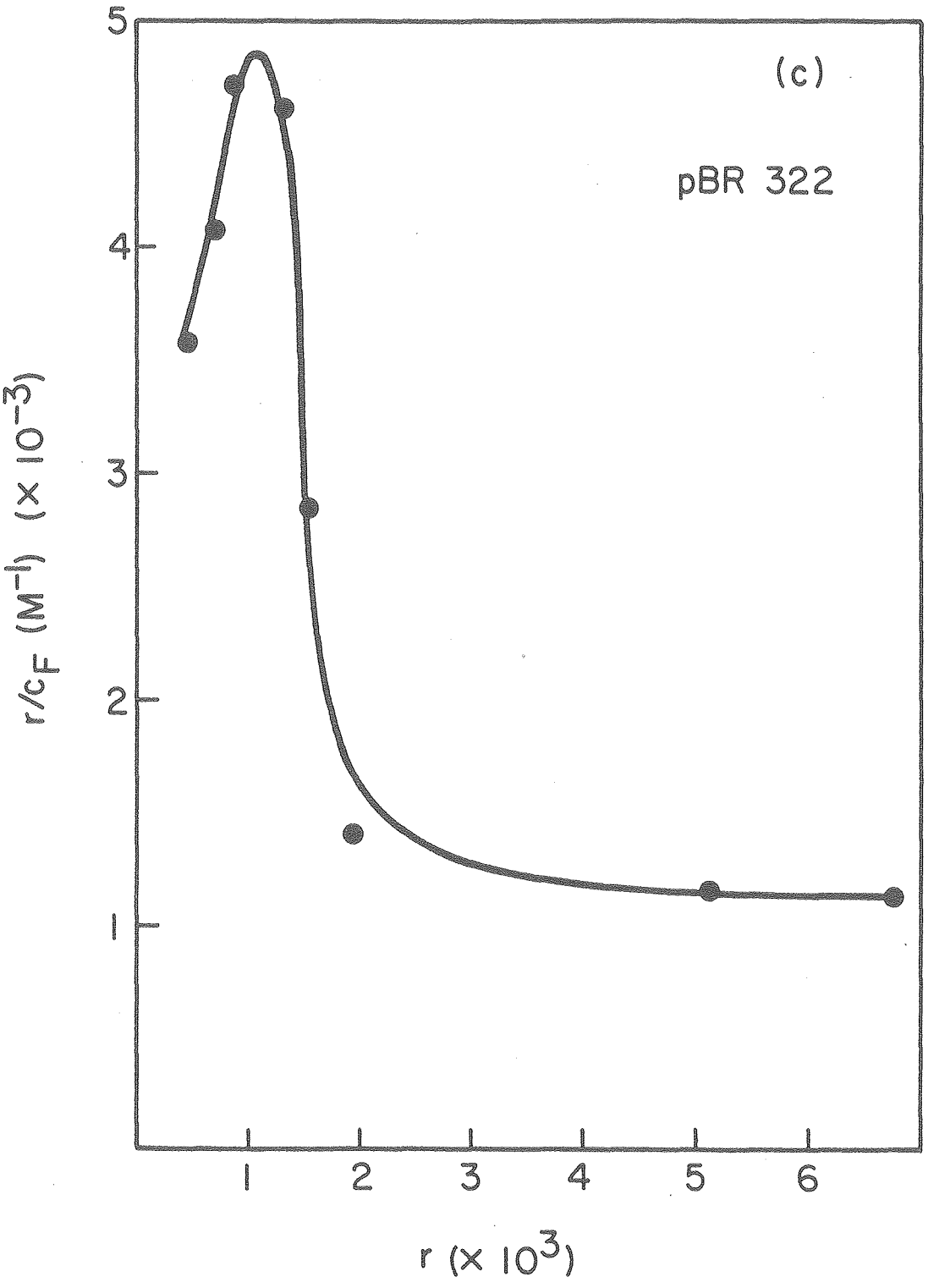

XBL 798-10856

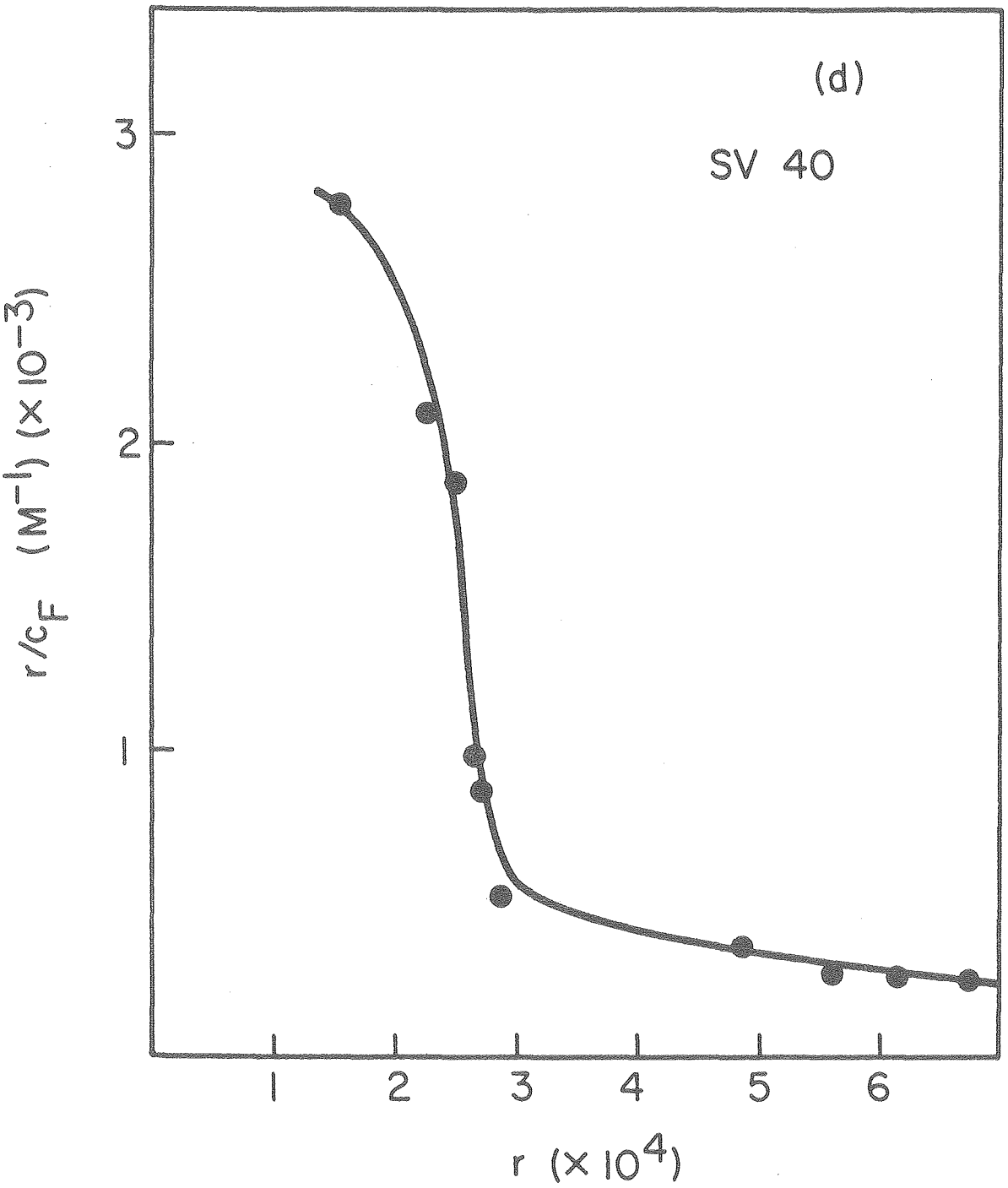

XBL 798-10857

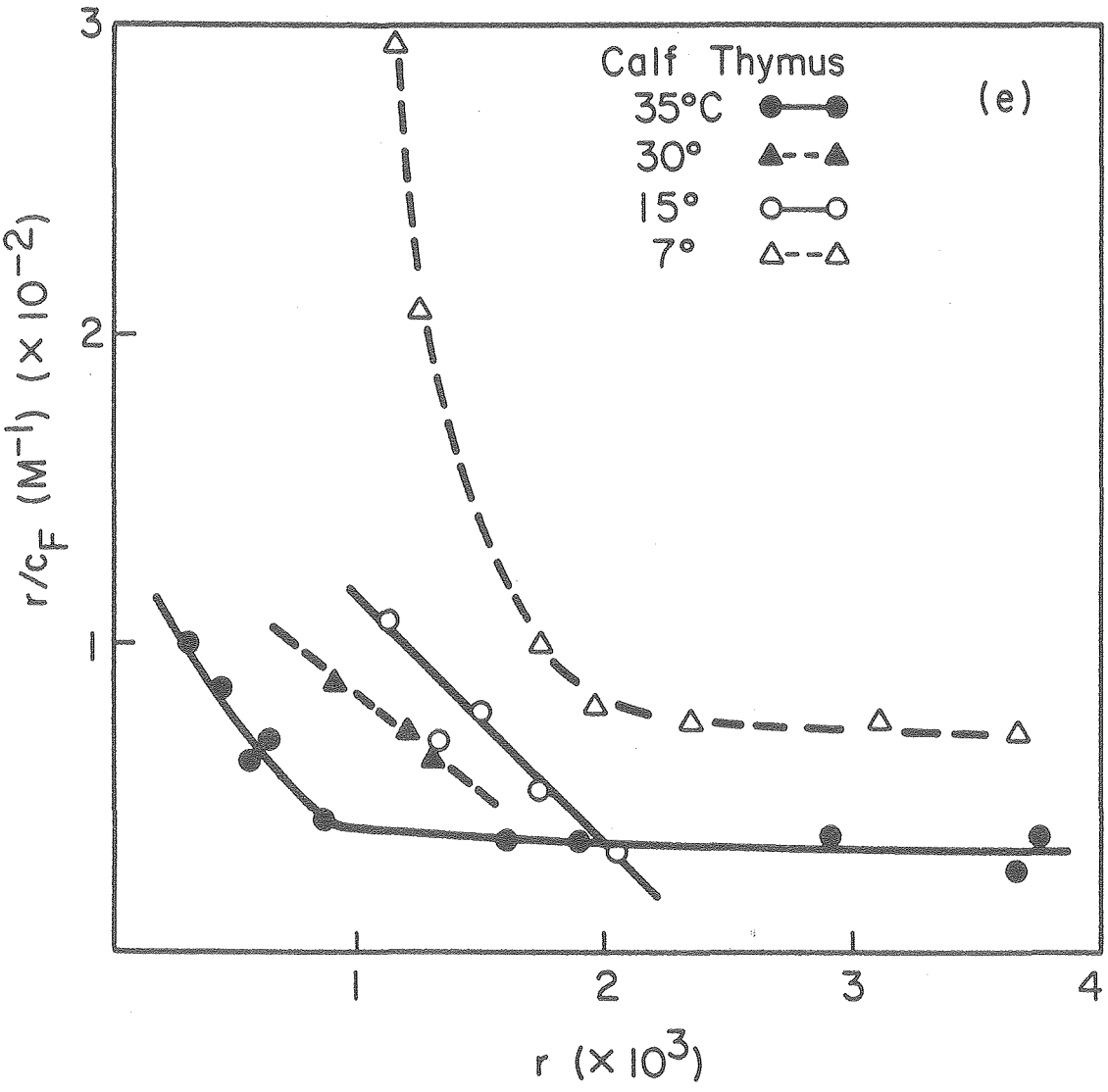

XBL 798-10858

The degree of cooperativity was assayed using Hill plots, $\ln(\bar{r}/N-\bar{r})$ vs. $\ln c_F$, where $\bar{r} = rR$ and N is the number of NQO molecules binding cooperatively. If N molecules are binding cooperatively, the slope of the plot will equal N. As a first approximation, the values of R were taken from the Scatchard plots (figure 12) by extrapolating the downward slope of the curve to the r-axis. This is similar to how R may be determined for "normal" Scatchard plots. The values of N tried were 1, 2, and 3. The data for r and c_F was that used in the Scatchard plots (figure 12a-d). A representative Hill plot is shown in figure 13. At the higher r values [the less negative $\ln(\bar{r}/N-\bar{r})$ values] the plot deviates from linearity. At these higher r the strong binding sites are filling (or are filled since R is only approximate) and there may be some binding to weaker sites. Accordingly, the slope of the plot was determined by taking those points up to where the plot begins to curve (as is shown). The best fits of the data for all four DNA's (at 25°C) occurred with N=2, two NQO molecules bound per site. At this value of N the slopes came the closest to equaling N.

An equation similar to the Scatchard equation used above was derived for a binding model in which two NQO molecules bind in a highly cooperative fashion to independent sites: $(2KR/r) - K = 1/c_F^2$, or $K(2R-r) = r/c_F^2$.

Figure 13: Hill plot for calf thymus DNA + NQO (25°C). Data is that used in Scatchard plot (fig. 12a). R = 100 used to calculate $\bar{r}$'s. This R determined in figure 14a as described in text. The points labeled ® used to determine slope.

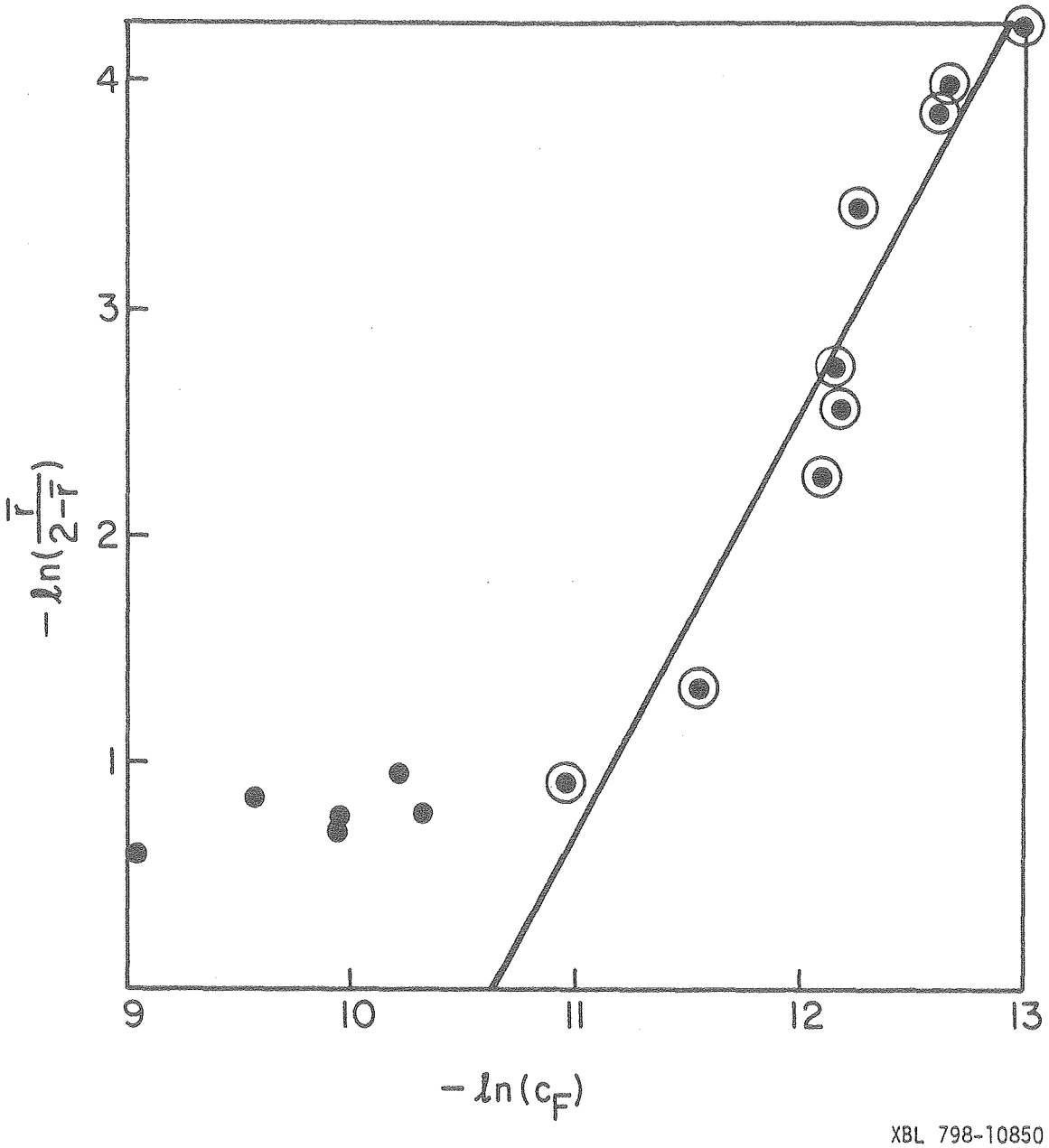

XBL 798-10850

In these equations, R is still the number of sites but there are now two NQO molecules per site. Thus, where $r/c_F^2 = 0$, the value of r equals the binding rates in terms of the number of NQO molecules per residue or the number of sites per base pair. The data for the different DNA systems at 25°C, calf thymus, E. coli, SV 40 (superhelical and linear), pBR 322 (superhelical and linear) are given in figures 14 a-d. The equilibrium constants and binding ratios from these plots are presented in Table VIII. As a check on the Hill plots constructed as described earlier with the approximate R values from the Scatchard plots in figures 12 a-d, new Hill plots were made using the R values from the plots in figures 14 a-d. As with the Hill plots described above, the slopes of this second set of plots also equaled two (approximately), supporting the use of the two NQO molecules per site equations.

The binding of NQO to superhelical SV 40 DNA in the presence of ethidium was also explored. The binding data, obtained using the phase equilibrium method, was fitted to the 2 NQO molecules per site equation, as is shown in figure 14e. The equilibrium constant obtained from this plot is 6×10^{12} M^{-2} and the binding ratio is 1 site per 1700 base pairs.

Figure 14:

(a) Calf thymus DNA + NQO binding data (25°C) using the equation $(2KR/r) - K = 1/c_F^2$.

(b)-(d) Binding data (25°C) for E. coli, pBR 322, SV 40 + NQO using the equation $2KR-rK = r/c_F^2$.

For (a)-(d), $[DNA]_T$ ranged from 8×10^{-6} to 6×10^{-3} M; $[NQO]_T$ (in aqueous phase) from 2×10^{-8} to 3×10^{-4} M in cacodylate buffer (pH 7.0).

(e) SV 40 DNA + NQO binding data (25°C) in the presence of ethidium. $[DNA]_T = 1.0\times10^{-4}$ M; $[NQO]_T$ (in aqueous phase) $\simeq 2.9\times10^{-7}$ M; $[ethidium]_T \simeq 8\times10^{-7}$ M in cacodylate buffer (pH 7.0). Equation used: $2KR - rK = r/c_F^2$.

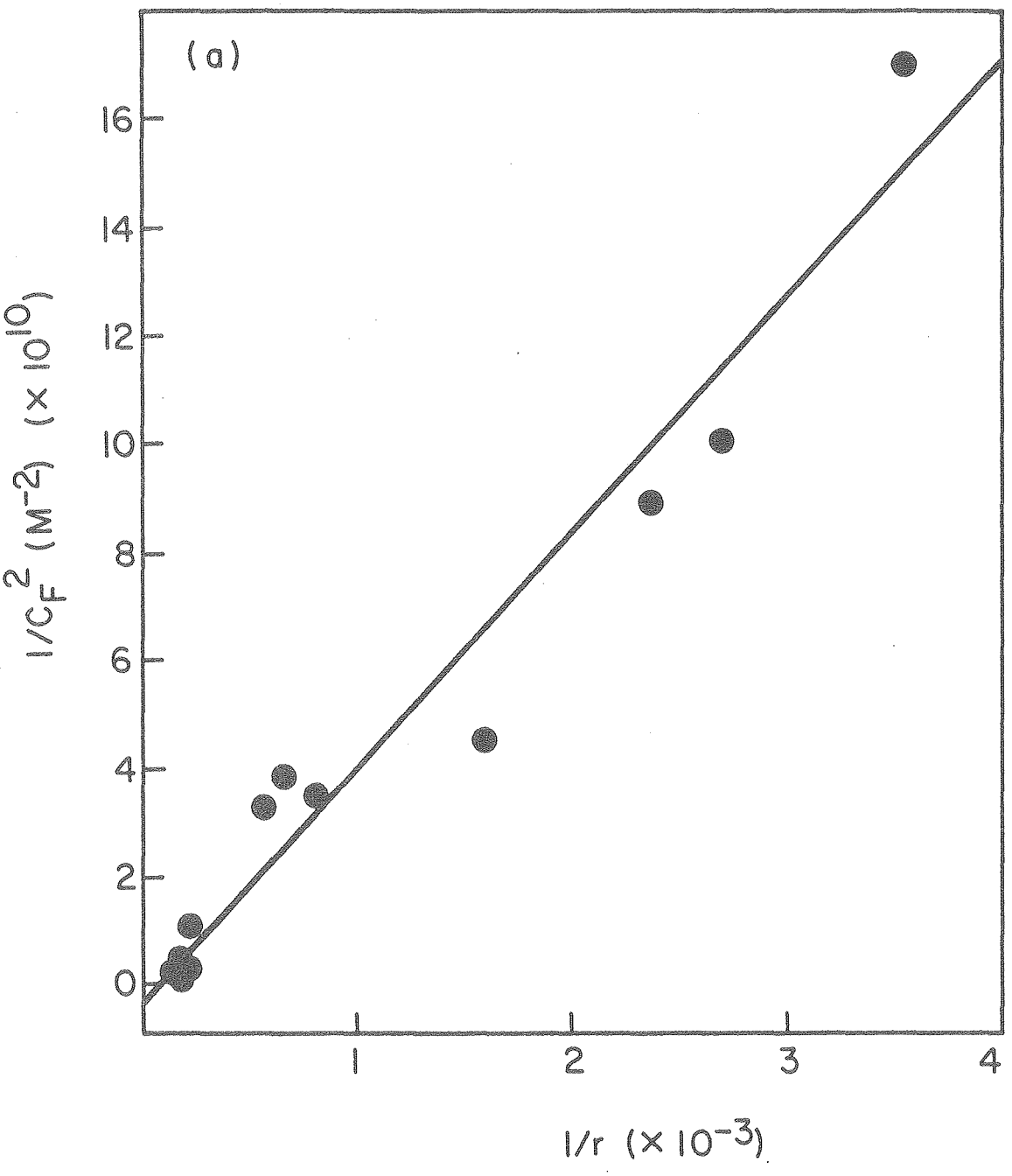

XBL 797-10714

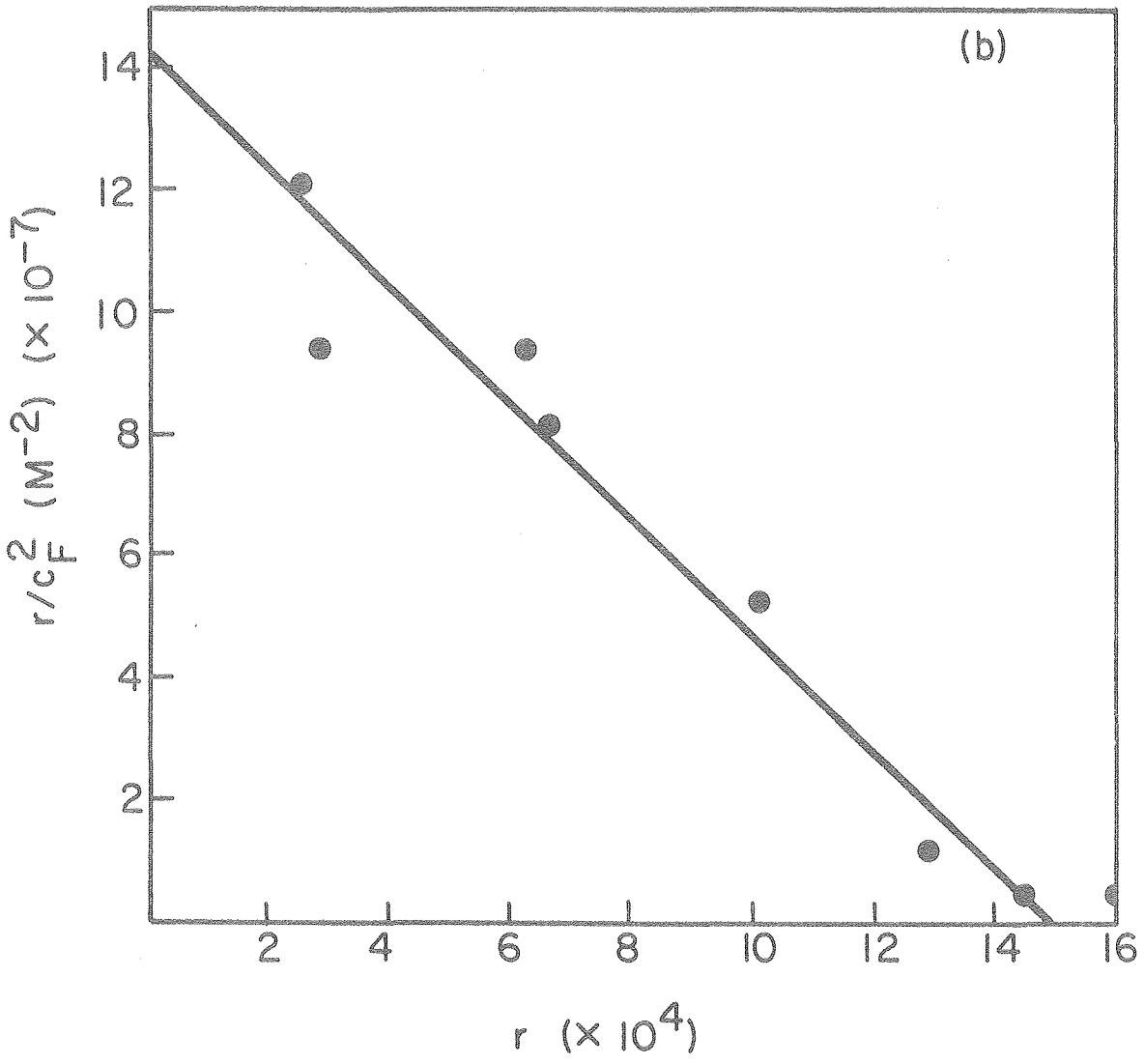

XBL 798-10853

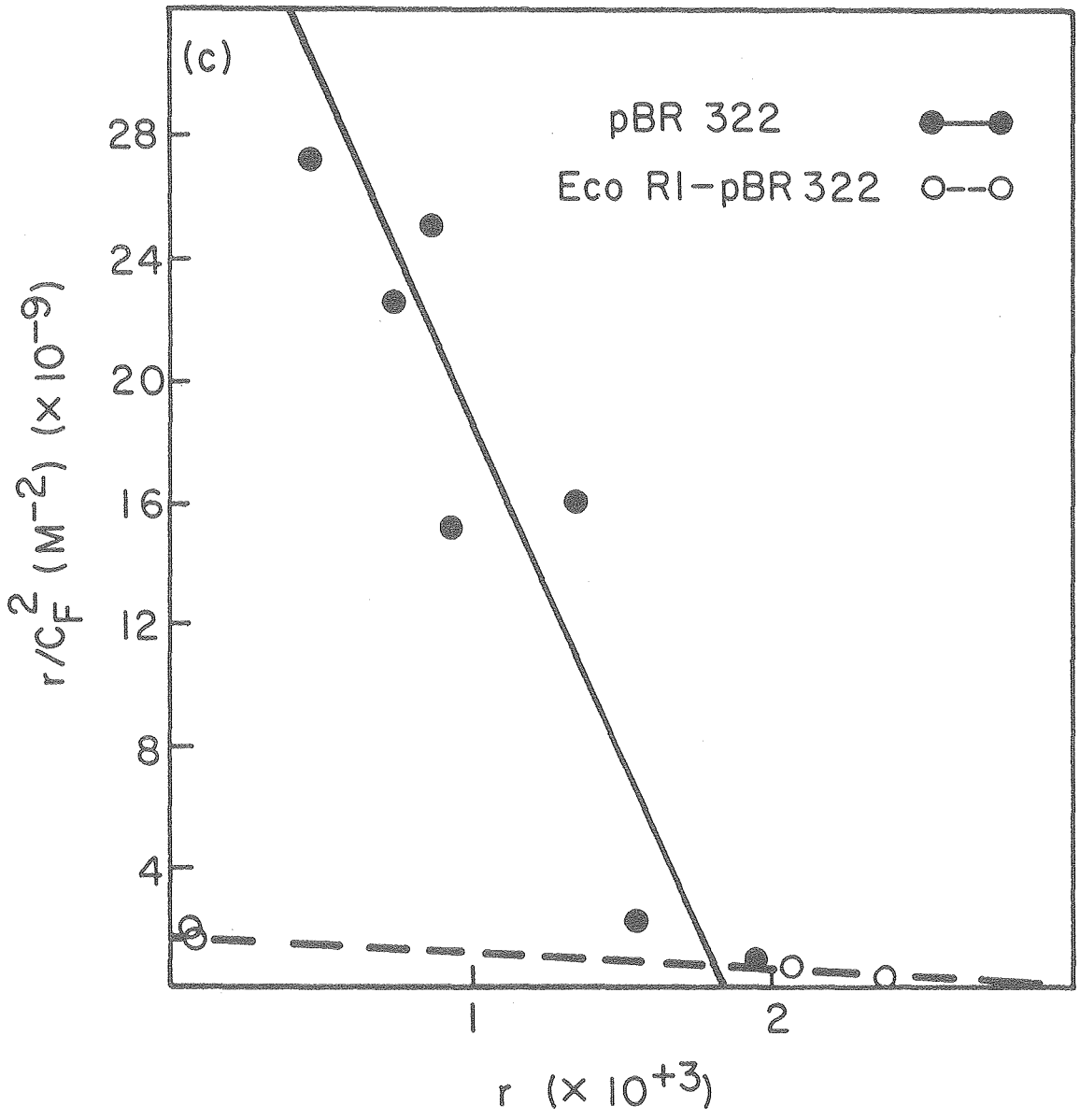

XBL 797-10713

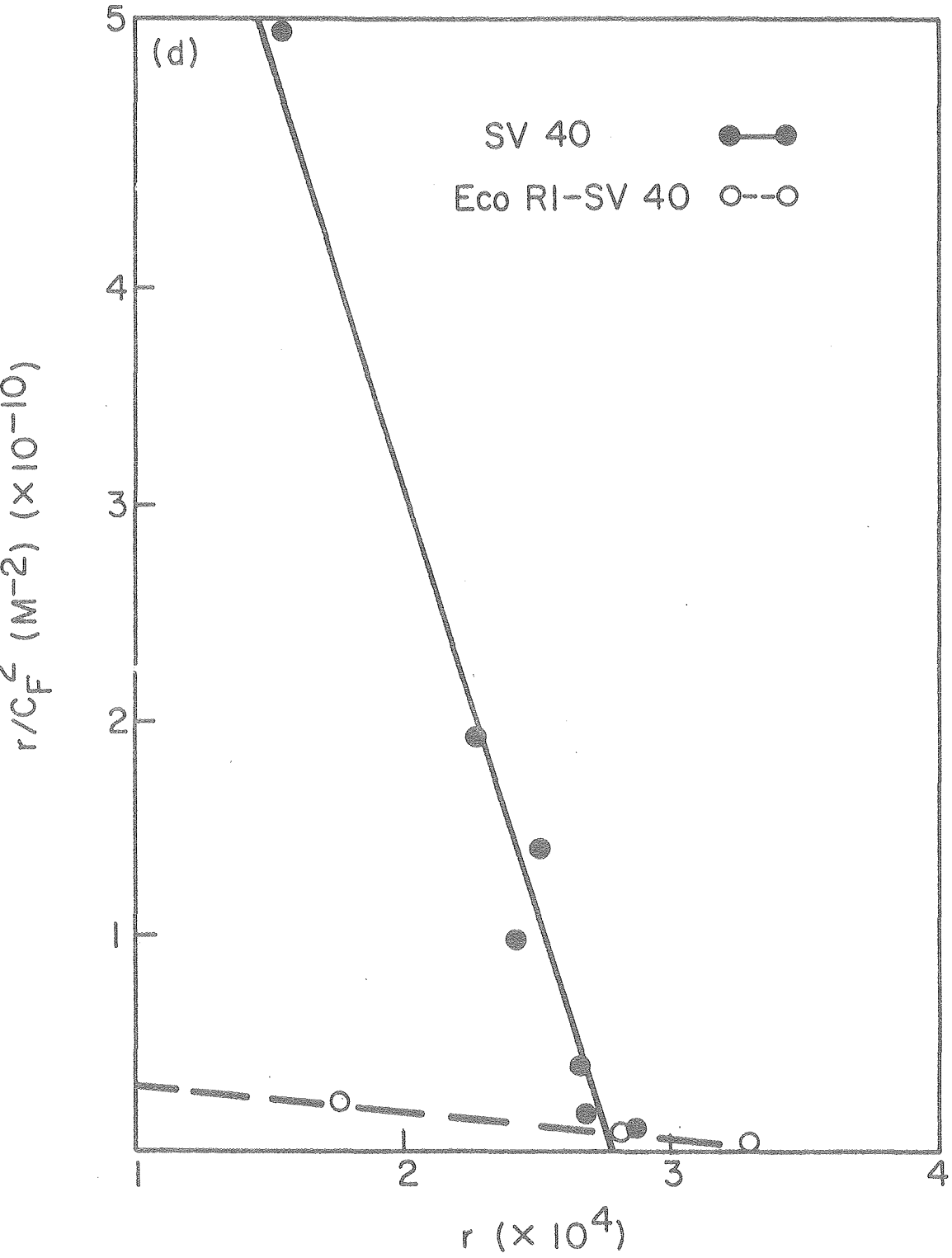

XBL 797-10712

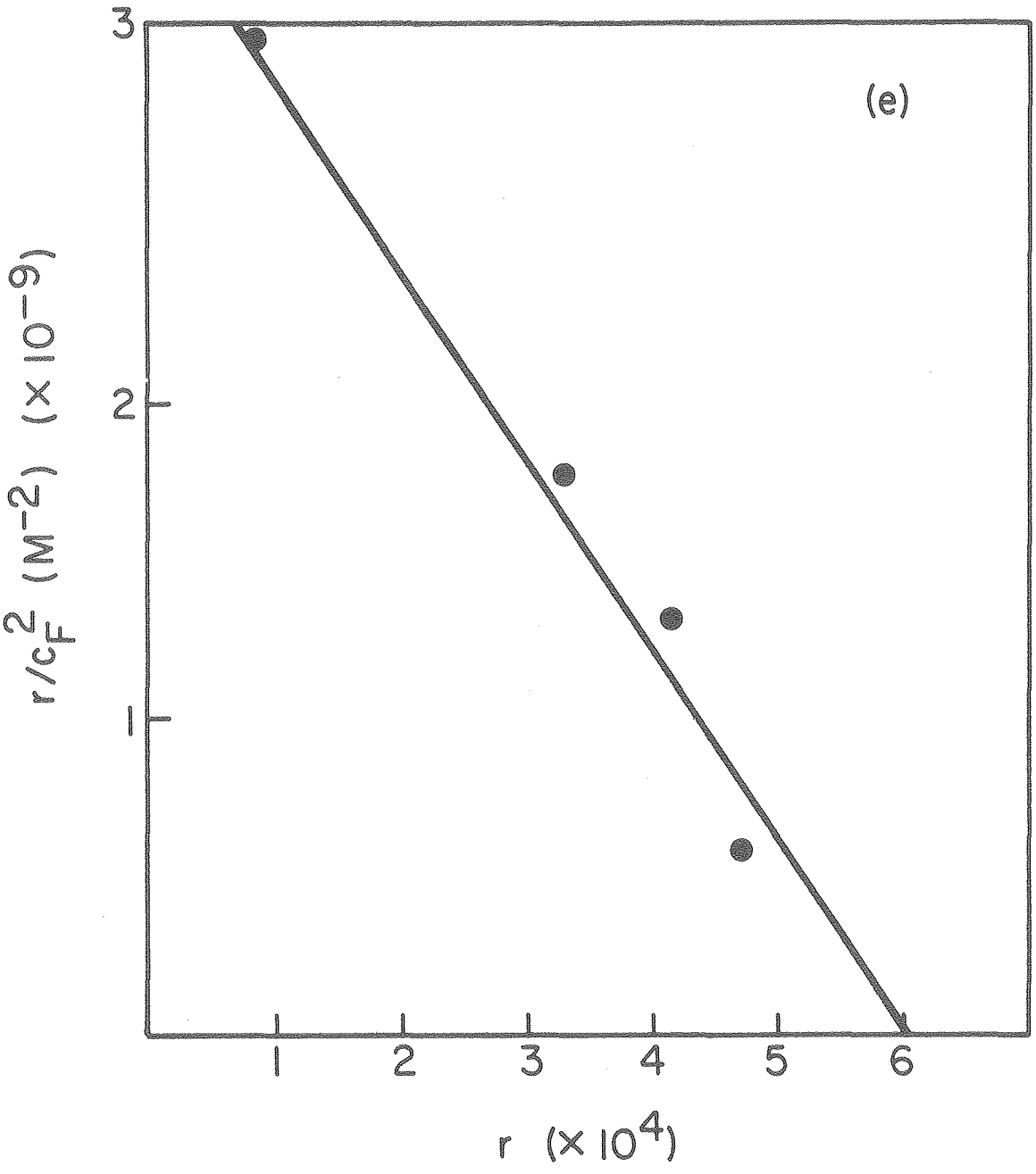

XBL 798-10854

TABLE VIII

Equilibrium Constants (K)[a] and Binding Ratios (R)

for NQO Bindint to Various DNA's at 25°C

DNA	K (M^{-2})	R ($\frac{\text{Base Pairs}}{\text{Site}}$)
calf thymus	$4.3\pm0.7\times10^{9}$	100±30
E. coli	$9.7\pm0.7\times10^{10}$	670±30
pBR 322 linear	$6.8\pm0.6\times10^{11}$	350±50
superhelical + relaxed circular[b]	$2.2\pm0.6\times10^{13}$	540±50
SV 40 linear	$1.3\pm0.5\times10^{13}$	3000±100
superhelical + relaxed circular[c]	$4.0\pm0.5\ 10^{14}$	3600±100

[a]Equilibrium constants and binding ratios determined for two NQO molecules binding cooperatively into non-interactive sites (as described in text).

[b]From gel electrophoresis on 1% agarose, the pBR 322 used was approximately 2:1 superhelical:relaxed

[c]From gel electrophoresis on 1% agarose, the SV 40 used was approximately 8:2 superhelical:relaxed.

The Scatchard plots of the binding data for the calf thymus DNA-NQO interaction at various temperatures were given in figure 12e. The binding ratios at these temperatures were obtained by extrapolating the plots in figure 12e to $r/c_F = 0$. The value of r at $r/c_F = 0$ gives the binding ratio in terms of the number of NQO molecules per residue which is equal to the number of sites per base pair (since there are two NQO molecules per site). The binding ratio at 25°C was obtained from the two NQO per site plot (figure 14a). The binding ratios obtained (base pairs/site) were plotted vs. temperature (figure 15) to assay the dependence of the binding ratio on temperature.

The binding of NQO to denatured calf thymus DNA was investigated by both the optical and phase partition methods. No significant NQO binding was observed for denatured calf thymus DNA.

Figure 15: Plot of Base Pairs/Site for calf thymus DNA + NQO vs. temperature. $[DNA]_T \simeq 2\text{-}6\times10^{-3}$ M; $[NQO]_T$ 6×10^{-6} to 3×10^{-4} M in cacodylate buffer, pH 7.

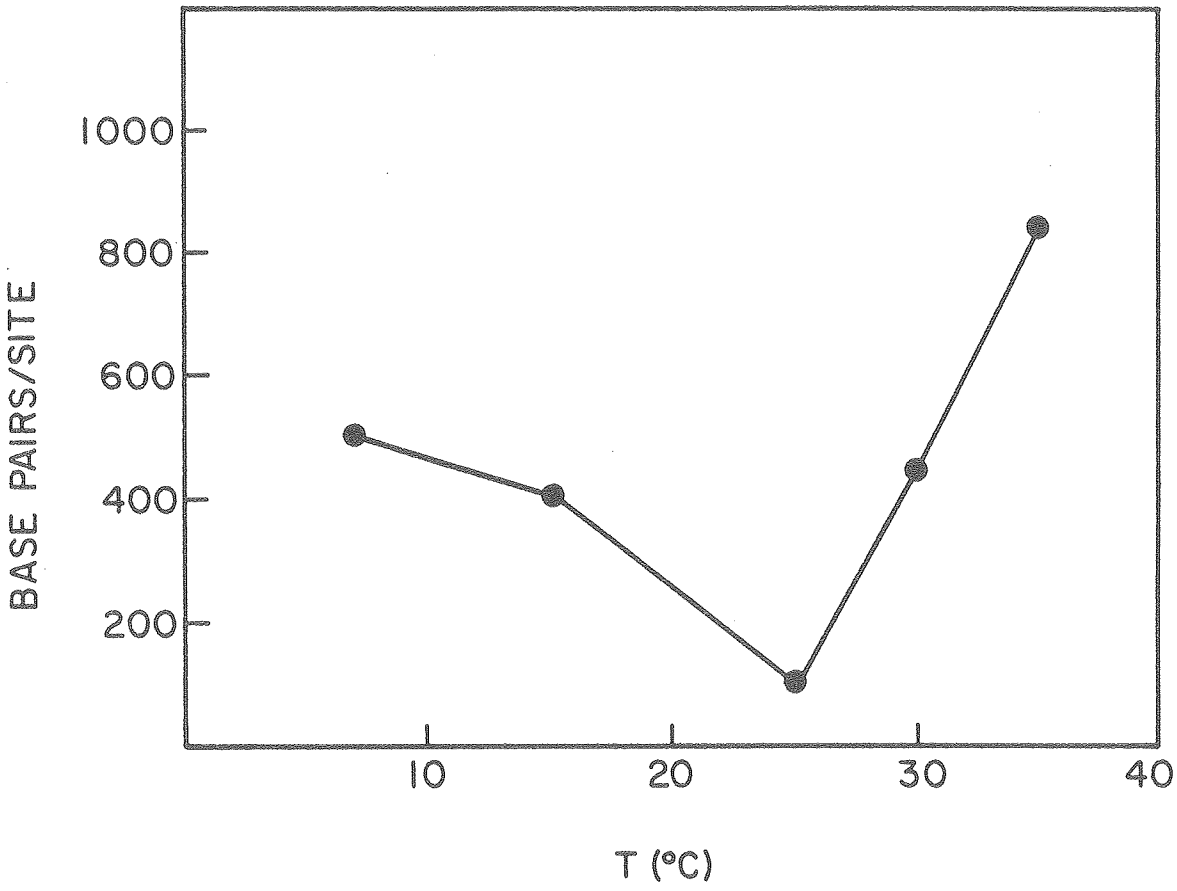

XBL 797-10709

DISCUSSION

The charge transfer bands from the NQO-DNA base interactions occur at $\lambda_{max} \simeq 415$ nm which is similar to the wavelengths for the mononucleotide complex bands (Chapter II) and the dimer complex bands (Chapter III). The ε_c's of the DNA interaction(s) are roughly one-half those for either the dimers or monomers. This could imply less overlap of the bases and NQO in the DNA complexes, leading to weaker charge transfer transitions.

The Scatchard plots in figure 12 suggest that the biinding of NQO to the high affinity binding sites is highly cooperative. Analysis of the data using Hill plots indicates that there are two NQO molecules per site. By applying the binding data to the two NQO per site equation, equilibrium constants for the DNA-NQO noncovalent interaction were determined (Table VIII). These equilibrium constants are quite large. They represent the binding of two NQO molecules to the DNA and may include a component due to the formation of the binding site. The reaction might be represented as:

(1) $$DNA_{(1)} \overset{K_1}{\rightleftharpoons} DNA_{(2)}$$

(2) $$DNA_{(2)} + NQO \overset{K_2}{\rightleftharpoons} DNA_{(2)} \cdot NQO$$

(3) $$DNA_{(2)} \cdot NQO + NQO \overset{K_3}{\rightleftharpoons} DNA_{(2)}(NQO)_2.$$

The first equilibrium represents the possible conversion of the DNA from the normal double strand to a second type of structure. (Chapter VI will deal with the possibility of this equilibrium.) The experimentally determined K is equal to $K_1K_2K_3$. Thus the binding constant for binding one NQO may not be unreasonably large. Of course, it is possible that the binding of the first NQO would have a small K and the second a much larger K.

Recently Hogan, et al. (1979), published data on the binding of the drug distamycin to sonicated calf thymus E. coli DNA. The binding to calf thymus DNA was highly cooperative, giving the same type of Scatchard curve as the DNA-NQO system. They did not observe a cooperative binding curve for E. coli DNA. It could be possible that their distamycin to residue ratios were too high in this latter system. For NQO, it was necessary with some of the DNA systems to use NQO concentrations which were much lower than those in the 25°C calf thymus DNA-NQO study. In Hogan et al's interpretation of the cooperativity of distamycin binding, the distamycin was affecting allosterically the long range structure of the DNA - changing the DNA from one form to another, e.g., B form to A form. They did not suggest that multiple drugs might be binding per site. The cooperative binding of NQO might then be explained in terms of the first NQO stabilizing an alternate structural form or causing the formation of an alternate form.

The high base pair to NQO binding ratios tabulated in Table VIII suggest that NQO binds into a highly specific set of sites. The binding ratio for calf thymus DNA at 25°C does correlate fairly well with the nearest neighbor frequency of CG in calf thymus DNA (Swartz, et al., 1962). However, E. coli DNA has a much higher nearest neighbor frequency for CG (Subah-Sharpe, et al., 1966) but with E. coli DNA the base pair to NQO ratio is much higher than with calf thymus DNA. Thus, no consistent correlation with any dinucleotide sequence frequency was found. As the experiments in Chapter III showed, NQO displays no great preference for any of the particular dinucleotides studied, CG, GC, AT, TA, CA-TG.

The temperature lability of these strong bonding sites in calf thymus DNA (figure 15) could be an argument for NQO bonding to an alternate structural feature of the DNA. At low temperatures, too much energy would be needed for the formation of the feature and at higher temperatures the feature would melt out. Also it is somewhat difficult to imagine a short DNA sequence, dimer, trimer, or other oligomer, which would show such "melting" behavior.

For both pBR 322 and SV 40 DNA, the number of base pairs per DNA is known, 4362 (Sutclffe, 1978) and 5224 (Buchman, Burnett & Berg, SV 40 sequence Manual, 1978) base pairs, respectively. The binding ratios from Table VIII may be

converted to the number of sites per molecule. For pBR 322, there are 8 sites per molecule while for SV 40 DNA the binding ratio converts to 1.5 sites per molecule.

Unless the sites within a set of binding sites on DNA are identical, the equilibrium constants for binding to the different sites will vary somewhat. With a large number of sites, as with calf thymus or E. coli DNA, these differences are not noticed. With a small number of sites per molecule, as with pBR 322 or SV 40, the differences may be observed. There is sufficient scatter in the plotted data to cover up the difference to the extent that the data give a linear plot. The K from this plot is an "average" for all the sites. The intercept of the plot is weighted by the equilibrium constants of the various sites and will not necessarily give the exact number of sites. Accordingly, the Scatchard plot for SV 40 yielded an apparent 1.5 sites/SV 40 molecule probably because one of the sites has a larger K than the other. There are probably 2 sites for NQO binding on SV 40 DNA.

It might be argued that the NQO is binding to single strand regions or nicks in the calf thymus DNA and E. coli. However, no significant binding of NQO to denatured calf thymus DNA was observed. The equilibrium constants for NQO binding to the SV 40 and pBR 322 DNA's were very high. These DNA's both contained sizable percentages of superhelical DNA (80-90% and 60%, respectively) which are not nicked.

The equilibrium binding data for linear pBR 322 and linear SV 40 DNA are compared in figures 14c and d and Table VIII with that for mixtures of the superhelical and relaxed circular DNA's. When either DNA is linearized by cutting with the restriction enzyme Eco R1, the equilibrium constant drops markedly relative to the circular forms. With various other DNA-interacting molecules no such large changes have been observed. For example, with the psoralen 4'-aminomethyl trioxsalen, the association constant in 0.15 M NaCl is 7×10^3 M^{-1} for supercoiled Col El DNA and is 4×10^3 M^{-1} for linear Col El DNA. For trimethylpsoralen in 0.15 M NaCl, the K for supercoiled Col El DNA is 4×10^3 M^{-1}; for linear Col El, it is 2×10^3 (Hyde & Hearst, 1978). This increase in K for NQO binding may be discussed in terms of the generalized equilibrium expressions given earlier in this section. As has been noted by Hsieh and Wang (1975) and by Valogodshii et al. (1979), the presence of supercoiling increases the possibility of the formation of denatured or alternately structured regions in a DNA. (This will be discussed in more detail in Chapter VI). The equilibrium

$$DNA_{(1)} \overset{K_1}{\rightleftharpoons} DNA_{(2)}$$

where $DNA_{(1)}$ is the normal double strand DNA is assumed to be shifted by the presence of superhelical turns towards the alternate form $DNA_{(2)}$- that is, K_1 increases. The intrinsic

K's (K_2 and K_3 in the reaction scheme) are assumed to not be changed by the presence of the supercoils. The apparent or observed K which is equal to $K_1K_2K_3$ is thus increased by the increase in K_1. Thus it seems that in the presence of superhelical turns, the binding of NQO is enhanced.

CONCLUSION

The DNA-NQO equilibrium binding data indicate that NQO binds in a highly cooperative fashion into a specific type of sites (with two NQO molecules per site). The equilibrium constants obtained, which appear quite large, represent the overall equilibrium of the two NQO molecules binding and represent the possible formation of the site, as well. The data raise the possibility that the binding sites could be some type of alternate DNA structure rather than a particular set of sequences. In the next chapter, experiments which aid in defining the nature of the binding sites will be discussed.

CHAPTER VI

NATURE OF THE NQO BINDING SITES IN DNA

INTRODUCTION

In forming noncovalent complexes with various DNA's NQO has been shown (Chapter V) to bind very strongly in a cooperative fashion into specific types of sites. The experiments discussed in Chapter V suggested some details aobut these binding sites. The sites appear to be temperature dependent and the binding of NQO to the DNA is enhanced when the DNA possesses supercoils. The temperature lability and lack of correlations with nearest neighbor frequencies argue against the sites being particular short sequences. Hogan, et al. (1979) have previously suggested that distamycin, which also binds cooperatively, alters the DNA structure.

The experiments in Chapter 5 gave data on the strength of binding and the nuber of binding sites. These experiments did not offer a clear picture of the nature of the binding sites. In this chapter, the results of various experiments dealing with the details of NQO bindint to SV 40 and pBR 322 will be presented. The SV 40 and pBR 322 DNA's are used because they have been sequences and restriction mapped and because they are superhelical. The presence of this latter property allows the study of the unwinding, if any, of DNA by NQO.

The techniques used for these studies differ from those in the previous chapters. The experiments involve the use of several enzymes, i.e., restriction enzymes, S_1 "single strand" specific endonuclease, and unwinding enzymes, and gel electrophoresis. Using the results of these studies, the approximate locations on the DNA of the NQO binding sites, the unwinding of DNA by NQO (both covalently and noncovalently bound) and the effects of NQO binding on S_1 cutting of supercoiled DNA will be discussed.

EXPERIMENTAL

Materials

The SV 40 and pBR DNA's were obtained as described in Chapter V. The DNA's were dissolved in the cacodylate buffer of Chapter III and concentrations measured as in Chapter V. The DNA's were transferred from one buffer to another by dialysis or by EtOH precipitation and redissolving.

The ^{3}H-NQO, prepared as in Chapter V, was kept in 1:1 n-amyl acetate:cyclohexane. For addition to the aqueous DNA solutions, ^{3}H-NQO in the organic solvent was shaken with the aqueous DNA solution. The aqueous layer was then separated and the amount of ^{3}H-NQO added determined by tritium counting.

Unwinding of SV 40 DNA by NQO

A. Noncovalent Unwinding

Solutions of SV 40 DNA (4×10^{-6}M to 1.7×10^{-3} M) and ^{3}H-NQO (8.8×10^{-9} to 5.1×10^{-8} M) were prepared in a buffer of 0.04 M Tris-HCl, 5 mM NaOAc, 0.5 mM EDTA, 0.2 M NaCl, pH 7.9.

To each NQO-SV 40 DNA mixture, 30 µl in volume, 3 µl of the HeLa nicking closing enzyme (obtained from Dr. Gary Wiesehahn) were added and the mixture kept at room temperature in the dark for 24 hr. Control reactions of equivalent SV 40 concentrations without NQO were also run. Before adding samples to the electrophoresis gel, 10 µl 10% sodium dodecyl sulfate (SDS) were added to each sample.

Samples with 5 µl dye marker (0.25% bromphenol blue, 0.25% xylene cyanole in 50% glycerol) were placed on a vertical 1% agarose gel made up in the "running buffer" 0.04 M Tris-HCl, 5 mM NaOAc, 0.5 mM EDTA, pH 7.9. The gel was electrophoresed at ca. 40 V, 35-50 mA for roughly 12 hr and was then stained in a dilute ethidium solution (ca. 1 µg/ℓ). The stained gels were photographed with Polaroid Type 107 film using a Mineralight C-51 UV light source to illuminate the gel and using an orange filter.

In an effort to move the partially relaxed DNA bands from near the relaxed SV 40 band and from the relatively insensitive region of the gel, ethidium bromide was added to each SV 40-NQO reaction mixture. The samples contained SV 40 DNA (1.50×10^{-5} M or 1.35×10^{-5} M) ^{3}H-NQO (2.8×10^{-8} to 1.2×10^{-6} M), ethidium (6.3×10^{-7} or 8.2×10^{-7} M), 3 µl HeLa nicking closing enzyme in a total reaction of volume of 39.5 or 38 µl. Control samples consisted of SV 40 DNA alone in the presence of the enzyme and SV 40 DNA with ethidium (concentrations as above). All samples were kept in the dark at room temperature for 24 hr. To each, 10 µl of 10% SDS was then added.

The gel electrophoresis was performed as before. The center of the collection of partially relaxed bands for each DNA sample was determined visually in the photographs of the gels. The displacement of the center band in the photographs for samples with NQO relative to the center band position in the absence of NQO was measured. Each sequential band on the gel representes the addition (or subtraction of one supercoil. Dividing the displacement distance by the average distance between neighboring bands gave the number of supercoils removed in each sample.

B. Unwinding of SV 40 by Covalently Bound NQO

Solutions of SV 40 DNA (3.2 µg/ml) with varied concentrations of added ^{3}H-NQO (initial concentrations, 1.0-5.4x10^{-8} M) were irradiated for 20 min at 20°C using the Hg-arc lamp source described in Chapter IV. Samples were placed on 1% agarose gels and electrophoresed as described above. Typical running times (at 30-40 V, ca. 50 mA) for these gels were 7 hr. After staining in an ethidium solution, photographs of the gels were made as described above.

To make the system more sensitive to small changes in the number of supercoils, partially relaxed SV 40 DNA was prepared. In 100 µl of a buffer consisting of 0.08 M phosphate, 3.5 mM $MgCl_2$, pH 7.7, 40 µg SV 40 DNA were dissolved. To this 5 µl of omega enzyme (approximately 0.5 mg/ml, obtained from Dr. Gary Wiesehahn) were added. The reaction

mixture was maintained at 37°C for 5 min and then was quenched by addition of 50 µl of 0.1 M EDTA (pH 7) and by chilling in an ice bath.

Samples of the partially relaxed SV 40 (1.3×10^{-5} M) with ^{3}H NQO (initial concentrations, 8.4×10^{-8} to 7.4×10^{-7} M) were irradiated for 10 min at 20°C using the Hg-lamp source. The reaction mixtures were applied to a 1% agarose gel and the electrophoresis and subsequent work up conducted as above Running time of the gel was about 12 hr.

Other samples of the partially relaxed SV 40 (4.04×10^{-5} M) with ^{3}H-NQO (initial concentrations ranged from 5.3×10^{-7} to 4.6×10^{-6} M) were irradiated at 415 nm for 1 min at room temperature on the Molectron pulsed dye laser system described in Chapter IV. The SV 40 DNA (with covalently bound NQO) was precipitated by adding two volumes of NaCl saturated 95% EtOH and then placing the mixtures in a freezer for 3 hr. The SV 40 was collected by centrifugation and redissolved in cacodylate buffer. Aliquots were tritium counted. Gel electrophoresis on the samples was carried out as before (running time 12 hr).

S_1 Reaction with Supercoiled DNA in the Presence of NQO

Samples of either pBR 322 (ca. 1 µg/ml) or SV 40 DNA (ca. 3.5 µg/ml) in S_1 buffer (300 mM NaOAc, 50 mM NaCl, 1 mM $ZnSO_4$, 5% glycerol, pH 4.6) were reacted with the endonuclease S_1 (obtained from Dr. Gary Wiesehahn) both in the

presence and absence of ^{3}H-NQO. For pBR 322, $[NQO]_T$ ranged from ca. 1-5x10^{-7} M and the amounts of S_1 used were 5, 50, or 500 units. For SV 40 DNA $[NQO]_T$ was 2-7x10^{-8} M and the amounts of S_1 were 15 or 50 units. All S_1 reactions were for 30 min at 37-40°C. Samples were then loaded onto 1% agarose gels and the electrophoresis and workup were performed as before. Gel running times were about 7 hr at 40 V, 50 mA. For pBR 322 additional samples were prepared in which the ^{3}H-NQO was extracted with $CHCl_3$ prior to addition of 5 u S_1. Additional samples of SV 40 and ^{3}H-NQO were irradiated for 20 min at 20°C on the Hg source then dialysed to remove NQO photo-"breakdown" products and unreacted NQO before the addition of 15 u S_1.

The possibility of inhibition of S_1 by action of NQO on the enzyme itself was assayed using heat denatured calf thymus DNA according to the procedure in Worthington Biochemical Corp. Enzyme Manual (1972). Heat denatured calf thymus DNA (6.7x10^{-5} M) was incubated with S_1 in the presence of and absence of ^{3}H-NQO. In the samples with NQO, $[NQO]_T$ ranged from ca. 1.9x10^{-7} to 5.4x10^{-6} M and the amounts of S_1 used were 50 or 500 u. All samples (reaction volume 75 µl) were incubated for 30 min at 35°C. To precipitate the nonreacted DNA, 150 µl of 7% $HClO_4$ were added to each sample and the samples were cooled for 10 min in an ice bath. To each sample, 1 ml cold H_2O was added. The absorbances at 256 nm of the final solutions were read versus H_2O on a Cary 118 spectrometer.

Location of Covalently Bound NQO in SV 40 DNA and pBR 322. Restriction Enzyme Digests.

A. pBR 322

Approximately 20 µg pBR 322, dissolved in Hpa II buffer (20 mM Tris-HCl, 7 mM $MgCl_2$, 1 mM dithiothreitol, pH 7.4), were reacted with 30 units of the restriction enzyme Hpa II (Bethesda Research Laboratories) for 2 hr at 37°C. After the enzyme was extracted with 90% phenol, the DNA was precipitated with 2 volumes 95% EtOH and dissolved in cacodylate buffer. The cacodylate solution was shaken in ice for 3 hr with an n-amyl acetate:cyclohexane (1:1) solution of ^{3}H-NQO to add NQO (about 7×10^{-7} M). After removing the organic layer, the aqueous DNA solution was irradiated at 406 nm for 5 min, 25°C using the Molectron pulsed dye laser (average power ca. 2 mW). The solution was dialyled at 4°C vs. cacodylate buffer overnight. The DNA was precipitated using 2 volumes 95% EtOH and dissolved in the electrophoresis buffer. A 6% acrylamide tube gel (23 cm) was prepared by combining 10 ml of degassed acrylamide solution (7.4 ml H_2O, 2 ml 30% polyacrylamide solution (60:1 acrylamide:N,N'-methylene-bis-acrylamide (BIS)), 0.5 ml of 20 x electrophoresis buffer) with 10 µl of 10% ammonium persulfate and 7 µl N,N,N',N'-Tetramethylene-diamine in the plastic tube. The gel was run at 300 V for approximately 6 hrs. The running buffer was that described

above. After staining in an ethidium solution, the DNA fragment bands, visualized with the UV light source, were sliced from the gel. Gel slices were solubilized by the addition os sufficient fresh 99:1 H_2O_2(30%):NH_4OH (concentrated) to cover the slices and placement in an oven at 37°C overnight. Sufficient cacodylate buffer to bring the aqueous volume to 1 ml was added followed by 10 ml of counting fluid. The gel slice solutions were counted on the Beckman liquid scintillation counter described previously. Background counting was obtained by counting slices taken from the gel in regions near the DNA fragment bands.

B. SV 40 DNA

A solution of SV 40 DNA (approximately 20 µg) and NQO ($7x10^{-7}$ M) was irradiated for 20 min at 20°C on the Hg source. The DNA was precipitated with two volumes of NaCl saturated 95% EtOH and redissolved in Hind III buffer (20 mM Tris-HCl, 7 mM $MgCl_2$, 60 mM NaCl, pH 7.4). About 75 units of Hind III restriction enzyme was added and the mixture incubated at 37°C for 3.5 hr. The sample was then loaded onto a 6% acrylamide tube gel (approximately 23 cm) and electrophoresed at 200 V in the standard buffer. The 6% acrylamide gel was prepared as above except the acrylamide solution used was 30:1 acrylamide:BIS. The DNA fragment bands were sliced from the gel and solubilized by addition of 1 ml 99:1 H_2O_2 (30%):NY_4OH (concentrated) to each slice. Counting was done as before. Again background counts were obtained by counting "blank" slices.

Approximately 30 µg SV 40 DNA with ^{3}H-NQO (ca. $3x10^{-7}$ M) in cacodylate buffer were irradiated for 10 min at 17°C. The DNA was precipitated with two volumes of cold NaCl saturated 95% EtOH and redissolved in Hae III buffer (50 mM Tris-HCl, 5 mM $MgCl_2$, 0.5 mM dithiothreitol, pH 7.5). To this solution, 134 u restriction enzyme Hae III were added and the mixture was incubated at 37°C for 2 hr. The mixture was applied to a 6% acrylamide gel and the electrophoresis conducted exactly as with the Hind III digest of SV 40. In the Hae III gel, the smaller fragment bands were blurred and there appeared to be partial digest bands. Where distinct bands were seen, the bands were sliced as before. In the region of the smaller fragment bands, the entire "smear" was sliced into sections. Background slices were taken as before. The solubilization of the gel slices adn counting were done as above.

RESULTS

In figure 16, a 1% agarose gel of the SV 40 DNA relaxed with the HeLa nicking-closing enzyme in the presence and absence of NQO is shown. The samples with NQO present may have shown more partially relaxed bands than the two samples (on the ends) without NQO. However, all of the samples ran close to the fully relaxed DNA band. This made it difficult to discern how much the NQO unwinds the DNA.

Figure 16: 1% agarose electrophoresis gel of SV 40 relaxed using HeLA nicking-closing enzyme in presence of NQO. $[DNA]_T$ from 4.4×10^{-6} to 1.7×10^{-5} M; $[NQO]_T$ from 8.8×10^{-9} to 5.1×10^{-8} M. Control samples (DNA alone) labeled "C". Electrophoresis at 25°C with 40 V, $\sim$ 40 mA.

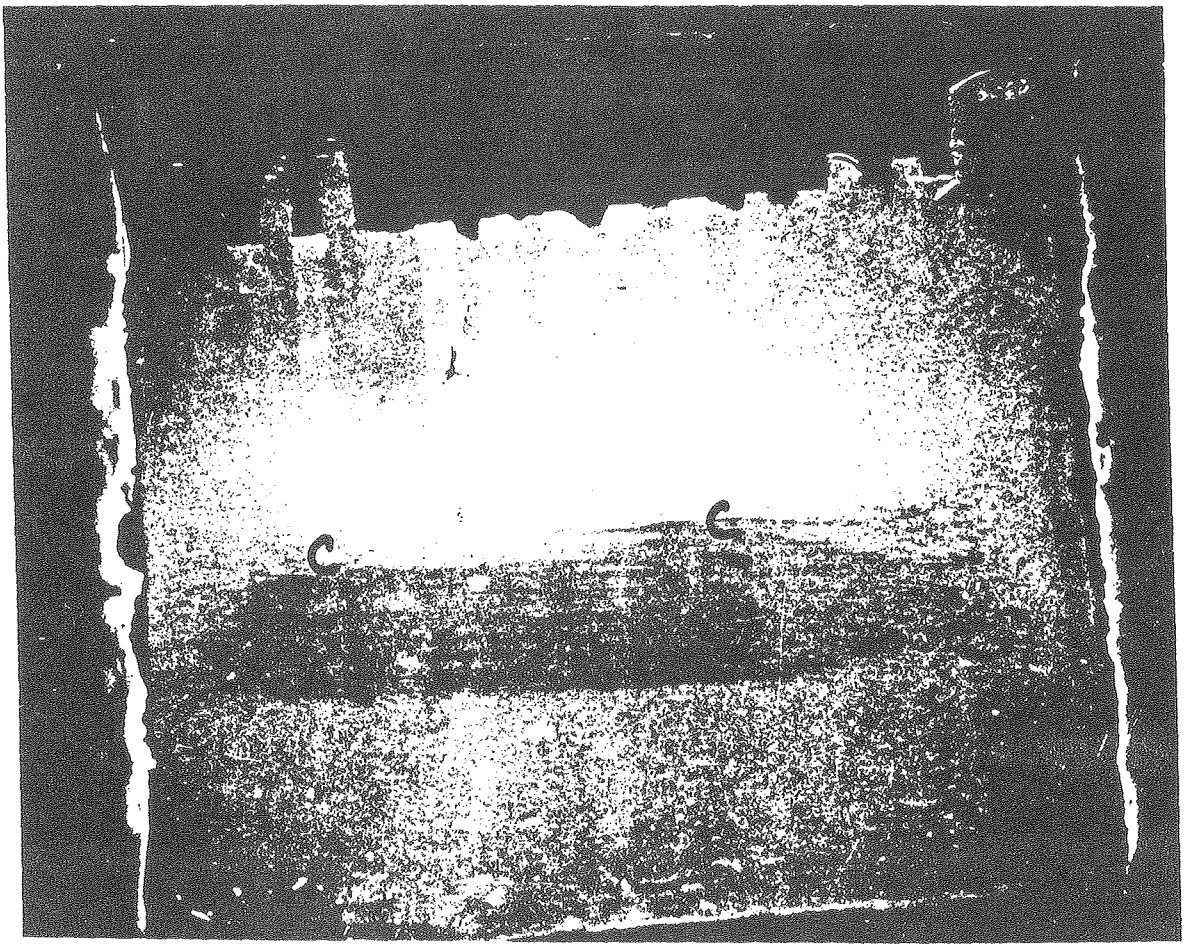

In the unwinding experiments involving the use of HeLA nicking-closing enzyme, the supercoiled DNA and NQO were combined and the enzyme then added. If the interaction of the NQO with the DNA unwinds the DNA, the result would be a partial removal of superhelical turns per NQO bound. The presence of n NQO molecules bound results in the removal of N supercoils (where N may be a fraction). The enzyme relaxes the DNA to an "apparently" fully relaxed state. Thus, with no NQO present in a DNA with an initial x superhelical turns, the enzyme will remove all x superturns. The presence of the n NQO molecules gives a DNA with an apparent x-N supercoils, which the enzyme will remove. When the NQO is then taken out, as on a gel, the DNA would then have N supercoils (or appear as partially relaxed). The more bound NQO, the greater N will be and the further the DNA (after enzyme treatment) wil travel on the gel, relative to the fully relaxed DNA. (Supercoiled DNA travels faster than relaxed DNA.)

With SV 40 DNA, there were only two high affinity sites for NQO binding - four NQO molecules binding per DNA molecule. Hence the NQO concentrations in the samples were limited to amounts which would give no more than four NQO/DNA. With such small concentrations of NQO bound, the numbers of supercoils removed by NQO binding should be small. It was not surprising to observe (figure 16) that most of the DNA relaxed in the presence of NQO appeared almost as relaxed

as the control DNA. There may have been partially relaxed DNA bands in the samples with NQO present, but determining the band centers would have been difficult.

To "move" the partially relaxed DNA to a region of the gel where small changes could be seen, ethidium was added. The ethidium, with an unwinding angle of 26° (Wang, 1974) removes some of the supercoils. The presence of NQO removes additional superhelical turns. Using an argument analogous to the one in the last paragraph, the DNA with ethidium and NQO present would have N more supercoils (for n bound NQO molecules) than the DNA with only ethidium. The samples with NQO and ethidium would run farther on the gel than samples with only ethidium (in a concentration equal to that in the samples with NQO). This is shown in figure 17. Thus, in the presence of a fixed ethidium concentration, the unwinding due to the binding of NQO to the DNA could be observed.

The amount of NQO bound (noncovalently) to the SV 40 DNA in each sample was calculated using the equilibrium constant and binding ratio determined in Chapter V for NQO binding to SV 40 DNA in the presence of ethidium, i.e., $K = 6 \times 10^{12}\ M^{-2}$, $R = 6 \times 10^{-4}$. It should be noted that these values are for $[\text{ethidium}]_T = 8.22 \times 10^{-7}$ M which was the ethidium concentration used in some of the samples. At the ethidium concentration, 6.30×10^{-7} M, used in the other samples, the values of K and R would be somewhat different. Thus, using these values for K and R for the latter samples is an approximation.

Figure 17: 1% agarose electrophoresis gels of SV 40 DNA relaxed by HeLa nicking-closing enzyme in the presence of fixed ethidium concentrations.

(a) $[DNA]_T = 1.35 \times 10^{-5}$ M; $[NQO]_T = 2.8 \times 10^{-8}$ to 1.1×10^{-7} M; [Ethidium] = 8.22×10^{-7} M.

(b) $[DNA]_T = 1.50 \times 10^{-5}$ M; $[NQO]_T = 1.1 \times 10^{-7}$ M to 1.2×10^{-6} M; [Ethidium] = 6.30×10^{-7} M

Control samples (DNA + ethidium, only) are labeled "C". Samples with NQO on each gel are numbered sequentially in order of increasing $[NQO]_T$. Electrophoresis at 25°C using 40 V, ~ 40 mA.

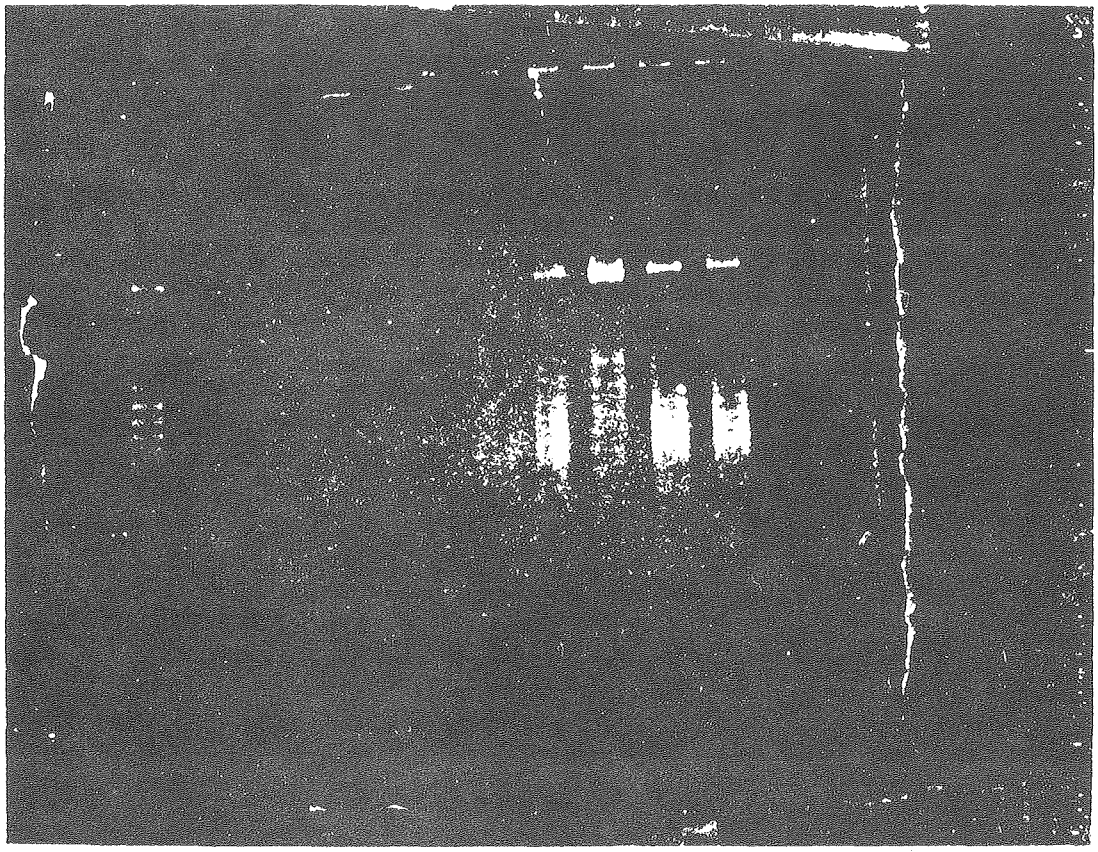

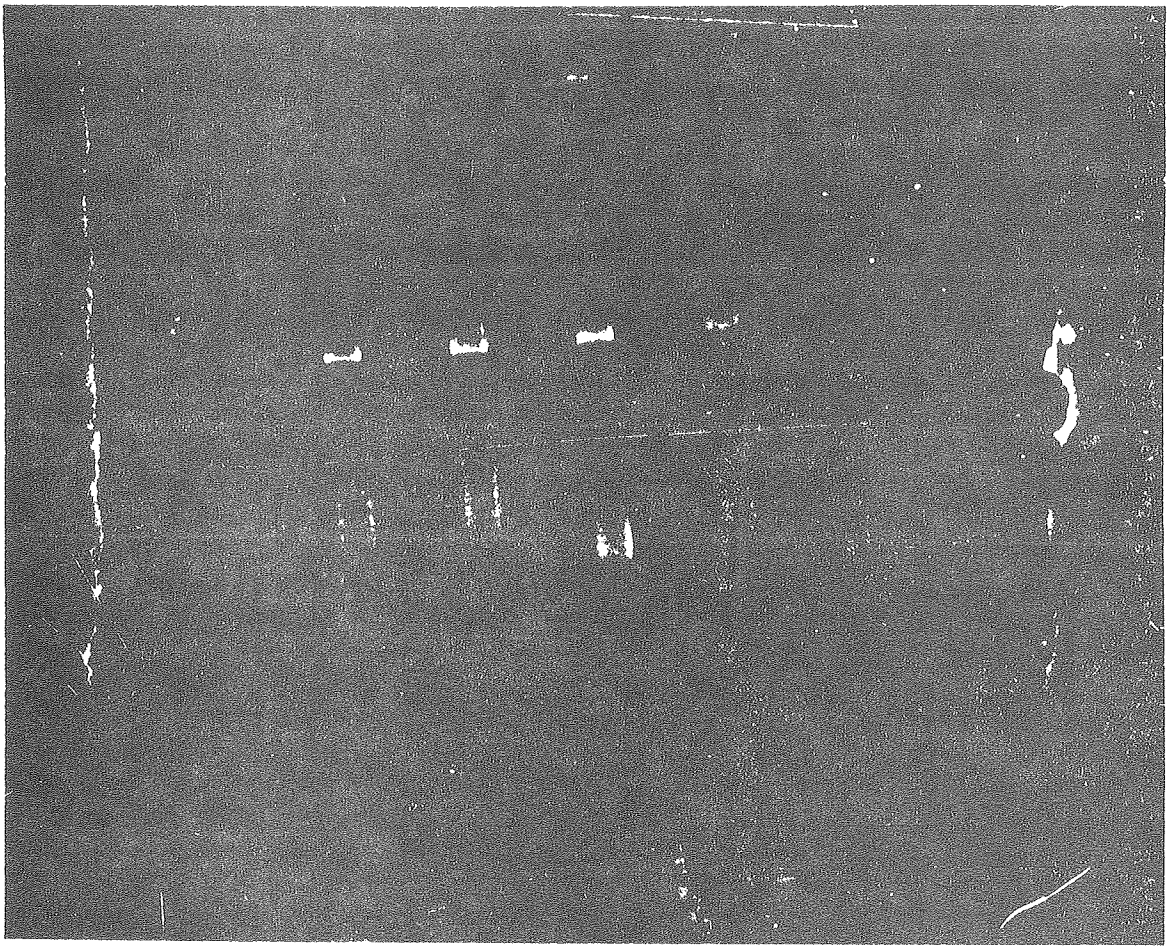

Sample one in figure 17 had insufficient complexed NQO to produce a noticeable change. Sample seven appears anomalous but the amount of complexed NQO was much greater than the number of primary binding sites. Thus, in this sample, some effect of binding to the secondary sites may be what is observed.

For the other samples the number of superhelical turns removed by the binding of NQO was determined by measuring the displacement of the band center in the presence of NQO related to that in the absence of NQO. These distances divided by the average distance between consecutive bands give the number of supercoils removed. The unwinding angle for each number of NQO's bound per DNA molecule was calculated:

$$\text{unwinding angle} = \frac{(\text{number of supercoils removed}) \times 360^\circ}{(\text{number of NQO molecules per DNA molecule})}$$

It should be noted that the number of NQO molecules bound is taken per molecule, not per residue or base pair. The concentration of SV 40 molecules equals the concentration of residues divided by the number of residues (5224x2). For the noncovalent binding of NQO to SV 40 DNA, the unwinding angle came out to 830°±60° per NQO bound or 1700°±100° per site filled (with 2 NQO molecules per site). This apparent unwinding angle is very large, much larger than the 26°

observed for ethidium, (Wang, 1974), for example. This suggests as will be discussed in detail later, that the binding of NQO to DNA is not the "normal" intercalative binding.

Irradiation of supercoiled SV 40 with the Hg arc lamp source in the presence of ^{3}H-NQO did not produce any significant change in the position of the supercoiled band on a 1% agarose gel nor did it produce any partially relaxed bands (figure 18). The irradiation did produce an increase in the amount of relaxed SV 40 DNA as was shown by an increase in the size of the relaxed DNA gel band and concomitant decrease in the superhelical band's size. The cause of this relaxing is not known exactly but could be explained by nicking due to the irradiation. In support of this, irradiated SV 40 and NQO samples which were heated then quickly cooled gave on the electrophoresis gel smears characteristic of denatured DNA.

The use of partially relaxed DNA moved the DNA bands to the more sensitive middle of the gel where the expected small changes might be seen. Samples one and four in figure 19 did not have covalently bound NQO (as was shown by the tritium counting of aliquots). Accordingly, the bands shown correspond to partially relaxed and nicked circular and/or fully relaxed DNA. Sample three had 1.0 NQO/SV 40 molecule while sample two had 1.8 NQO/SV 40 molecule. The unwinding

Figure 18: 1% agarose electrophoresis gel of SV 40 DNA irradiated in the presence of NQO. SV 40 DNA (3.5 μg) with $[NQO]_T$ = 1.0 or 3.9×10^{-8} M was irradiated on the Hg lamp source for 20 min at 20°C. Control SV 40 sample, no NQO or irradiation, labeled "C". Electrophoresis at 25°C using 40 V, ∿ 40 mA.

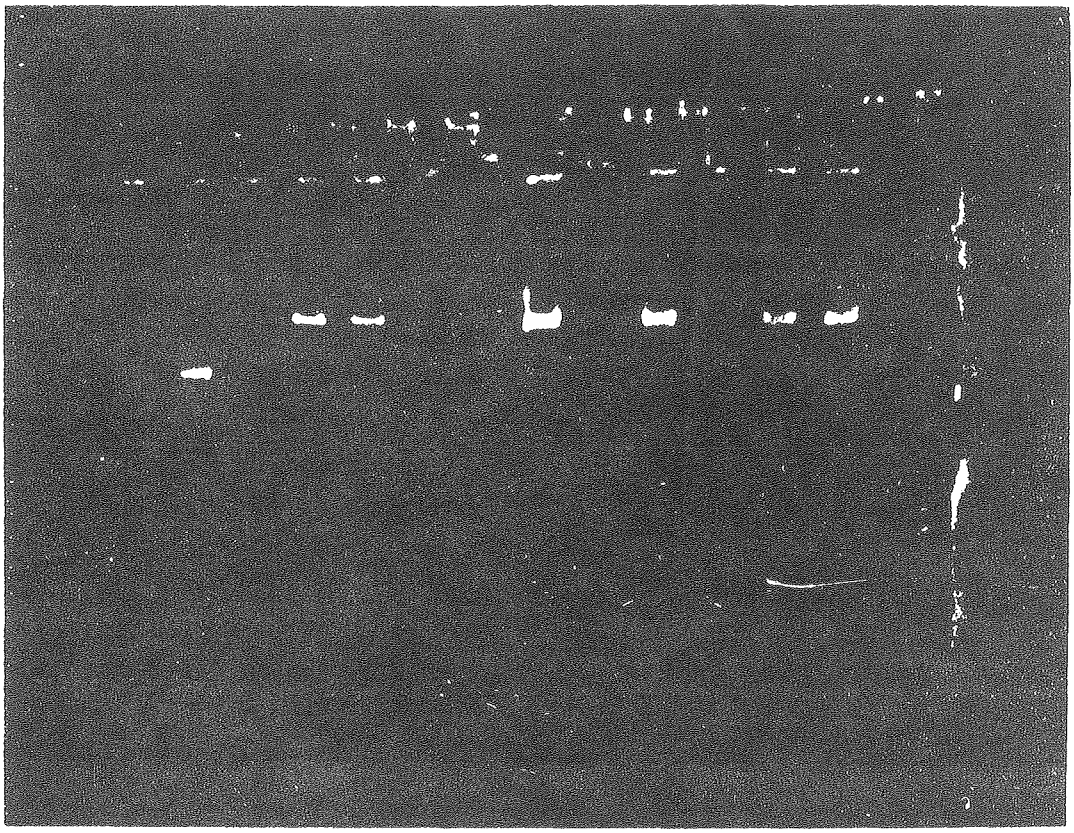

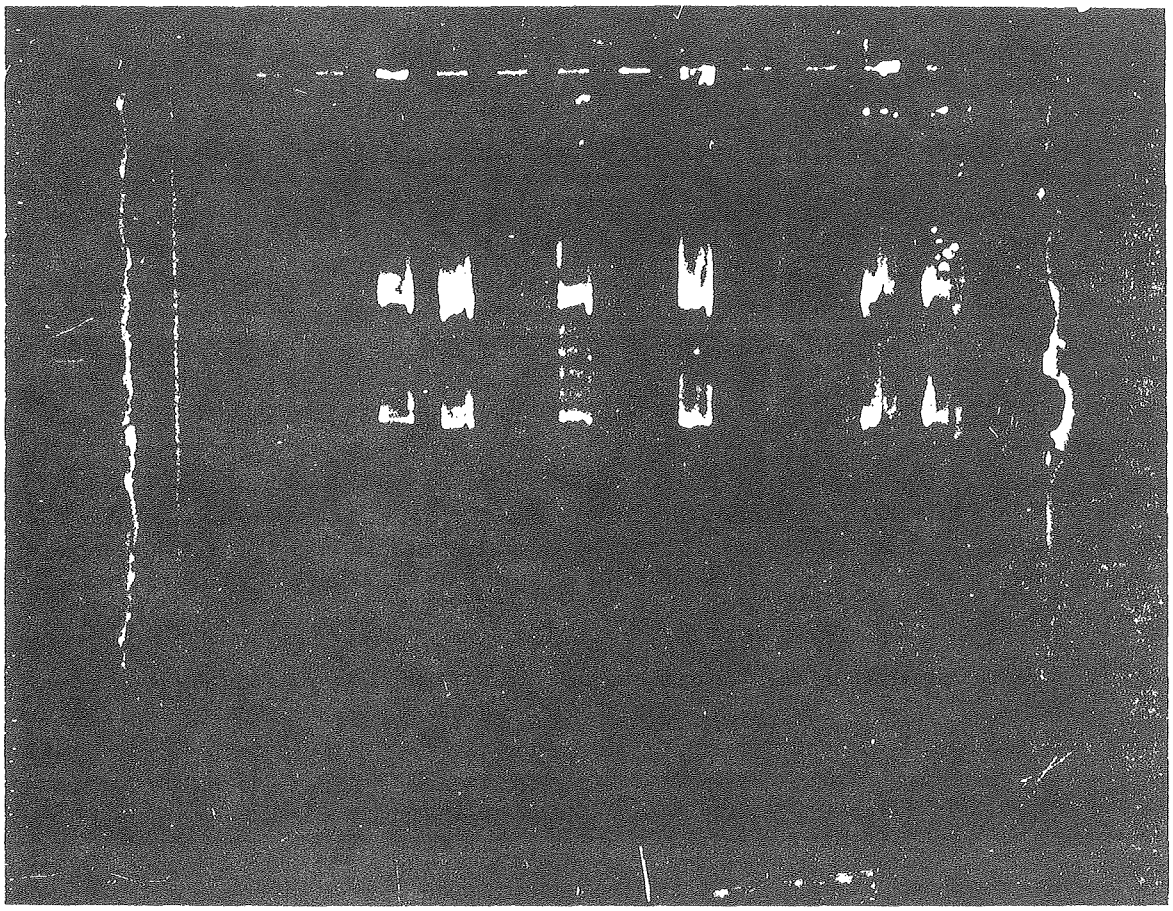

angle calculated as above came out to 770°±120° per bound NQO or 1540°±250° per site filled. This unwinding angle for covalently bound NQO is comparable to that given earlier for the noncovalent binding.

SV 40 DNA and pBR 322 with and without NQO present were incubated with S_1 nuclease, which cuts single strand DNA or non-hydrogen bonded DNA. As Beard, et al. (1973) have reported, S_1 cuts superhelical SV 40 first to the nicked circular form then to the linear form. Thus the extent of S_1 reaction with a superhelical DNA can be crudely judged from the increase of the amount of relaxed DNA and linear decrease coupled with the decrease of the amount of supercoiled DNA. With pBR 322 (1 µg/ml) the presence of low concentrations of NQO inhibited the S_1 reaction in 110 mM salt when 5 units of S_1 were used (figure 20a) but not at the higher S_1 concentrations, 50 and 500 units. The pBR 322 DNA that had been mixed with NQO and then had the NQO extracted reacted the same as the control DNA. With SV 40 DNA (3.5 µg/ml), NQO inhibited the S_1 reaction in 110 mM salt with 15 units S_1 used (figure 20b) but not with 50 units S_1. The SV 40 with NQO that had been irradiated to produce photoadducts prior to reaction with 15 units S_1 also showed inhibition of S_1 cutting.

Figure 20: 1% agarose electrophoresis gel of superhelical DNA's reacted with S1 in the presence of NQO.

(a) pBR 322 (1 μg/ml) reacted with 5 u S_1 (30 min, 37°C). Sample (1) - no NQO; sample (2) with $[NQO]_T = 5.4 \times 10^{-7}$ M; sample (3) mised with $[NQO]_T = 5.4 \times 10^{-7}$ M and NQO extracted prior to adding S_1; control DNA, no NQO or S_1, labeled "C".

(b) SV 40 (3.5 μg/ml) reacted with 15 u S_1 (30 min, 37°C). Samples (1), (2), (5) no NQO; sample (3), with $[NQO]_T = 5.0 \times 10^{-9}$ M; sample (4) with $[NQO]_T = 2.9 \times 10^{-8}$ M; sample (6) with $[NQO]_T = 1.9 \times 10^{-8}$ M; sample (7) with $[NQO]_T = 1.9 \times 10^{-8}$ M, irradiated Hg lamp source, 20 min at 20°C; control DNA, no NQO or S_1, labeled "C".

Electrophoresis conditions: 25°C, 40 V, ∿ 40 mA.

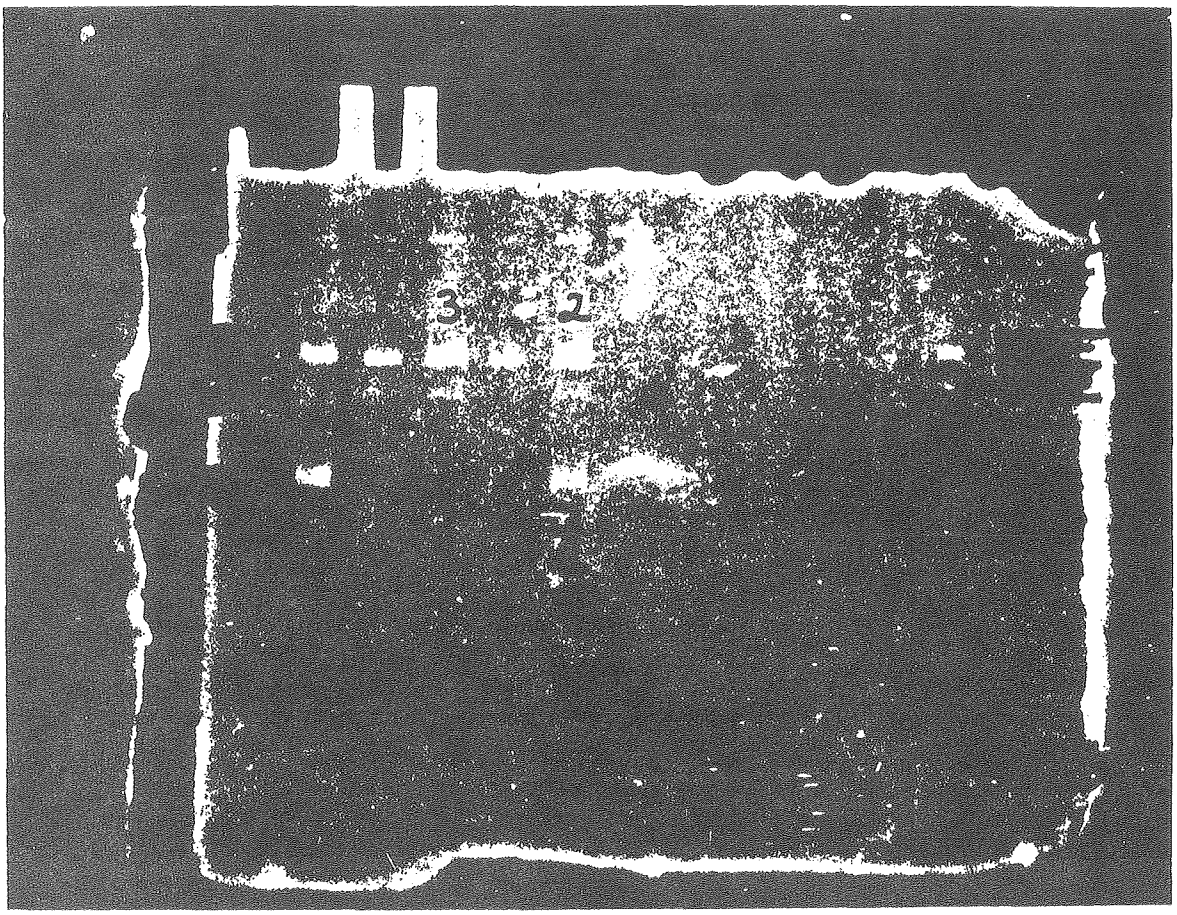
3
2

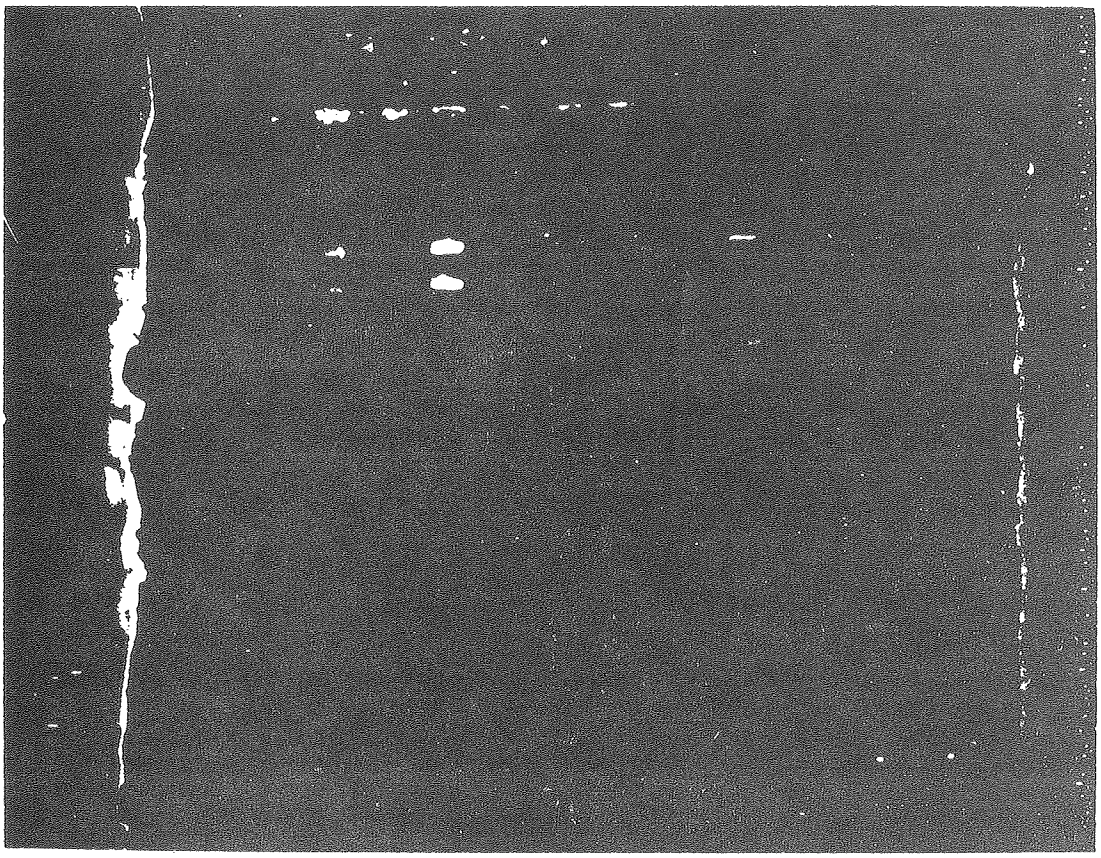

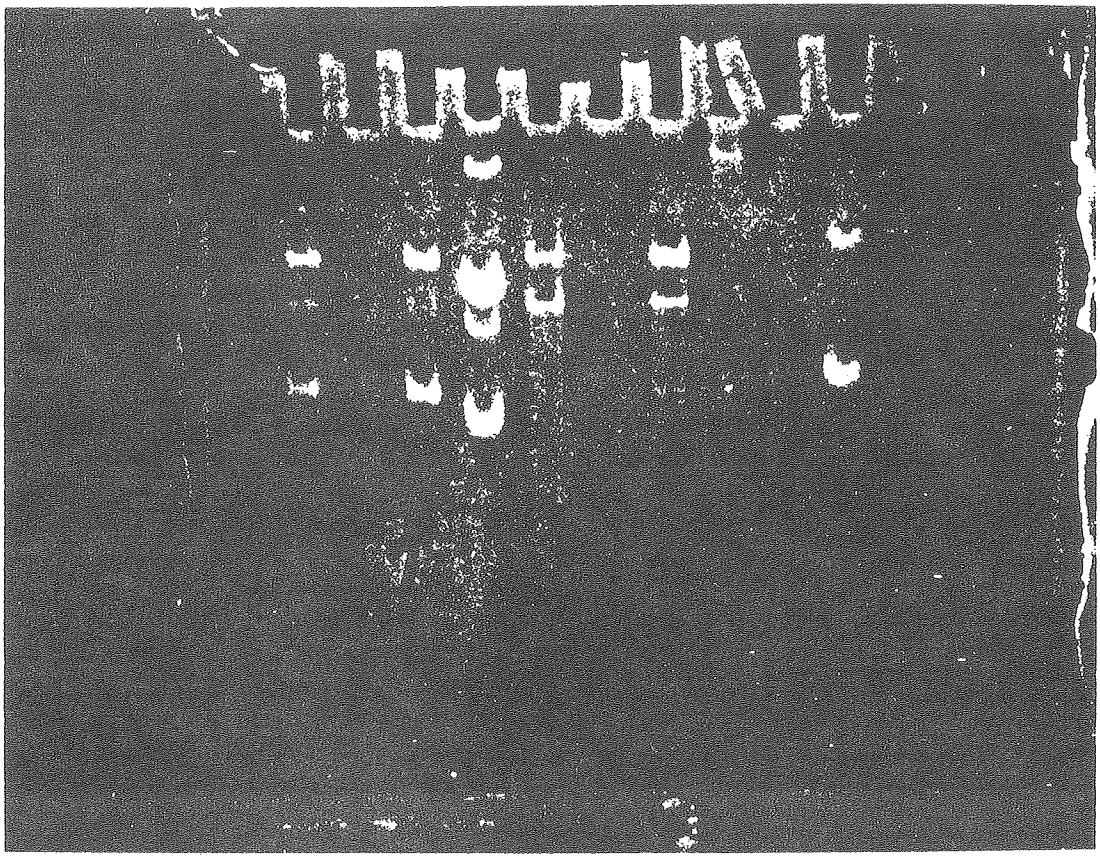

Denatured calf thymus DNA does not bind NQO (Chapter V). It was therefore used to tell if the NQO inhibition of S_1 cutting of DNA resulted from interaction with the enzyme rather than the DNA. The reaction of S_1 on denatured DNA produces acid soluble monomers. After using 7% $HClO_4$ to precipitate unreacted DNA, the amount of monomers produced was assayed by recording the absorbance at 256 nm of the supernatant. The concentration of monomers produced by S_1 reaction on heat denatured DNA was not diminished by the presence of NQO.

The 6% acrylamide gel of the Hpa II digested pBR 322 with covalently bound ^{3}H-NQO gave sixteen fragment bands with one additional band attributed to a partial digest fragment. This band was considerably fainter (under UV lamp after ethidium staining) than the other bands, and did not match well in position on the gel with any of the restriction fragments. The sixteen bands were assigned to the sixteen largest Hpa II fragments. The ℓn(fragment size) was plotted vs. distance moved on the gel using this assignment of fragments to gel bands. The plot was reasonably linear (with some expected curvature at the ends) as it should be, supporting this band assignment. In figure 21 is a histogram showing number of gel slice tritium counts per gel band using the above assignments. Having assigned the gel bands to the restriction fragments and knowing which bands

Figure 21: Histogram of tritium cpm for the sixteen gel gands from a 6% acrylamide electrophoresis gel of Hpa II digested pBR 322 reacted with ^{3}H-NQO. The five bands possessing significant amounts of tritium (and hence NQO) are indicated (↓). Electrophoresis at 300V at 25°C.

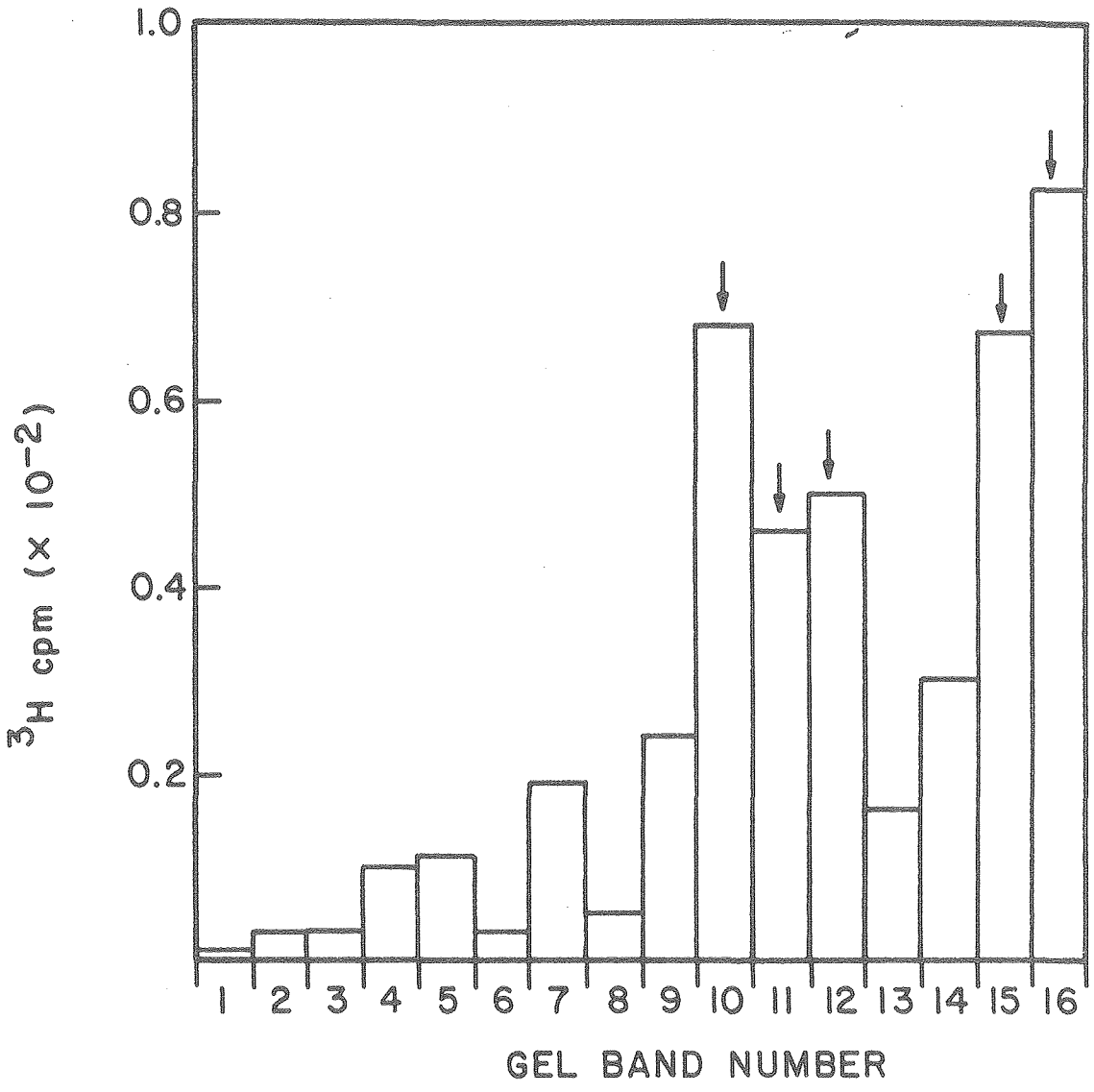

XBL 797-10710

contain a significant number of counts (as indicated in figure 21) gives the fragments containing bound NQO. The positions of the fragments with the largest number of counts (and hence the most bound NQO) are shown on a Hpa II map of pBR 322 in figure 22. One of the 'hot' gel bands represented two fragments of the same size. Thus the NQO could be bound to either of these two fragments, as is indicated in figure 22. In addition there are two other fragments which had significantly lower but possibly still significant amounts of radioactivity. These two fragments are indicated as possible binding sites. The positions of the fragments containing NQO binding sites are given in Table IX.

With the 6% acrylamide gel of Hind III digested SV 40 with covalently bound ^{3}H-NQO, there were six bands and there are six fragments expected (according to the SV 40 sequence). The band representing the smallest fragment was somewhat smeared. The ℓn(size) vs. distance plot of this assignment of fragments to gel slices was reasonably linear. The histogram of the number of gel slice tritium counts per gel band is in figure 23a. Again, having assigned the gel bands to fragments and knowing the amount of radioactivity per band gives the fragments containing bound NQO. The position of the fragments showing a significant number of counts is shown on a Hind III map of SV 40 in figure 24.

Figure 22: Hpa II restriction map of pBR 322 (Sutcliffe, 1978) showing fragments containing significant levels of bound NQO. The fragments labeled (■) contain NQO binding sites. An additional site is found in either of the fragments labelled (▥). Two additional fragments containing possible sites are labeled (▤). The origin of replication, ampicillin resistance (A_p^r) and Tetracycline resistance (T_c^r) genes are indicated. Numbering is clockwise from the Eco R1 restriction enzyme cutting site.

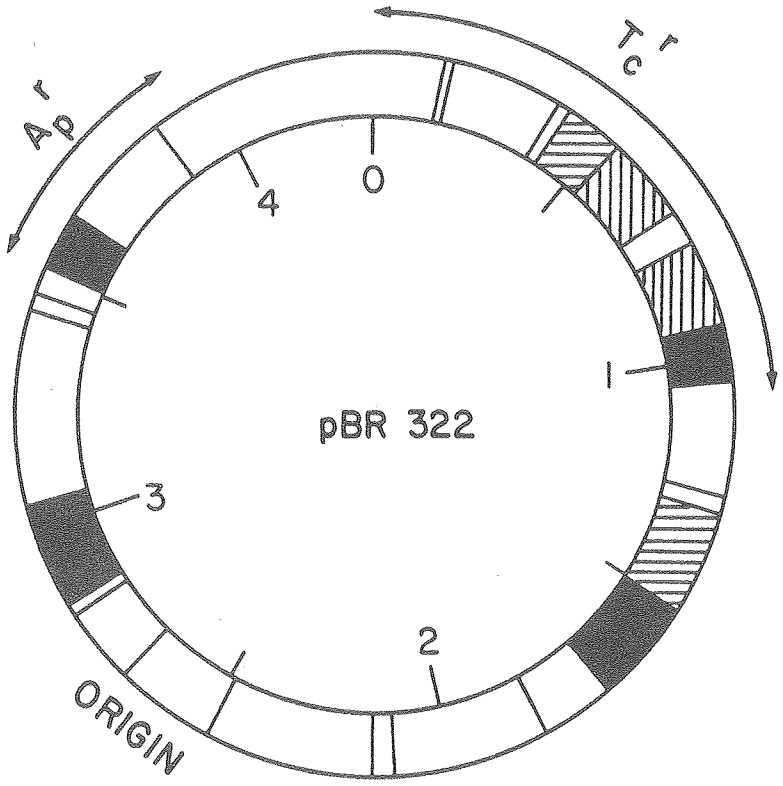

XBL 797-10707

TABLE IX

Positions of NQO Binding Sites on pBR 322 and SV 40

Positions of Restriction Fragments Containing Bound NQO

A. NQO Binding Sites on pBR 322.

Hpa II Digest Fragments[a] Containing Bound NQO

533-693 or 769-929[b]

929-1019

1484-1664

2854-3044

3549-3659

B. NQO Binding Sites on SV 40.

Composite of Hae III and Hind III Digests

Positions[c]	Eco R1 map units
2550-3070	0.80-0.90
4120-4640	0.42-0.59

[a]according to the restriction map of Sutcliffe (1978).

[b]two equally sized fragments; NQO binding site could be in either.

[c]according to the sequence numbering of Buchman, Burnett & Berg, SV 40 Sequence Manual, 1978.

Figure 23: Histograms of tritium cpm for gel bands from 6% acrylamide electrophoresis gels of the (a) Hind III digest or (b) Hae III digest of SV 40 DNA reacted with ^{3}H-NQO. The one Hind III gel band and two Hae III gel bands possessing significant amounts of tritium (and hence NQO) are indicated (↓). Electrophoresis at 200 V at 25°C.

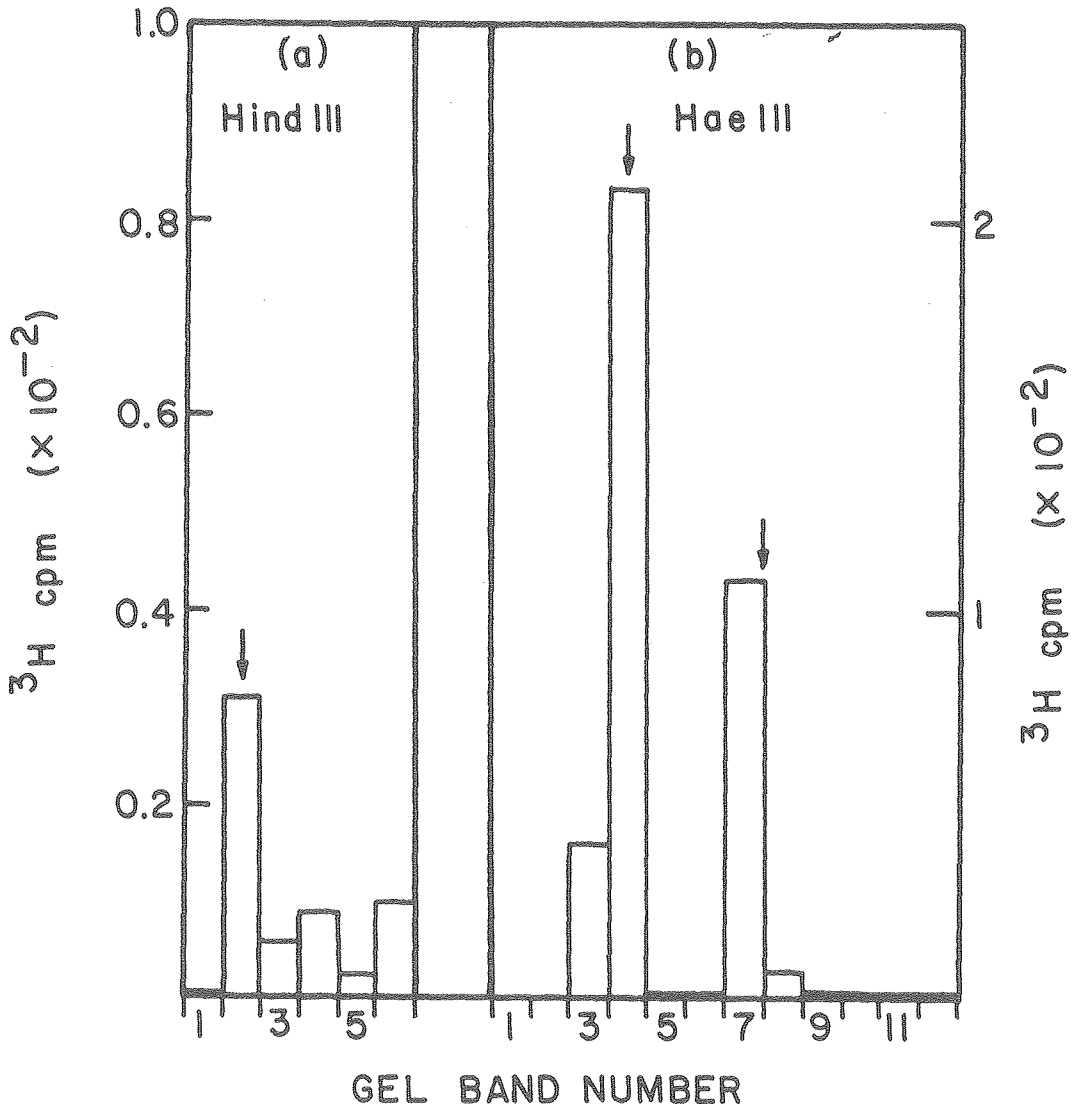

XBL 797-10711

Figure 24: Hind III (inner circle) and Hae III (outer circle) restriction maps of Sv 40 DNA (Bethesda Research Laboratories 1979 catalogue) showing fragments containing significant levels of bound NQO. The fragments labeled (▮) contain NQO binding sites. The two S_1 cutting sites (Beard, et al., 1973) are indicated (⊢S_1⊣). The (↓) indicates the T4 gene 32 protein binding site (Morrow & Berg, 1973). Also indicated are the origin of replication, early and late m RNA's (arros heads denoting 3' ends), and regions coding for known proteins (from Hsu & Jelinek, 1977). The numbering is that of Buchman, Burnett and Berg, SV 40 Sequence Manual, 1978.

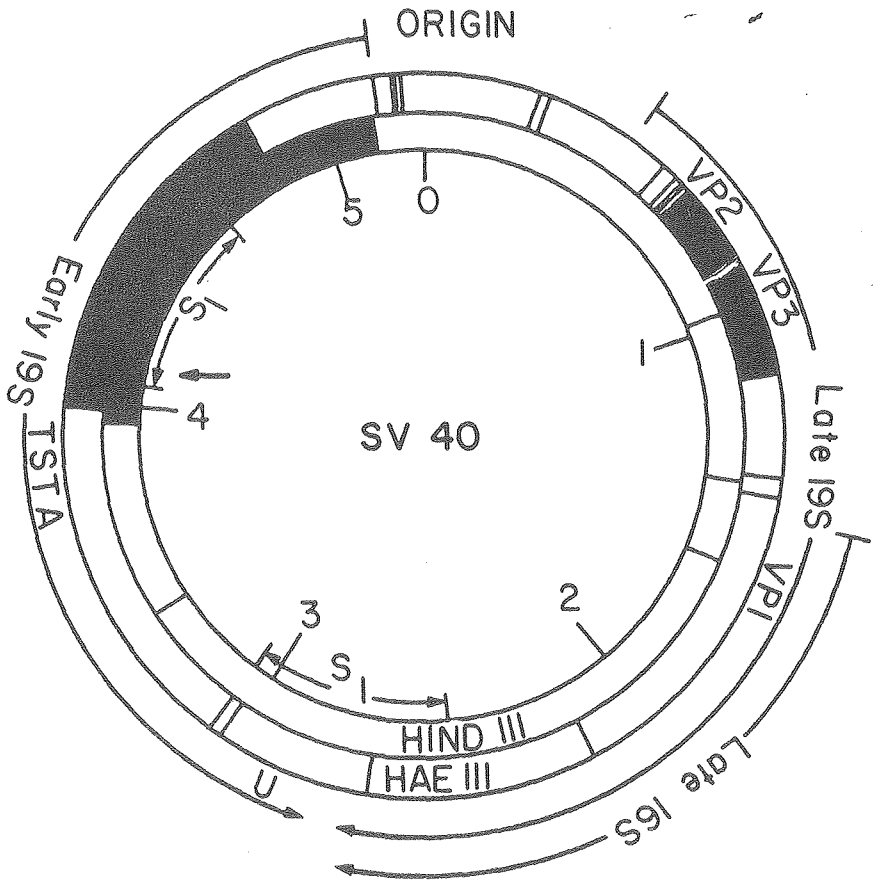

XBL 797-10708

For the Hae III digest of SV 40 with ^{3}H-NQO covalently bound, the 6% acrylamide gel showed a smear in the ragion where smaller fragments should appear. There were partial digest bands as well. The positions of the sliced gel bands and smear sections were compared to the Hind III ℓn(size) vs. position plot. Since the two gels were prepared and electrophoresed identically, fragments of the same size should have traveled the same distance on each gel. Using the position of each slice from the Hae III gel, the approximate size of the DNA in that slice was determined. The histogram of gel slice tritium counts per fragment is presented in figure 22b. The positions of the two hot fragments are displayed in the Hae III map in figure 24. One of the two fragments was a partial digest fragment consisting of the two indicated adjacent fragments. The other fragment overla-ped in position with the NQO binding fragment of the Hind III digest. The NQO binding site is in the region of the overlap. The positions of these two binding sites are given in Table IX.

DISCUSSION

As discussed in the Results section of this chapter, when SV 40 was relaxed using HeLa nicking-closing enzyme in the presence of NQO, the samples with NQO gave about the same amounts of partially relaxed and relaxed DNA as did the control DNA (without) NQO). Addition of a fixed quantity of ethidium resulted in an apparent "shift" of the partially relaxed DNA down the gel away from the fully relaxed DNA. The unwinding of the SV 40 by the NQO (in the presence of fixed ethidium concentrations could then be observed.

To determine the amounts of NQO noncovalently bound to the DNA in the presence of ethidium, it is necessary to know the equilibrium constant and binding ratio for this system. The equilibrium constant for NQO binding to SV 40 DNA in the presence of ethidium was given in Chapter V, $K_e = 6 \times 10^{12}\ M^{-2}$. This K_e is much smaller than the equilibrium constant determined for NQO binding to superhelical SV 40 - $K = 4 \times 10^{14}\ M^{-2}$. One possible explanation is that the ethidium is binding into the NQO binding sites, resulting in competition for these sites. The measured K_e would then be diminished relative to the K in the absence of ethidium. Ethidium, in binding to the superhelical DNA, unwinds the DNA. The amounts of ethidium used in the NQO unwinding experiments gave roughly 120 to 160 ethidium

molecules bound per SV 40 molecule. This corresponds to an unwinding by the ethidium of approximately 9 to 12 superhelical turns. This amount of unwinding of the SV 40 by the ethidium could possibly inhibit the binding of NQO to the SV 40.

In studying the covalent binding of NQO to supercoiled DNA; it was not necessary to use a relaxing enzyme to obtain the unwinding angle. Because the covalent binding of NQO results in an unwinding of the supercoiled DNA, the DNA with NQO adducts is partially relaxed. It therefore runs slower on an electrophoresis gel than the native superhelical DNA. The case of partially relaxed DNA was necessary, however, to move the DNA to a region where small changes in the number of supercoils could be seen. The displacement of the DNA with bound NQO relative to the unreacted partially relaxed DNA gave the unwinding angle for covalently bound NQO. The amounts of covalently bound NQO were directly determined by tritium counting the DNA after removal of NQO not covalently bound to the DNA.

The unwinding angles for the noncovalent and covalent binding of NQO to SV 40 DNA were 830°±60° per NQO bound per SV 40 and 770°±120° per NQO bound per SV 40, respectively. In Chapter V, it was reported that two NQO molecules bind to each strong binding site. The above unwinding angles correspond to, then, 1700°±100° per site filled per SV 40

for noncovalent binding and 1500°±300° per site filled per SV 40 for covalent binding. The values for noncovalently and covalently bound NQO are within experimental error of being equal.

That these apparent unwinding angles are very large is perhaps an understatement. They correspond to an unwinding of the superhelical DNA by roughly four to five superhelical tuerns. The unwinding angles for noncovalent ethidium binding (Wang, 1974) and covalent 4'-aminomethyl trioxsalen binding (Wiesehahn & Hearst, 1978) were both 26°-28° per bound drug per DNA. A large apparent unwinding angle for the covalently bound benz(a)pyrene diol epoxide has been observed by Gamper (H. Gamper, personal communication). By intercalation between the base pairs of DNA, drugs may change the twist angle of the base pairs from the B form 36°. For example, ethidium with an unwinding angle of 26° (Wang, 1974) changes the twist angle to 10°. It is difficult to account for the large apparent unwinding angles of NQO or BaP diol epoxide using such a mechanism.

If the drug binding resulted in localized denaturing of the DNA, this would account for a large amount of observed apparent unwinding. Hsieh and Wang (1975) discussed the unwinding of supercoiled DNA by the denaturation of base pairs. Denaturation of one base pair could result in unwinding the DNA helix by 0.1 turn. The energy lost by breaking a base pair is made up by relieving through unwinding the strain caused by the supercoiling. Hsieh

and Wang concluded that in naturally occurring superhelical DNA's, there are too few supercoils to account for a significant population of denatured base pairs. The presence of bound drug molecules could stabilize denatured native superhelical DNA's possess too few supercoils to give the energy (which would be gained by supercoil removal) needed to support the double strand-cruciform conversion. Thus they concluded that in native superhelical DNA's such structures are not stable - without some additional energy source. More recently, Vologodskii, et al. (1979) presented a theoretical discussion of the possibility of cruciforms in superhelical DNA's. Their conclusion was that with the amounts of superhelicity found in native supercoiled DNA, cruciforms would only exist "transiently". As with denatured regions, the presence of bound drug molecules could stabilize cruciforms. In structures such as cruciforms, there are new intrastrand base pairs formed which add to the stability of these structures. There is less of an "energy gap" between the normal double strand DNA and the regions, leading to larger amounts of unwinding (and removal of supercoils) than could be explained by the straightforward intercalation mechanism.

DNA segments which possess a twofold rotational symmetry may form intrastrand base pairs as opposed to interstrand base pairs. This results in the formation of cruciforms. Hsieh & Wang (1975) stated that cruciform formation would result in a decrease in the number of

superhelical turns in the DNA. Again, formation of such structures would be stabilized by relief of the strain produced by supercoiling. Hsieh & Wang approximated the free energy change for the conversion of a double stranded DNA sequence to the cruciform structure. Based on their studies on the free energy of supercoil formation, they showed that alternate cruciform structure than between the normal structure and the equivalent denatured DNA. Of course, any alternate structure could be a combination of hairpins and denatured regions.

Beard, et al. reported in 1973 that the endonuclease S_1, which is single strand specific, cuts superhelical SV 40 DNA resulting in linear SV 40 molecules. Nicked, circular SV 40 DNA was also converted to linear DNA. They suggested that the S_1 first converts the super coiled DNA to the nicked circular form, then to the linear form. In their paper, Beard et al. showed that S_1 cuts in 0.75 mM salt in one of two sites - at 0.15 to 0.25, or 0.45 to 0.55 SV 40 fractional length, mapped clockwise from the Exo R1 site. In higher salt, 250 mM, cutting at the 0.45-0.55 site dominated. The S_1 cutting was inhibited by the presence of T4 gene 32 protein which binds at 0.46 fractional length. Although the T4 gene 32 protein is selective for single strand DNA (Alberts and Frey, 1970), it binds to SV 40 (superhelical and non-superhelical) (Delius, et al. 1972).

Beard and coworkers attributed the inhibition by T4 gene 32 protein of S_1 cutting to either blockage of the attack site by the protein or to relaxation of superhelical SV 40 due to protein binding.

As was shown in figures 20a and 20b, the presence of noncovalently bound NQO inhibited the S_1 cutting in 110 mM salt of superhelical SV 40 DNA and pBR 322 at low enzyme concentrations. These "low" enzyme concentrations were sufficient to remove most or all the superhelical DNA from samples of equal [DNA] but without NQO. Since NQO did not inhibit the S_1 reaction with heat denatured calf thymus DNA, the inhibition does not result from a protein-NQO interaction.

This inhibition could arise, as with the T4 gene 32 protein, from one of two causes. The bound NQO could block the S_1 reaction site. One of the NQO binding sites on SV 40 (0.42-0.59 map units relative to the Eco R1 site) coincides with the 0.45-0.55 map unit S_1 cutting site. The binding of NQO has been shown to result in a sizable amount of unwinding, possibly through denaturation or cruciform formation or a combination of both. The alternate explanation for S_1 inhibition would be that NQO binding, resulting in alteration of DNA structure and unwinding, in one region decreases the probability of local denaturation in another region - such as the S_1 site. This is similar to the second argument proposed by Beard et al. (1973) to explain the S_1 inhibition by T_4 gene 32 protein.

Beard et al. (1973) placed emphasis in their discussion of the S_1 cutting sites on denaturable regions of the SV 40. Both of their S_1 cutting sites are within regions that are most easily denatured at high pH (Mulder and Delius, 1972). As discussed earlier, it would seem preferable to have the formation of some alternate secondary structure rather than the simple denaturation of the DNA. The base pairs formed in the alternate structure would stabilize that structure. In Chapter V, it was noted that NQO does not bind appreciably to single stranded DNA. It would therefore seem unlikely that NQO would be binding into a solely denatured region of DNA. It is possible that the binding sites are a combination of denatured regions and hairpins.

All the S_1 reactions conducted on the DNA or the DNA-NQO mixtures were run for the same length of time. The time dependence of NQO inhibition was not assayed. It is possible that if the reactions of S_1 on the DNA-NQO mixtures had been allowed to continue for longer than 30 min., the DNA in the presence of NQO would have been cut eventually.

SV 40 DNA with covalently bound ^{3}H-NQO was digested with the restriction enzymes Hind III or Hae III to locate the NQO binding sites. The NQO concentrations used in the adduct forming reaction mixtures were kept low to insure that NQO was bound to only the primary sites. There are probably two such sites in SV 40, as determined in the equilibrium

binding study in Chapter V. From the Hind III digest only one binding site was located (figures 23a and 24). With the Hae III digest two binding sites were found. The site having the larger amount of bound NQO corresponds to the binding site found in the Hind III experiment. Bound NQO was also found in a gel band which corresponds to a fragment consisting of two adjacent Hae fragments, as is indicated in figure 24. The maps in figure 24 are numbered according to the sequence map developed by Buchman, Burnett & Berg, SV 40 Sequence Manual, 1978, that is relative to the center of the palindrome of the Bql I restriction enzyme site. In Table IX, the positions of the NQO binding sites are also given in map units relative to the Eco Rl site, 0.42-0.59 and 0.80-0.90 map units.

The equilibrium binding data for pBR 322 presented in Chapter V suggested tha there are eight strong binding sites. Using the Hpa II digested pBR 322 with covalently bound ^{3}H-NQO, five binding sites were identified. There were two other possible sites but the binding to these two was considerably less. As was touched upon in Chapter V, the strong binding sites do not necessarily have identical structures. Since there will then be variances in the strengths of equilibrium binding by NQO to these sites, the amounts of NQO covalently bound to the different sites will vary. If some of the sites have equilibrium binding constants which are significantly

weaker (but of the same magnitude) than others, binding to these sites may not be detected. This observation is based on the reasoning that noncovalent binding precedes the covalent reaction. This could also explain why, with SV 40, only one binding site was detected in the Hind III experiment. The site found in the Hind III digest corresponded to the site from the Hae III digest having more bound NQO.

Comparison of the locations of the NQO binding sites on pBR 322 with the gene map of pBR 322 shows that some of the binding sites occur near the ends of the sequences for the ampicillin resistance gene (A_p^r) and the two tetracycline resistance genes (T_c^r). A computer assisted hairpin search of the pBR 322 sequence was done using a program developed by Dr. James McMahon. The minimum number of base pairs in each helical region and the maximum number of unbonded bases in the loops were specified to be five and twenty, respectively. A very large number of hairpins was found (244). Most of these were eliminated because of too few (less than four) or too many bases (more than seven) bases in the loop or because the loop contained more than three guanines or cytosines (an arbitrarily picked number). The calculated energies of the predicted hairpins should be compared to the energies of the corresponding double stranded DNA sequences since the interest is in double strand-cruciform conversions. Thus, if a loop contains four guanines or cytosines, this represents a loss of the energy of four GC base pairs. (Of course there is an

energy gain resulting from relief of the supercoil strain when the cruciform is formed). The computer search did not allow for structures with bulged bases or unbonded regions (interior loops). With some of the computer predicted hairpins with large loops, it is possible, by allowing for either bulges or interior loops, to create additionsl base pairs. Additional hairpins with bulges or nonbonded bases were found by a visual search of the NQO binding regions of pBR 322. These searches suggested that hairpins (cruciforms) are possible in the NQO binding regions. The computer predicted hairpin with the highest energy is in one of the NQO binding regions. Though most of the "reasonable" hairpins fall within one of the NQO binding regions it should be noted that there are hairpins that do not. Although hairpins have been predicted in the NQO binding regions, this does not necessarily mean that NQO would bind in these structures.

With SV 40 DNA, it has already been mentioned that one of the two NQO binding sites (0.42-0.59 map units) coincides with one of the S_1 cutting sites. This NQO binding site also encompasses the T4 gene 32 protein site. This NQO binding site is in the same region as the start of one of the SV 40 proteins (TSTA) as is shown in the gene map. The other binding site (0.90-0.90 map units) is in the same same region as within it the start of one capsid protein (VP3) and the end of another (VP2).

Shen & Hearst (1977), using trioxsalen crosslinking of the single strand SV 40 followed by electron microscopy, mapped the sequences of 2-fold symmetry axes (i.e. hairpins) relative to the Eco R1 site. In 30 mM NaCl, they found six hairpin loops - at 0.16, 0.26, 0.68, 0.84, 0.94 map units and near the Eco R1 site. The hairpin loop found at 0.84 map units is within the 0.80-0.90 NQO binding fragment. Hsu and Jelinek (1977) used electron microscopy of single stranded linear DNA to map inverted repeat sequences- at 0.11-0.30, 0.47-0.52, 0.63-0.68, 0.70-0.76, 0.90-0.96 Eco R1 map units. The inverted repeat at 0.47-0.52 falls within one of the NQO binding fragments (0.42-0.59). The 0.90-0.96 inverted repeat is at the end of the other NQO site. Both groups of authors pointed out that their mapped regions occur near either the positions of SV 40 replication origin or termination or near the end positions of transcription of the different mRNA's.

CONCLUSION

The experiments in this chapter were designed to help in answering the question: What is the nature of the DNA binding sites of NQO?

The unwinding experiments showed that both covalently and noncovalently bound NQO give large apparent "unwinding" angles. NQO inhibits the action of S_1 endonuclease, which attacks single stranded DNA. In SV 40, NQO was shown to have

a binding site in the same region as one of the S_1 sites. The equilibrium binding of NQO to superhelical DNA's is greater than the binding to linear versions of the same DNA's. The presence of supercoiling apparently enhances the binding. The binding sites in calf thymus DNA are temperature labile; the number of sites vs. temperature goes through a maximum. The equilibrium binding to the various DNA;s is cooperative with two NQO molecules bound per site. The number of binding sites for each type of DNA was small.

All of these results suggest that, rather than intercalating into a particular sequence (dimer, trimer, or other short oligomer), NQO binds into some type of alternate DNA secondary structure, e.g., cruciforms. It is difficult to see how any intercalative binding into double stranded DNA would be cooperative or require two drug molecules per site. Double stranded DNA should not show the temperature vs. number of binding sites plot found for NQO binding. Denatured regions or cruciforms show an enhanced stability in superhelical DNA. This coincides with the enhanced equilibrium binding of NQO to supercoiled DNA. The inhibition of S_1 by NQO binding to the DNA in the region of S_1 activity suggests that NQO binds into the cleavage site of S_1, i.e., a site containing single strand DNA. (Cruciforms, hairpin structures,

possess unbase-paired regions). The unwinding angles observed is much larger than can be explained by intercalation into normal double stranded DNA. This can be explained by NQO binding into and stabilizing (or creating) some form of non-double stranded regions in the supercoiled DNA. Finally, Shen and Hearst (1977) and Hsu and Jelinek (1977) observed hairpins in the single stranded DNA in regions where NQO binding sites are found.

All of the above information supports the proposition that NQO binds into (and stabilizes) an alternate DNA secondary structure. These structures most likely contain cruciform-like features and may have denatured sequences on either side of the hairpins. The results do not indicate where in such structures the NQO would bind. It was noted in Chapter 5 that the DNA-NQO complex molar absorptivities, ε_c, are roughly one half of those for the dinucleotide- or mononucleotide-NQO complexes. This suggests less overlap of the NQO with the aromatic bases of the DNA than with the bases of the monomers or dimers. This could be explained by binding into either the loops of the two hairpins or into the junctions of the hairpins with the rest of the DNA. Binding the NQO into these sites, especially the first, would further explain NQO inhibition of S_1 activity. Such binding would also explain why there are two NQO molecules per site - there are two loops.

Obviously this is speculative and further experiments are necessary to clarify this. One such set of experiments would be to isolate the NQO containing fragments from a restriction enzyme digest of some DNA and sequence those fragments. This would locate the base(s) to which the NQO is covalently attached. Further restriction enzyme digests using different enzymes of NQO bound DNA's again using SV 40, would narrow down the locations of the regions of NQO binding. Isolation of sufficient quantities of the NQO binding restriction fragments form pBR 322 or other plasmid would permit equilibrium binding studies with the fragments, e.g., equilibrium constant determination.

Several of the NQO binding sites in SV 40 and pBR 322 coincided with what are "control regions" of various gene coding sequences in the DNA's. There has been speculation in the literature that proteins binding into the gene control regions are attached to alternate secondary structures. Regions of two fold symmetry have been found, for example, near the promoter regions in prokaryotic DNA's (Pribnow, 1975; Shaller, et al., 1975; R. Dickson, et al., 1975). Such regions may form hairpins. Shen & Hearst (1977) and Hsu & Jelinek (1977) have previously reported the presence in SV 40 of hairpins near regions of importance for replication or transcription. It is possible that NQO binds into similar structures. At present, this is merely speculation. Further

refinements of the locations of NQO binding sites in the DNA's would help determine this. It would be interesting to look at the effects of NQO binding on RNA polymerase binding and reactivity.

CHAPTER VII

CONCLUSIONS

This investigation represents an effort to trace the noncovalent interactions of NQO with nucleic acids from the mononucleotide level up to DNA. The work began with spectroscopic investigations of the noncovalent binding of NQO to mononucleotides, then to dinucleotides. These studies were relatively straightforward. During the course of the dinucleotide study, the photochemistry of NQO was discovered. A side trip into the realm of the photoreactions of NQO was made prior to returning to the noncovalent interactions with DNA. The results of research on DNA-NQO noncovalent equilibria created a desire to determine the nature of the NQO binding sites in DNA. The previously explored photoreactions of NQO with DNA proved a useful tool for "permanently" placing NQO molecules into these binding sites. Based on the experiments exploring facets of the NQO binding to DNA, models for NQO binding could be speculated on.

Noncovalent interactions of NQO with the 5'-deoxy-mononucleotides were studied using absorption and NMR spectroscopy. The equilibrium constants obtained for the formation of 1:1 complexes suggested a preference for purine bases over pyrimidines. Analysis of the NMR spectra of NQO-dpA and NQO-dpG mixtures led to proposed structures for these two complexes.

The dinucleotide-NQO systems were investigated using methods very similar to those in the monomer studies. The equilibria data obtained indicate that the NQO binding strengths are greater when the dimers or dimer mixtures can form DNA-like minihelices. No great sequence preference is manifested on the dimer level. NQO forms 2:1 complexes with specific structures with the four selfcomplementary dimers. The orientations of the NQO in the CG and GC complexes and in the TA and AT complexes are similar to the NQO to base orientations in the dpG and dpA complexes, respectively.

The experiments with the monomers and dimers gave results which were similar to those reported with previously studied mutagens. Other carcinogens have shown a preference for purine binding. The equilibrium constants with the dimers are roughly of the same order of magnitude as for other molecules, e.g., ethidium (Krugh & Reinhardt, 1975). The lack of any sequence specificity on the dimer level was different from previous studies with ethidium and other molecules. In addition, the indications that NQO, in the noncovalent binding, does not unwind the dimer, differed from past mutagen studies. One of the novel results of these studies was the discovery of the photoreactivity of NQO.

As discussed in Chapter 4, the reactivity of NQO towards nucleophiles and its ability to form free radicals have been previously noted. The results of this study indicated that NQO will undergo catalyzed nucleophilic substitution at the 4-position, for example, to produce 4-hydroxyquinoline-1-oxide. NQO reacts photochemically with adenine, cytosine and uracil (and probably with guanine). At least some of the photoreactions with nucleic acids involve exciting the charge transfer bands. NQO will react, unmetabolized, with DNA in the dark, suggesting that *in vivo*, metabolic activation of the NQO is not necessary (though the metabolism, of course, occurs with much of the ingested NQO). The establishment of the existence of NQO photoaddition to DNA creates a tool to be used in probing NQO binding to DNA.

NQO binds very strongly and cooperatively to a select group of sites in the DNA. Two NQO molecules bind per site. A variety of experiments were conducted to look at these binding sites. The large DNA unwinding angle of NQO, the inhibition of S_1 cutting of superhelical DNA by NQO, the increased binding in the presence of superhelical turns, the cooperativity of the binding, the temperature lability of the binding sites all argue for NQO binding into (and stabilization of) some DNA structure different from the normal double helix. All of these characteristics of the NQO binding are consistent with NQO binding into cruciform-like structures. These structures could be hairpins

(cruciforms) surrounded by stretches of denatured DNA. In the locations of the NQO binding sites on SV 40, hairpins have been observed using electron microscopy on single stranded SV 40 (Shen & Hearst, 1978; Hsu & Jelinek, 1978).

It has been noted that the hairpins observed in SV 40 occur in control regions of the DNA. In pBR 322, some of the NQO binding sites are near the beginnings or ends of various protein coding regions. It is of interest to speculate on the consequences of NQO binding to such control retions of the DNA.

NQO molecules covalently bound into cruciforms could theoretically stabilize such structures indefinitely. When the DNA polymerase reads to a cruciform or hairpin stabilized by an NQO adduct, it could probably follow one of three courses of action. The polymerase could stop, period, in which case the DNA would not be replicated.

The polymerase could unzip the hairpin and read through it. In this case, the NQO could cause some form of misreading, e.g., a frameshift mutation. Since such a mutation is not in the protein coding region, the structure of future protein molecules would not be affected. Removal of bases in the cruciform could be crucial, however, to the formation of the hairpins. A decrease in the ability of the DNA to form this hairpin would impair the control of the gene in question.

In the third possibility, the polymerase could skip past the cruciform. Alternatively, some repair process could be called in which would remove the offending piece of DNA, i.e., the hairpin. In either of these cases, the daughter DNA's would be missing a sizable piece of one of their gene control regions. This would seriously change the production of the gene product by the DNA.

Thus it can be seen that the binding of NQO into control region cruciforms of the DNA of the parent cell could alter the nature and production rates of the gene products made by the daughter DNA's.

If these gene products are necessary for maintaining cell size or controlling replication, altering the mechanism of their production could have interesting consequences.

This discussion of what cruciform stabilization by NQO could lead to is obviously, at this time, speculation. The studies presented here on NQO binding to nucleic acids form a basis from which many types of studies might be begun. Some of these have been mentioned in earlier chapter. In addition to those proposed avenues of research, it would be of value to investigate DNA replication in the presence of boune NQO. Binding studies like those presented with NQO using other carcinogens would establish whether the highly specific binding into select regions of altered DNA structure is a general feature of carcinogen binding.

If such binding is common, this could provide insight as to why certain compounds are carcinogens and how they produce cancer.

REFERENCES

Alberts, B. and Frey, L. (1970) Nature 227, 1313.

Allen, F.S., Gray, D.M., Roberts, G.P. and Tinoco, I., Jr. (1972) Biopolymers 11, 853.

Beard, P., Morrow, J.F. and Berg, P. (1973) J. Virology 12, 1303

Benesi, H.A. and Hildebrand, J.H. (1949) J. Am. Chem. Soc. 71, 2703.

Cheney, B.V. and Grant, D.M. (1967) J. Am. Chem. Soc. 89, 3319.

Davanloo, P. and Crothers, D.M. (1976) Biochemistry 15, 4433

Dejangh, D.C. (1973) in Synthetic Procedures in Nucleic Acid Chemistry, vol. 2, W.W. Zorbach and R.S. Tipson, Eds., Wiley-Interscience, New York, NY. p. 145.

Delius, H., Mantell, N. and Alberts, B. (1972) J. Mol. Biol. 67, 341.

Endo, H. (1958) Gann 49, 151.

Fasman, G.D., Ed. (1976) CRC Handbook of Biochemistry and Molecular Biology, rrd ed., CRC Press, Cleveland Ohio.

Fink, L., Nishimura, S. and Weinstein, I. (1970) Biochemistry 9, 496.

Frimer, A.A., Havron, A., Leonov, D., Sparling, J. and Elad, D. (1976) J. Am. Chem. Soc. 98, 6026.

Giessner-Prettre, C. and Pullman, B. (1970) J. Theor. Biol. 27, 87.

Giessner-Prettre, C. and Pullman, B. (1976) Biochim. Biophys. Res. Commun. 70, 578.

Hanna, M.W. and Ashbaugh, A.L. (1964) J. Phys. Chem. 68, 811.

Hogan, M., Dattagupt, M. and Crothers, D.M. (1979) Nature 278, 521.

Hsieh, T.-S. and Wang, J.C. (1975) Biochemistry 14, 527.

Hsu, M.T. and Jelinek, W.R. (1977) Proc. Natl. Acad. Sci. USA 74, 1631.

Hyde, J.E. and Hearst, J.E. (1978) Biochemistry 17, 1251.

Isaacs, S.T., Shen, J. C.-K., Hearst, J.E. and Rapoport, H. (1977) Biochemistry 16, 1058.

Jain, S.C., Tsai, C.-C. and Sobell, H.M. (1977) J. Mol. Biol. 114, 317.

Jennete, K., Jeffrey, A., Blobstein, S., Beland, F., Harvey, R. and Weinstein, I. (1977) Biochemistry 16, 932.

Jeffrey, A.M., Jennette, K.W., Blobstein, S.H., Weinstein, J.B., Beland, F.A., Harvey, R.G., Kasai, H., Miura, I. and Nakanishi, K. (1976) J. Am. Chem. Soc. 98, 5714.

Karplus, M. and Pople, J.A. (1963) J. Chem. Phys. 38, 2803.

Karreman, G. (1962) Ann. N.Y. Acad. Sci. 96, 1029.

Kataoka, N., Imamura, A., Kawazoe, Y., Chihara, G. and Nagata, C. (1966) Chem. Pharm. Bull. (Tokyo) 14, 897.

Kawashima, S. and Tomoeda, M. (1970) Chem. Pharm. Bull. (Tokyo) 18, 620.

Kawazoe, Y. (1971) in Recent Results in Cancer Research, vol. 34, H. Endo, T. Ono, T. Sugimura, Eds., Springer, New York, NY Chapter 2, p. 3.

Kawazoe, Y. and Araki (Tachibana), M. (1970) in Chemical Tumor Problems, W. Nakahara, Ed., Japan Soc. Promotion Sci. Publishers, Tokyo, p. 45.

Kawazoe, Y., Araki, M. and Nakahara, W. (1969b) Chem. Pharm. Bull. (Tokyo) 17, 544.

Kawazoe, Y. and Ohnishi, M. (1967) Chem. Pharm. Bull. 15, 828.

Kawazoe, Y. and Tachibana, M. (1967) Chem. Pharm. Bull. (Tokyo) 15, 1.

Kawazoe, Y., Uehara, N., Araki (Tachibana), M. and Tamura, M. (1969a) Gann 60, 617.

Koreeda, M., Moore, P.D., Yagi, H., Yeh, H.J.C. and Jerina, D.M. (1976) J. Am. Chem. Soc. 98, 6720.

Kriek, E., Miller, J.A., Juhl, U. and Miller, E.C. (1967). Biochemistry 1, 177.

Krugh, T.R., Laing, J.W. and Young, M.A. (1976) Biochemistry 15, 1224.

Krugh, T.R. and Reinhardt, C.G. (1975), J. Mol. Biol. 97, 1933.

Krugh, T.R., Wittlin, F.N. and Cramer, S.P. (1975) Biopolymers 14, 197.

McCann, J., Choi, E., Yamasaki, E. and Ames, B.N. (1975) Proc. Natl. Acad. Sci. USA 72, 5135.

Morrow, J.F. and Berg, P. (1973) J. Vriol. 12, 1631.

Mulder, C. and Delius, H. (1972) Proc. Natl. Acad. Sci. USA 69, 3215.

Nagata, C., Imamura, A., Fukui, K. and Saito, H. (1963) Gann 54, 401.

Nagata, C., Kodama, M., Tagashira, Y. and Imamura, A. (1966) Biopolymers 4, 409.

Nakanishi, K., Kasai, H., Cho, H., Harvey, R.G., Jeffrey, A.M., Jennette, K.W. and Weinstein, I.B. (1977) J. Am. Chem. Soc. 99, 258.

Nakahara, W. (1964) Arzneimittel-Forsch. 14, 842.

Neidle, S., Achari, E., Taylor, G.L., Berman, H.M., Carrell, H.L., Glusker, J.P. and Stallinger, W.C. (1977) Nature 269, 304.

Ochiai, E. (1953) J. Org. Chem. 18, 534.

Ochiai, E., Ohta, A. and Nomura, H. (1957) Chem. Pharm. Bull. (Tokyo) 5, 310.

Okabayaski, T. (1953) J. Pharmaceut. Soc. Japan 73, 94.

Okamoto, T. and Itok, M. (1963) Chem. Pharm. Bull. (Tokyo) 11, 785.

Okano, T., Maenosono, J., Tetsuya, K. and Onoda, I. (1973) Gann 64, 227.

Okano, T., Nittsuma, A. Takadata, A. and Uekama, K. (1969a) Gann 60, 97.

Okano, T., Takadata, A. and Kano, T. (1969c) Gann 60, 557

Okano, T. and Uekama, K. (1968) Chem. Pharm. Bull. (Tokyo) 16, 1411.

Paul, J.S. and Montgomery, P. O'B. (1970) Mol. Pharmacol. 6, 315

Sakore, T.D., Jain, S.C., Tsai, C.-C. and Sobell, H.M. (1977) Proc. Natl. Acad. Sci. USA 74, 188.

Schweizer, M.P., Broom, A.D., Ts'o, P.O.P. and Hollis, D.P. (1968) J. Am. Chem. Soc. 86, 696.

Sobell, H.M., Tsai, C.-C., Gilbert, S.G., Jain, S.C. and Sakore, T.D. (1976) Proc. Natl. Acad. Sci. USA 73, 3068.

Subah-Sharpe, H., Bürk, R.R., Crawford, L.V., Morrison, J.M., Hay, J., Kein, H.M. (1966) Cold Spring Harbor Symposium 31, 737.

Sugimura, T., Okaba, K. and Nagao, M. (1966) Cancer Res. 26, 1717.

Sutcliffe, J.G. (1978) Nucleic Acids Res. 5, 2721.

Swartz, M.N., Trautner, T.A. and Kornberg, A. (1962) J. Biol. Chem. 237, 1961.

Tachibana, M., Sawaki, S. and Kawazoe, Y. (1967) Chem. Pharm. Bull. (Tokyo) 15, 1112.

Tada, M. and Tada, M. (1976) Biochim. Biophys. Acta 454, 558.

Tada, M., Tada, M. and Takabashi, T. (1967) Biochem. Biophys. Res. Comm. 4, 469.

Valogodskii, A., Lukashin, A., Anghelevich, V. and Frank-Kamenetskii, M. (1979) Nucleic Acids Res. 6, 1967.

Wang, J.C. (1974) J. Mol. Biol. 89, 783.

Waring, M. (1975) Biochem. Biophys. Acta 407, 200.

Wiesehahn, G. and Hearst, J.E. (1978) Proc. Natl. Acad. Sci. USA 75, 2703.

Young, M.A. and Krugh, T.R. (1975) Biochemistry 14, 4841.

For a review of work on NQO through 1972, see:

Arcos, J.C. and Argus, M.F. Eds. Chemical Induction of Cancer. Structural Bases and Biological Mechanisms, vol. IIB (1974) Academic Press, New York, NY. Various chapters.

APPENDIX I

PROCEDURES FOR HANDLING 4-NITROQUINOLINE-1-OXIDE (NQO) AND OTHER CARCINOGENS

Stephen Winkle, March 1977

1. Solid NQO must be handled in the glove box. For making up solutions of NQO, dissolve NQO in the solvent in the glove box and use UV to determine concentration. If the solution is saturated, i.e., contains particulate, filter off solid in the glove box. If it is necessary to weigh NQO, as when doing a reaction, NQO is to be placed in the weighing vessel in the glove box. The vessel is then sealed with Parafilm, wiped off with acetone in the glove box, then taken out for weighing.
2. When transporting NQO, wolid or solution, the vessel containing the NQO is placed inside a second container, e.g., a plastic beaker. The vessel containing the NQO directly should be sealed with parafilm. Prepared NQO solution should be stored in sealed bottles inside plastic beakers.
3. Obviously, plastic gloves must be worn while handling the NQO solutions outside the glove box. When adding or removing something from the blove box, use plastic gloves.
4. Reactions, recrystallizations, etc., must be done in the glove box.

5. As stated in (1), all NQO solution preparation must be done in the glove box. However, preparation of solutions, e.g., dilutions, NQO-nucleotide mixtures, from these "stock" solutions may be done at the designated bench in 407 Hildebrand. For working with NQO solutions, work in the metal bucket labeled for carcinogen use lined with absorbent paper. Preparation of samples for nmr, UV, etc., is to be done in this bucket. In addition, transferral of samples to the UV spectrometer or to other locations are to be made using this bucket.
6. Transfer NQO to sample tubes using small glass tuberculin syringes (so that volume, flow, etc., may be controlled). Keep the amount thus transferred small, e.g., 0.250 ml.
7. When running UV (or other absorption type experiments) rinse cells thoroughly 4 times into a waste container, or a storage flask (for recycling) in the case of dimers or other oligonucleotides, before using the cell washer. Similarly rinse nmr tubes 3 times with water and 2 times with acetone into a waste container. All other glassware is to be similarly rinsed into the waste container. If the object remains discolored, try acid. If this doesn't work, discard the glassware into solid waste container.

8. Hopefully, by having only small amounts of the solution transferred at a time, there will be no spills. However, if a spill occurs, immediately blot up the spilled material, rinse the area 4 times with H_2O and twice with acetone. The final acetone wipe should be "clear".
9. Waste disposal - all solid material, e.g., Kimwipes, pipettes, glassware, etc. shall be placed in the plastic bag in the labeled solid waste box in 402 Hildebrand. Do not allow this box to become too full. The amount of waste in the bag should not exceed an amount which would allow for tying off the bag. Tie off the bag when full and tape shut. Highly carcinogenic solid waste, including filter paper (from filtering mixtures containing NQO), kimwipes that have wiped up concentrated NQO solutions, (of course) solid NQO, should be put in a zip lock plastic bag before placement in the general solid waste box. All solid waste from the glove box should be put in a ziplock bag before discarding. Liquid waste shall be placed in the liquid waste container in 402 Hildebrand.

APPENDIX II

^{13}C NMR SPECTRAL DATA FOR NUCLEIC ACIDS

TABLE X

^{13}C Chemical Shifts[a] for 5'-deoxymononucleotides

monomer	Chemical Shift (ppm)										
a. pH 5	2	4	5	6	8	m_e(T)	1'	2'	3'	4'	5'
dpG	158.14	155.51	120.38	163.12	141.73		87.76	43.01	75.64	90.00	68.88
dpC	167.35	158.12	98.84	144.91			88.86	42.16	73.60	88.42	67.18
dpA	155.36	151.91	121.92	158.42	143.39		87.11	42.50	74.61	89.20	67.96
dpT	154.24	169.04	114.18	139.89		14.06	87.58	41.28	73.68	88.10	66.84
b. pH 7											
dpG	156.39	153.74	118.58	161.45	140.17		85.82	41.15	74.02	88.71	66.33
dpC	168.87	160.15	99.17	144.56			88.45	42.01	73.66	88.70	66.25
dpA	155.64	151.61	121.57	158.58	143.10		86.48	42.03	74.37	89.29	66.68
dpT	154.38	169.16	114.31	140.20		14.22	87.64	41.07	73.84	88.52	66.63

[a]All spectra obtained at 35°C on the 180 MHz system described in Chapter III. $[dpN]_T \approx 10$ mM. Buffer 0.1 M NaCl, 0.01 M Na cacodylate, 0.2 mM EDTA (pH 7, 30% D_2O). DSS Reference.

TABLE XI

^{13}C Chemical Shifts[a] for Deoxydinucleotide Aromatic Carbons

dimer	Chemical Shift (ppm)								
	C2 \	C4	C5	C6	G2	G4	G5	G6	G8
dpCpG	168.56	156.43	99.28	143.80	159.66	153.98	118.66	161.31	140.22
dpGpC	168.19	159.53	98.35	143.66	156.27	153.61	118.68	161.37	139.96
	T2	T4	T5	T6	A2	A4	A5	A6	A8
dpTpA	153.83	168.83	114.43	139.53	155.46	151.44	120.96	158.06	142.56
dpApT	155.22	---[b]	113.77	139.30	153.74	151.12	121.27	158.14	142.62

[a]All spectra obtained at 35°C on the 180 MHz system described in Chapter III. $[dpN_1pN_2]_T \simeq 4.0$ mM. Buffer 0.1 M NaCl, 0.01 M Na cacodylate, 0.2 mM EDTA (pH 7, 30% D_2O). DSS reference

[b]Not observed.

Figure 25. ^{13}C NMR spectra of denatured calf thymus DNA.
(a) Heat denatured DNA. $[DNA]_P \simeq 5$ mM. pH 7.
(b) pH denatured DNA. $[DNA]_P \simeq 8$ mM. pH 12.
Both spectra obtained at 40° in 0.1 M NaCl, 0.01 M Na cacodylate, 0.2 mM EDTA on the 180 MHz system. 8 K data points, 70° pulse, 1 sec delay with ^{1}H decoupling.

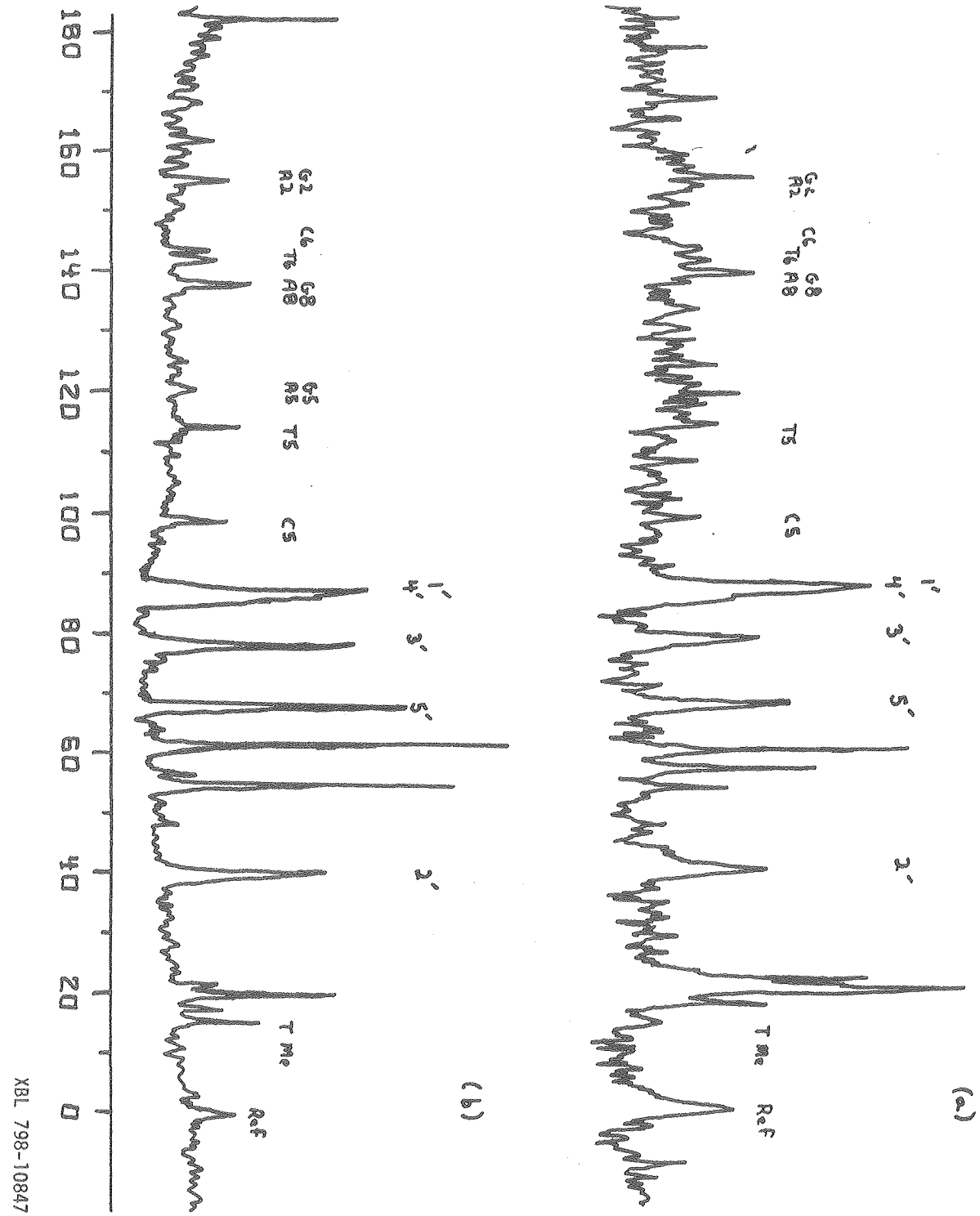

XBL 798-10847

U.S.GPO:1979-689-169 (F)82

TECHNICAL INFORMATION DEPARTMENT
LAWRENCE BERKELEY LABORATORY
UNIVERSITY OF CALIFORNIA
BERKELEY, CALIFORNIA 94720